NASA Contractor Report 187040

Solar Dynamic Heat Receiver Technology

Final Report

Leigh M. Sedgwick
The Boeing
Company
Seattle, WA

January 1991

Prepared for
Lewis Research Center
Under Contract
NAS3-24669

National Aeronautics and
Space Administration

NASA Contractor Report 187040

Solar Dynamic Heat Receiver Technology

Final Report

Leigh M. Sedgwick
The Boeing
Company
Seattle, WA

January 1991

Prepared for
Lewis Research Center
Under Contract
NAS3-24669

National Aeronautics and
Space Administration

NASA
National Aeronautics and Space Administration

Report Documentation Page

1. Report No.	2. Government Accession No.	3. Recipient's Catalog No.
NASA CR-187040		

4. Title and Subtitle	5. Report Date
Solar Dynamic Heat Technology Final Report	January 1991
	6. Performing Organization Code

7. Author(s)	8. Performing Organization Report No.
Leigh M. Sedgwick	D180-32598-1
	10. Work Unit No. 474-52-10

9. Performing Organization Name and Address	11. Contract or Grant No.
Boeing Aerospace & Electronics P.O. Box 3999 Seattle, WA 98124-2499	NAS3-24669
	13. Type of Report and Period Covered Contractor Report Final

12. Sponsoring Agency Name and Address	14. Sponsoring Agency Code
National Aeronautics and Space Administration Lewis Research Center Cleveland, Ohio 44135-3191	

15. Supplementary Notes

Project Managers, Kerry L. McLallin and Thomas W. Kerslake,
Systems Engineering and Integration Division, NASA Lewis Research Center

16. Abstract

A full-size, solar dynamic heat receiver has been designed to meet the requirements specified for electrical power modules on the U.S. Space Station, Freedom. The heat receiver supplies thermal energy to power a heat engine in a closed Brayton cycle using a mixture of helium-xenon gas as the working fluid. The electrical power output of the engine, 25 kW, requires a 100 kW thermal input throughout a 90 minute orbit, including when the space craft is eclipsed for up to 36 minutes from the sun. The heat receiver employs an integral thermal energy storage system utilizing the latent heat available through the phase change of a high-temperature salt mixture. A near eutectic mixture of lithium fluoride and calcium difluoride is used as the phase change material. The salt is contained within a felt metal matrix which enhances heat transfer and controls the salt void distribution during solidification. Fabrication of the receiver is complete and it has been delivered to NASA for verification testing in a simulated low-Earth-orbit environment. This document reviews the receiver design and describes its fabrication history. The major elements required to operate the receiver during testing are also described in this document.

17. Key Words (Suggested by Author(s))	18. Distribution Statement
Closed Brayton cycle Heat receiver Solar dynamic power Space power Thermal energy storage	Unclassified - Unlimited Subject Category 18

19. Security Classif. (of this report)	20. Security Classif. (of this page)	21. No. of pages	22. Price
Unclassified	Unclassified	129	

NASA FORM 1626 OCT 86

ABSTRACT

A full-size, solar dynamic heat receiver has been designed to meet the requirements specified for electrical power modules on the U.S. Space Station, Freedom. The heat receiver supplies thermal energy to power a heat engine in a closed Brayton cycle using a mixture of helium-xenon gas as the working fluid. The electrical power output of the engine, 25 kW (e), requires a 100 kW thermal input throughout a 90 minute orbit, including when the space craft is eclipsed for up to 36 minutes from the sun. The heat receiver employs an integral thermal energy storage system utilizing the latent heat available through the phase change of a high-temperature salt mixture. A near eutectic mixture of lithium fluoride and calcium difluoride is used as the phase change material. The salt is contained within a felt metal matrix which enhances heat transfer and controls the salt void distribution during solidification. Fabrication of the receiver is complete and it has been delivered to NASA for verification testing in a simulated low-Earth-orbit environment (except for gravity). This document reviews the receiver design and describes its fabrication history. The major elements required to operate the receiver during testing are also described in this document. These hardware components include a closed Brayton cycle engine simulator that conditions the helium-xenon gas mixture to meet the interface requirements of the receiver (pressure, temperature, and flow rate), a quartz lamp heater used to provide a realistic distribution of input energy in the receiver cavity, and a structure to support the receiver during testing and provide an interface with the vacuum facility.

KEY WORDS

Calcium Fluoride
Closed Brayton Cycle
Electrical Power Generation
Energy Storage
Heat Receiver
Helium-Xenon
High-Temperature
Lithium Fluoride
Low Earth Orbit
Phase Change
Quartz Lamp
Solar Dynamic Heat Receiver
Solar Dynamic Power Generation
Space
Space Station Freedom
Test Plan
Test Procedures
Thermal Energy Storage
Vacuum

ACKNOWLEDGEMENTS

The faith in the receiver design and the constructive program guidance afforded by the following personnel of the NASA Lewis Research Center is gratefully acknowledged:

Mr. Kerry McLallin	SDHRT Project Manager
Mr. Steve Johnson	SDHRT Consultant and Past SDHRT Project Manager
Mr. Steve Cohen	SDHRT Consultant and Past SDHRT Project Manager
Mr. Thomas Kerslake	Staff Member

The assistance of the following personnel at Rocketdyne, the prime contractor to NASA on the Space Station Freedom electrical power system, is gratefully acknowledged.

Mr. Chuck Kudija	CBC Project Engineer
Mr. Jerry Friefeld	Space Station R&D Manager
Mr. Ken Santarelli	SD Power Module Integration Manager

Lukas Machine located in Seattle, WA was the major subcontractor to Boeing responsible for the fabrication of the receiver structure and pressure piping components, assembly of the receiver, fabrication and assembly of the CBC engine simulator, and the fabrication of many component level hardware used throughout the program. Sincere appreciation is expressed to Mr. Michael Iles (Project Manager), Mr. Herb Neff (welding), and Mr. Ray Motishka (component assembly, Q/A, and leak checking). Without their creative planning, hard work, and incredible speed in accomplishing difficult tasks, the SDHRT heat receiver would have never been completed.

The following subcontractor personnel also provided significant input to the SDHRT program and are gratefully acknowledged.

Mr. Tim Koert	Tofle America - Exton, PA
Mr. Marc Acton	Belfab - Daytona Beach, FL
Mr. Richard Larsen	Robertshaw - Cookeville, TN
Mr. Bob Barber	Barber-Nichols Eng. - Arvada, CO
Mr. Randy Petri	Inst. of Gas Tech. - Chicago, IL
Mr. Patrick Heller	Manville Insulation - Elkhart, IN
Mr. George Morrison	Valley Metals - El Cajon, CA
Mr. Dick Crawford	Nat'l Standard - Corbin, KY
Mr. George Robinson	Rembar - Dobbs Ferry, NY
Mr. Dean McCarthy	Rembar - Dobbs Ferry, NY
Mr. Dennis Lawton	Inco Alloys Int. - St Louis, MO

ACKNOWLEDGEMENTS (con't)

The assistance of Dr. Hal J. Strumpf of the Allied Signal Space Company is gratefully acknowledged, particularly for providing thermophysical property data for the LiF-CaF_2 salt.

Sincere appreciation is expressed to the following Boeing personnel for their assistance and participation on the SDHRT program.

Dr. Ted Kramer	AST Manager
Dr. Frank Marshall	AST Manager
Mr. Steve Goo	AST Manager
Mr. Harold Nordwall	SDHRT Program Manager
Mr. Leigh Sedgwick	SDHRT Principal Investigator
Mr. Ernie Valley	SDHRT Contracts
Mr. Kenneth Kaufmann	SDHRT Analysis/Design/Test
Mr. David House	SDHRT Mechanical Design
Mr. James Cotton	M&P - SDHRT Materials Engineer
Mr. Joe McCartney	TCPS - Salt Fill/Test Technician
Mrs. Rose Hall	Secretarial/Everything
Mr. Ron Zentner	SDHRT Consultant
Mr. John Laakso	Loads/Stress Consultant
Mr. Richard Schuller	Loads/Stress Analysis
Dr. Brad Kirkwood	M&P Materials Consultant
Mr. Gary Frankfurt	HTTES Setup/Test Consultant
Mr. Don Bartlett	SDHRT Consultant
Mr. Keith Warner	SDHRT Thermal Analysis
Mr. Chuck Domby	M&P - Materials Consultant
Mr. Jack Jorgensen	ETL - Test Planning
Mr. Scott Ulen	ETL - CBC Design/Test Planning
Ms. Peggy Lawrence	HTTES Facility Design and Operation
Mr. Greg Rhodes	HTTES Facility Design
Mr. Jim Lee	MR&D - EB Welding
Mr. Jeff Wills	M&P - Laser Welding
Mr. Ray Bower	M&P - Materials Consultant
Mr. Russ Crutcher	M&P - Salt Analyses
Mr. Warren Wascher	M&P - Salt Analyses
Mr. Colin Ferren	Licensed Transportation
Mr. Dan Peterson	TCPS Laboratory - Salt Filling

TABLE OF CONTENTS

TABLE OF CONTENTS (con't)

LIST OF FIGURES

LIST OF FIGURES (con't)

LIST OF FIGURES (con't)

NOMENCLATURE

AD	Advanced Development
ADRT	Advanced Development Receiver Thermal Vacuum Tests With Cold Wall
ASME	American Society of Mechanical Engineers
BOL	Beginning of Life
CaF_2	Calcium Fluoride
CBC	Closed Brayton Cycle
CDR	Critical Design Review
DACS	Data Acquisition and Control System
DAR	Design Analysis Report
DRS	Developmental Record System
EB	Electron-Beam
EOL	End of Life
GFP	Government Furnished Property
He	Helium
HTTES	High-Temperature Thermal Energy Storage
HX	Heat Exchanger
ID	Inner Diameter
LEO	Low Earth Orbit
LeRC	Lewis Research Center
LiF	Lithium Fluoride
NASA	National Aeronautics and Space Administration
OD	Outer Diameter
ORC	Organic Rankine Cycle
ORNL	Oak Ridge National Laboratory
PCM	Phase Change Material
PDR	Preliminary Design Review
QA	Quality Assurance
SD	Solar Dynamic
SDHRT	Solar Dynamic Heat Receiver Technology

NOMENCLATURE (con't)

SiO_2	Silicon Dioxide
SOW	Statement of Work
TES	Thermal Energy Storage
TSE	Test Support Equipment
Xe	Xenon

1.0 SUMMARY

The Solar Dynamic Heat Receiver Technology (SDHRT) contract was initiated by the NASA Lewis Research Center (LeRC) in October 1985. Completion was scheduled for 36 months later in September 1988. The primary objective of this contract was to design, fabricate, and test a full-size, solar dynamic (SD) heat receiver capable of meeting the requirements of the electrical power system on the U.S. Space Station, Freedom.

The contract was structured by specific tasks orders to (1) develop conceptual designs of SD heat receivers and thermal energy storage (TES) systems to meet Space Station electrical power and environmental requirements and conduct trade studies to determine those receiver and TES designs which best meet program objectives, Task 1; (2) identify the facilities and test support equipment required to conduct verification testing of a full-size SD heat receiver, Task 2; (3) identify and develop required fabrication techniques and the tooling needed to complete the fabrication of a full-size SD heat receiver, Task 3; (4) complete the detail design of the most promising receiver concept, Task 4; (5) fabricate a full-size solar heat receiver, Task 5; (6) fabricate test support hardware and conduct verification testing of the receiver in a vacuum environment, Task 6; and (7) deliver the heat receiver to NASA-LeRC and provide support to NASA during follow-on testing.

The final heat receiver configuration and details evolved through the conceptual and detailed design phases of the program. The completed receiver is pictured in Figure 1-1 mounted in a support fixture during preparation for testing. The receiver is shown without the aperture assembly in place. It has a cylindrical cavity 1778 mm (70 in) in diameter and 2032 mm (80 in) in length. The outer diameter (OD) is 2184 mm (86 in) and the total length is 2794 mm (110 in). The test receiver weighs 2178 kg (4,797 lbs).

The receiver heat exchange system is comprised of 24 parallel heat exchanger (HX) tubes, each surrounded by an annulus containing a salt/felt metal composite. The salt is a near eutectic mixture of lithium fluoride (LiF) and calcium difluoride (CaF_2) and is capable of storing about 72 kw-hrs of energy during its change of phase from solid to liquid at a temperature of 771°C (1420°F). The felt metal is used to improve the heat conduction across the salt annulus and to prevent the gravity force from controlling the locations of voids that form in the salt during solidification. Data collected during component tests demonstrated the felt metal concept and shows that the test data obtained from the receiver during ground verification testing will be representative of its operation in space.

The salt is contained around the HX tube by an exterior bellows. The bellows reduces the induced stress caused by differences in the thermal expansion of assembly materials and components. The operating life in space is predicted to exceed the 20 year Space Station requirement. The 24 heat storage tubes are cantilevered from the front end of the receiver to minimize the constraint of the axial growth. Each HX tube contains a smaller sealed tube to enable the internal convective heat transfer coefficient to be adjusted by changing the gas cross-sectional area. Gas flow is split to the 24 HX tubes by an inlet domed plenum and collected for return to the engine by an exit domed plenum. The plenum design minimizes the pressure drop, fabrication costs, and the constraint of the gas loop piping system.

Several significant advancements were made while developing SDHRT receiver fabrication methods and facilities including: (1) methods and a facility to cast molten salts into the full size heat storage tubes; (2) an improved electron-beam (EB) welded seal of the salt fill tubes; (3) a method to seal the TES by a laser weld of a thin bellows to a thick end-cap; and (4) a method of heat-treating the felt metal to remove contaminants and improve its wetability by the molten salt.

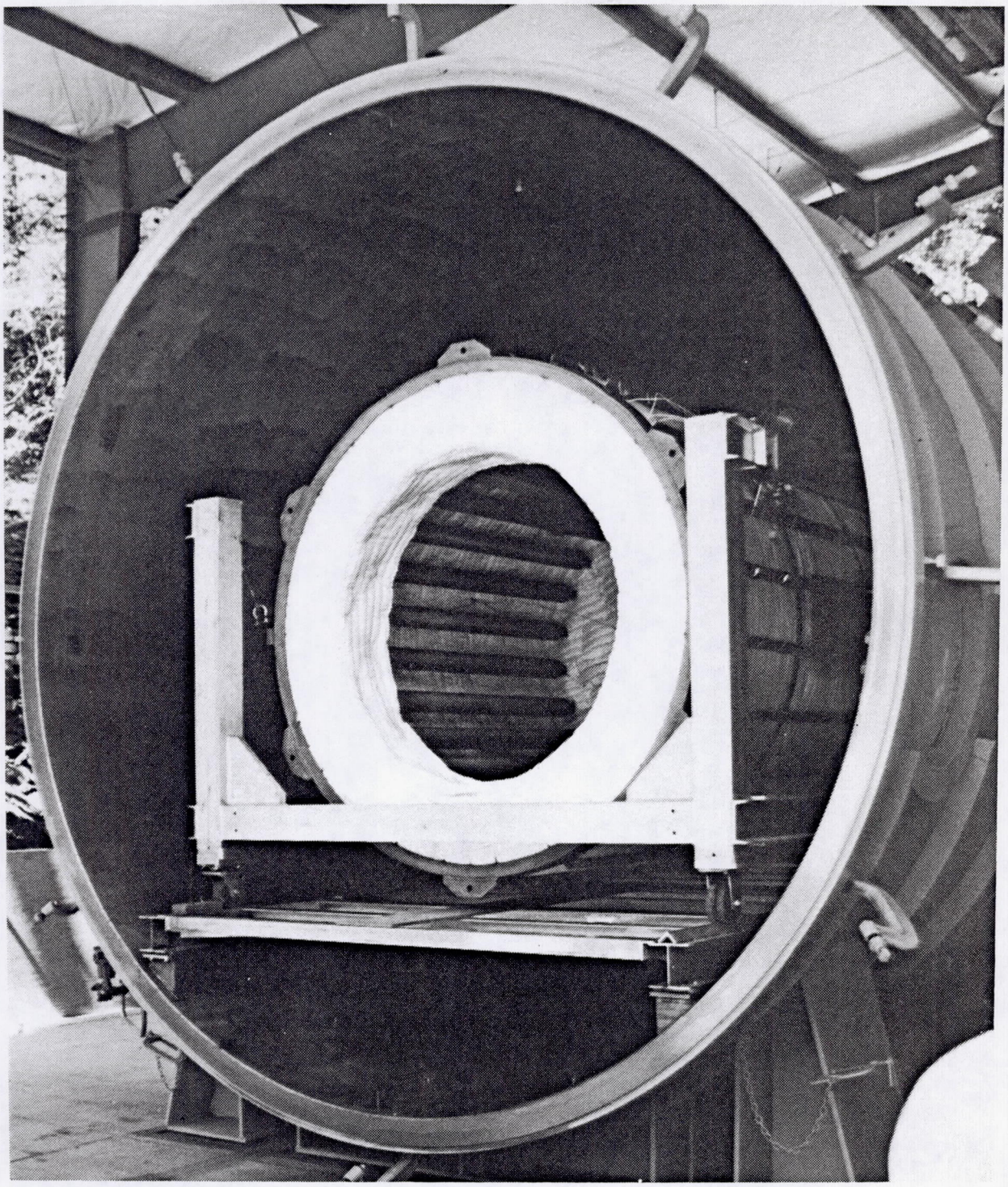

Figure 1-1: SDHRT SD Heat Receiver Ready for Test Assembly

The SDHRT receiver fabrication was completed in June of 1990, approximately 20 months later than originally planned. The most significant program delays resulted from (1) development of the laser weld seal of the bellows to the end-cap, (2) development of a reliable EB weld seal of the salt fill tubes, (3) an added requirement by NASA-LeRC to demonstrate a minimum 500 hour life of a heat storage canister prototypical of the full-size heat storage tube assemblies, and (5) molten salt filling of the receiver heat storage tubes with LiF-CaF_2.

The cost over-runs associated with these problems and their resulting delays caused NASA-LeRC to delete all of the verification testing from the SDHRT program and combine the testing into the NASA follow-on test program. This resulted in a more cost effective test program because all of the duplication in effort between the two programs was eliminated. The follow-on testing contract, NAS3-25716, is called the Advanced Development Receiver Thermal/Vacuum Tests With Cold Wall (ADRT).

All of the test hardware required for the testing of the SDHRT in a simulated low-Earth orbit (LEO) environment were designed and fabricated as part of the SDHRT program. The hardware items include (1) an engine simulator; (2) a 30 zone quartz lamp Sun simulator; (3) a receiver support structure to support the receiver inside the vacuum chamber; and (4) an aperture plug for the front end of the receiver that is integrated with the design of the quartz lamp heater. All of this hardware has been accepted by NASA-LeRC and has been transported to the test site. The hardware will be delivered to NASA-LeRC at the completion of the testing under the ADRT contract.

2.0 INTRODUCTION

An SD power module uses a reflective surface (the concentrator) to collect and focus solar energy onto HX surfaces (the heat receiver) that transfer the energy to a working fluid to drive an engine in a thermodynamic power cycle. SD electric power modules will be used to generate electricity for the U.S. Space Station Freedom, (reference 1). A closed Brayton cycle (CBC) using a single-phase, helium-xenon (He-Xe) gas mixture was chosen for the Space Station Freedom SD power modules. An SD power module used in space must also store energy to supply power when the spacecraft is eclipsed from the sun. Therefore, energy in excess of that needed by the power cycle is supplied by the concentrator during the sunlit period of orbit and is stored as latent and/or sensible heat for later use during eclipse. The heat receiver, due to its high operating temperature, cyclic solar energy input, and energy storage requirements is exposed to the most severe operating conditions of any of the SD power module components.

Early on in the Space Station program, key technologies were identified by NASA that would require development and demonstration prior to the design of the flight hardware. As part of this effort, an Advanced Development (AD) program was initiated by NASA-LeRC to develop a technology base to support the preliminary design of a flight qualified SD heat receiver. The Boeing Company was awarded the SDHRT contract, NAS3-24669, to design, fabricate, and test a full-size solar heat receiver to preliminary Space Station requirements. The work was performed during the period October 1985 through September 1990.

2.1 Program Objectives

The following program objectives were considered during the conduct of the SDHRT program:

1. Demonstrate that an adequate technology base exists to support the design and fabrication of a full-size heat receiver for Space Station application.
2. Provide experience to minimize the technical risks associated with the development, fabrication, and operation of heat receivers for flight operation.
3. Develop methods and provide experience to minimize the initial and life-cycle costs associated with the heat receiver component of a SD power module.
4. Demonstrate methods to maximize the reliability and life of a high-temperature SD heat receiver.
5. Develop tools and computer models to simulate and accurately predict the thermodynamic performance and component temperatures of the heat receiver operating in both a microgravity LEO environment and a 1-g simulated LEO environment.
6. Design a receiver that can operate in a 1-g simulated LEO environment and provide data that is representative of that which would be obtained if the same receiver were operated in space.
7. Provide a performance data base for the expected operating range of receiver interfaces and boundary conditions by testing the SDHRT heat receiver in a 1-g simulated LEO environment.
8. Correlate the measured receiver test data and the predicted thermal model data for the receiver operating in a 1-g simulated LEO environment.

2.2 Program Plan

The program plan was structured to be responsive to the SDHRT statement of work (SOW) as given in Part I, Section C of NAS3-24669. The work was implemented by specific contract task orders to:

1. Develop conceptual designs of different heat receiver and TES configurations for both a CBC and an organic Rankine cycle (ORC). Conduct trade studies to determine the CBC and ORC design concepts which best meet SDHRT program objectives (Task 1).
2. Identify and recommend the testing required for concept verification (Task 2).
3. Define/develop the required tooling and fabrication processes required for each of the conceptual designs (Task 3).
4. Perform detailed engineering design and analysis of both a CBC and an ORC receiver concept (Task 4). Only a single receiver will be chosen for fabrication and test.
5. Fabricate a single, full-size SD heat receiver and the required hardware to support the verification test program (Task 5).
6. Conduct component level demonstration tests and verification testing of the full-size heat receiver (Task 6).
7. Deliver the contract hardware to NASA and provide support for additional testing at a Government facility (Task 7).

The program was conducted within Boeing Defense & Space Group of the Boeing Aerospace & Electronics Division of The Boeing Company. The parent organization responsible for the program was Aerospace Systems Technology (AST), which is specifically structured to provide technical support from all functional areas on an as-needed basis, allowing the most cost effective program approach. The program organization is shown in Figure 2-1. The detailed program plan is documented in reference 2.

2.3 Program Overview

Work began on the SDHRT contract in November 1985 and the program was structured to be completed 36 months later in September 1988. However, problems were encountered during the receiver detailed design and fabrication tasks causing NASA to redirect contract resources to solve these problems. As a result, some of the original SOW tasks were eliminated from the scope of the SDHRT program and the program was extended by 24 months through September 1990. A brief history of the SDHRT program follows.

Conceptual designs of both ORC and CBC heat receiver were developed during Task 1. Barber-Nichols Engineering, located in Arvada, CO, was awarded a subcontract by Boeing to help develop the ORC receiver designs because of their experience from participation in several terrestrial ORC programs. A subcontract was also awarded to the Institute of Gas Technology in Chicago, IL to supply thermophysical properties of various TES materials for both sensible and latent heat storage systems. Methods of integrating the TES with the receiver were studied and analyses were conducted to quantify the performance of each of the conceptual designs. The testing requirements and fabrication issues associated with each concept were defined during test planning (Task 2) and fabrication planning (Task 3). These data were combined with the Task 1 trade study data to rank each of the receivers concepts by cost, performance, risk, and reliability. The results of these rankings showed several concepts to be competitive

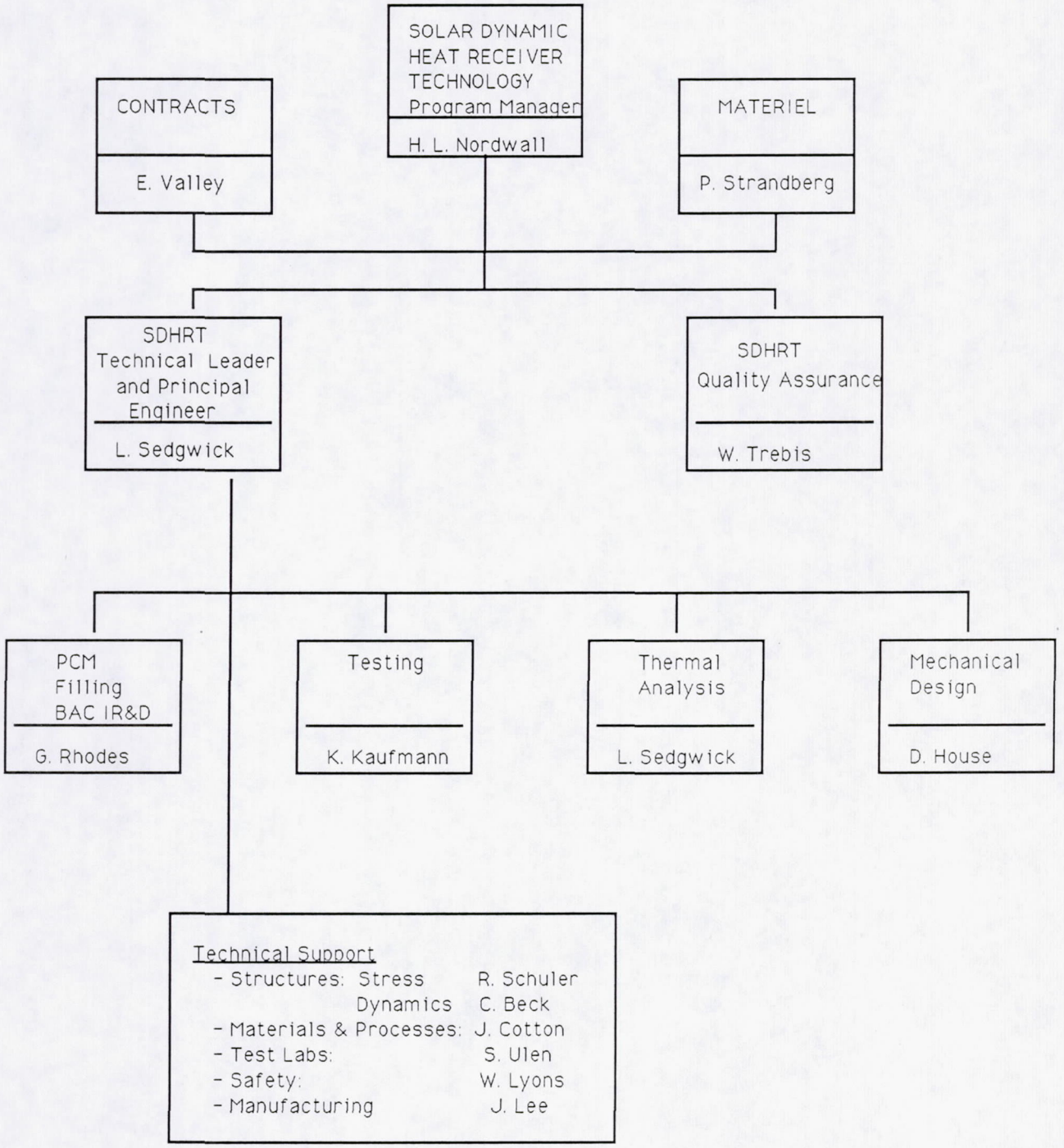

Figure 2-1: SDHRT Program Organizational Structure

in over-all ranking but that only a CBC receiver using parallel HX tubes with integral TES could be developed and fabricated with the available SDHRT funding. These data were presented to NASA at the SDHRT Preliminary Design Review (PDR) conducted in Cleveland, OH on 29 July 1986. The results of Tasks 1 through 3 are documented in the PDR data package, reference 3 and in reference 4.

After the PDR, direction was received from NASA-LeRC to continue with the detailed design of the parallel tube, integral TES CBC receiver concept but with 2 different heat storage materials; one using beryllium for sensible heat storage and the second using a eutectic mixture of LiF-CaF_2 as a phase change material (PCM). The program requirements used for the detailed design of the receiver are summarized in Figure 2-2 (references 5-10).

The beryllium receiver was chosen by NASA to eliminate some of the risks and design problems associated with latent heat energy storage systems. Beryllium can store thermal energy as sensible heat with a minimum temperature rise because it has a very high specific heat. Furthermore, its thermal conductivity is much larger than that of a fluoride salt, reducing temperature gradients and the resulting thermal stress. Problems associated with the large-density changes that occur in fluoride salts during phase change are eliminated. However, further study of a beryllium receiver revealed it had more difficult technical problems than those associated with the competing latent heat storage receiver designs.

Unacceptably high rates of sublimation of beryllium at operating temperatures in a space environment necessitated the use of a containment tube. No metallic elements were found to be compatible with beryllium at operational temperatures, therefore, a method to isolate the beryllium disks from the TES containment and HX tubes had to be developed. Beryllium oxide spacers were designed to support and separate the beryllium from the tube walls. A backfill of a highly conductive material was then required to reduce the increased thermal resistance of the resulting gaps. The beryllium had to be insoluble in the molten backfill material to prevent diffusion and subsequent interaction with the tube walls. Sodium was the most promising backfill material. However, a slight (approximately 1%) solubility of beryllium in sodium at 1500°F caused concern regarding eventual interaction with the containment alloy.

There are significant safety issues associated with handling and testing beryllium, beryllium oxide, and sodium at high temperature. Special facilities and procedures are required to mitigate the toxic hazards. Therefore, the cost of performing even simple compatibility tests was dramatically increased over those performed for a latent heat system. In addition, the beryllium raw material is very expensive as are beryllium manufacturing processes. Results of the beryllium study were presented to NASA-LeRC and it was recommended that further study and/or testing be cancelled. NASA-LeRC concurred with the Boeing recommendation and all activity related to this effort was suspended.

As the detailed design of the CBC heat receiver progressed during Task 4, SDHRT program resources were directed at the receiver components with the highest technical risks. The HX, thermal energy storage, and connecting piping encompass most of the heat receiver critical technologies. Two significant areas were not addressed because they were not required for ground testing the receiver in a vacuum chamber. The first is the design and maintenance of an aperture protection plate (thermal analysis of this component was conducted during Task 1). The long-term stability and life of this component must be addressed during a flight-design program. The second area not addressed directly by the SDHRT receiver is thermal control. The heat receiver is designed using an aphelion solar flux and end-of-life (EOL) concentrator optical properties, ensuring that sufficient energy is supplied to the heat engine during the entire life of the SD system. However, during a perihelion orbit at the beginning-of-life (BOL),

ORBIT PARAMETERS:	
Nominal Altitude	463 kM (288 miles)
Maximum Eclipse	36 minutes
Minimum Sun	58 minutes
Maximum Sun	66 minutes
Operational Life:	20 years
CBC Cycle Requirements:	
Working Fluid	Helium-Xenon gas (mol. wt. = 40)
Electrical Power To User	25 kW
Total Power Conversion η	24 %
CBC/Receiver Interfaces:	
Receiver Inlet Temperature	482°C (900°F) constant
Turbine Inlet Temperature	705°C ± 28°C (1300°F ± 50°F)
Receiver Inlet Pressure	630 kPa (92 psia)
Maximum Pressure Drop	5 %
Solar Environment:	1371 + 52 w/sq-m - 50 w/sq-m
Concentrator Properties:	
Reflectivity, ρ	0.95 beginning-of-life 0.90 end-of-life
Focal Length to Diameter Ratio, $\frac{f}{D}$	0.50
Intercept Factor, γ	0.95
Maximum Slope Error, σ	3 mrad

Figure 2-2: SDHRT Program Requirements Summary

approximately 45 kW-hrs of excess energy must be rejected by the SD module. It was shown during Task 1 that the choice of the most appropriate heat rejection method depends upon a total SD system performance and cost analysis. This was beyond the scope of the SDHRT program. It was decided that the capacity of the heat receiver to accommodate changes in the gas flow rate and inlet temperature measured during testing would provide a data base to quantify various thermal control options for the SD module.

Detailed thermal models of the heat receiver were developed to support the receiver and test hardware design during Task 4 (reference 11). Two separate models were created to simulate the receiver operating in either a space or a ground test environment. Performance data was generated for different receiver operating interfaces and natural environments. The ground test model was then used to design a cavity heater by matching predicted space data with predicted ground test data.

A number of component tests were conducted during Task 4 to demonstrate fabrication practices and performance of key receiver components (reference 11). These tests consisted of cycling sub-scale test canisters that were prototypical of full-size receiver heat storage tubes except for length. The canisters were cycled above and below the melt temperature of LiF-CaF_2. The purpose of the canister testing was originally to be concept verification but gradually they evolved into a life demonstration test. Several significant deficiencies were corrected in the design of the receiver heat storage tubes as a result of these tests, however, these tests caused a extension in the contract period of performance of about 13 months to December 1989. Delivery of the receiver, originally scheduled for February 1988, was delayed until October 1989. Contract funding was also increased to cover the additional costs associated with the component life testing and heat storage tube redesign efforts.

Tests to quantify the long-term compatibility between receiver alloys and molten LiF-CaF_2 were also conducted (reference 11-12). Small capsules were fabricated from candidate receiver alloys. A small amount of LiF-CaF_2 was loaded into each. Some of the capsules also contained metal felts of various alloys (the felt metals are used for thermal conductivity enhancement and void management through the salt). The capsules were heated to 871°C (1600°F) and held at temperature for up to 2500 hours. The capsules were then sectioned and metalographic analyses were conducted to look for evidence of interaction. These tests showed that the receiver high-temperature alloy, Inconel 617, was compatible with the LiF-CaF_2 salt in the molten state.

The detailed design effort was completed with a two-stage, Critical Design Review (CDR). Both of the CDR meetings were held at Boeing. The first CDR was conducted on 12 January 1988 and reviewed the receiver structure and pressure piping components and fabrication. A second CDR was held on 11 May 1988 to review the design of the heat storage tubes. Documentation of the entire detailed design effort is given in the SDHRT Design Analysis Report (DAR), reference 11.

Task 5, receiver fabrication, was begun with the procurement of long-lead materials with final authorization to proceed with the procurement received in October 1987. Authorization to proceed with the fabrication of the receiver structure and pressure piping components was given by NASA-LeRC shortly after the first CDR meeting in January 1988. The authorization to proceed with the fabrication of the receiver heat storage tubes was delayed until 23 September 1988; after 500 hours of canister cycling had been completed using the canister that had the design modifications made to correct problems associated with sealing the PCM containment.

The fabrication of the receiver, documented in section 4, proceeded smoothly until the operation to fill the heat storage tubes with molten LiF-CaF_2 at 927°C (1700°F). A special facility was designed and built by Boeing to cast molten salts into multiple, full-size heat storage components. The molten salt fill facility was demonstrated by successfully casting molten LiF-CaF_2 into a single full-size heat storage tube prior to attempting to fill SDHRT receiver hardware. However, the first 2 attempts to fill SDHRT receiver tubes, 6 at-a-time, failed to move salt into the containment volume and damaged the first 6 heat storage tubes (a more detailed description of this operation is given in section 4.2). Several iterations were required before problems with the salt and with the facility design were corrected. The molten salt filling problems caused an additional delay in the delivery of the heat receiver of 8 months, to June 1990 and resulted in a significant projected program cost over-run.

During Task 6, all hardware required to perform verification testing of the SDHRT heat receiver were designed and fabricated including (1) a CBC engine simulator; (2) a 30 zone quartz lamp Sun simulator; (3) a receiver support structure to support the receiver inside the vacuum chamber; and (4) an aperture plug for the front end of the receiver that is integrated with the design of the quartz lamp heater.

Changes in the availability of Government vacuum facilities prompted NASA to competitively bid the follow-on test program it had intended for the SDHRT heat receiver after completion of the SDHRT program. Boeing was awarded the ADRT contract by NASA-LeRC (NAS3-25716) in October 1989. Many of the ADRT test support equipment (TSE) set-up operations, TSE checkout operations, and receiver verification test modes duplicated those already defined during SDHRT test planning. A more cost effective approach was taken by NASA by performing the SDHRT test conduct tasks only once as part of the new ADRT test contract. This allowed all remaining SDHRT resources to be used to complete the fabrication of the heat receiver and the test support hardware (with the exception of a receiver cold shroud added to meet additional requirements of the ADRT program). The elimination of test set-up and conduct tasks from the SDHRT contract SOW allowed the SDHRT program to be completed with available funding.

The receiver and test hardware were delivered to NASA-LeRC at the Boeing Tulalip Test Site for testing under the ADRT contract in June 1990. Delivery of this final report completes the deliverable requirements of the SDHRT program.

2.4 Scope of Final Report

The SDHRT Final Report provides a summary description of the receiver and test support hardware configurations. A complete description of the receiver detailed design effort was already provided in the DAR (reference 11) and is not repeated here. The SDHRT Final Report also provides a detailed summary of the fabrication histories of the heat receiver and test support hardware. All of the heat receiver test set-up and conduct deleted from the SDHRT SOW will be documented separately in the ADRT Final Test Report when testing is completed in October 1990.

3.0 SDHRT CBC RECEIVER DESCRIPTION

The general configuration of the SDHRT SD heat receiver is illustrated in Figure 3-1 and dimensions are listed in Figure 3-2. Note that the receiver is shown without a front aperture cover. The receiver component and subsystem details are given the SDHRT fabrication drawing package, 180-60270, summarized in the drawing tree shown in Figure 3-3. A brief description of each of the receiver subsystems and components follows.

The HX and TES subsystems are integral and are comprised of 24 parallel tube assemblies. Each tube assembly consists of an inner HX tube surrounded by an annulus containing a PCM used to store energy. The PCM is contained by an outer corrugated tube that is sealed by welding at 2 end caps. The PCM is introduced into the TES assembly in the molten state through small PCM fill tubes in the end caps. The PCM tubes are sealed after filling by an EB weld made in vacuum. The HX tubes, corrugated TES containment tubes, end caps, and PCM fill tubes are all fabricated from Inconel 617, a nickel-based superalloy (reference 13-14). Inconel 617 is also the alloy recommended for use in a flight application. Inconel 617 was chosen over other candidate super-alloys because of its good creep properties, smaller thermal expansion coefficient, lower cost, compatibility with candidate TES materials, and availability (reference 11).

3.1 Thermal Energy Storage Concept

The PCM used in the SDHRT receiver is a mixture of 82_aLiF and $18_a$$CaF_2$ (atomic %). The mixture is slightly rich in LiF (with respect to the eutectic mixture) to ensure that all of the CaF_2 combines with LiF at the eutectic to prevent collection of solid CaF_2 during the salt filling process (described in section 4.2). Energy is stored in the salt as latent heat by changing its phase from solid to liquid. The energy is liberated and transferred to the working fluid during solidification back to the solid phase. The melting temperature of the eutectic mixture is approximately 771°C (1420°F), ideal for the CBC cycle requirements, and its latent heat of fusion, 816 kJ/kg (351 BTU/lbm), is among the highest of candidate materials (references 15-18).

Fluoride salts, such as LiF-CaF_2, are capable of storing a large amount of energy per unit mass but are very poor conductors of heat. Salt thickness must be kept thin to limit TES containment temperatures and achieve the desired operating life. Thus, the receiver size and the number of tube assemblies must increase as salt conductivity decreases. In addition, the density of LiF-CaF_2 increases substantially during solidification causing the formation of voids. Voids further decrease the effective thermal conductance through the salt, and their location is critical to the performance of the TES because salt void distributions in 1-g and microgravity environments may be quite different.

The gravitational force present during ground testing can cause molten salt to migrate into the voids located in the lower regions of the TES volume. The resulting region of solid salt can potentially damage or fail a containment structure by its expansion during subsequent remelting. In addition, the single large void that results in the upper regions of the TES containment volume can cause TES containment temperatures to rise above design values because higher temperatures are required to transfer the same quantity of energy by radiation across the gap. During space operation, the gravitational force is negligible and salt behavior may be quite different and, hence, ground test data for such a design would not represent that obtained during space operation.

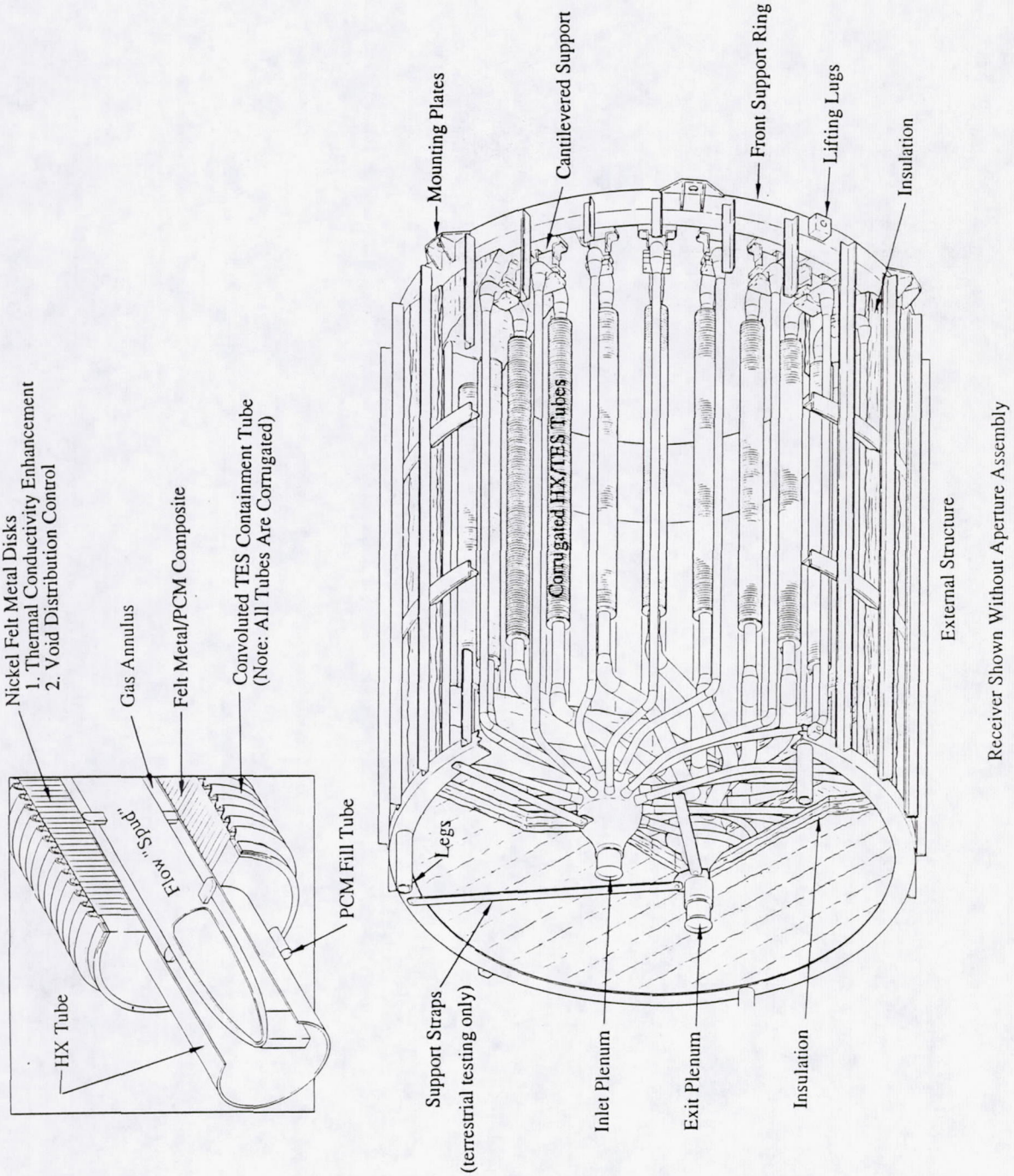

Figure 3-1: SDHRT Receiver Configuration

SUBSYSTEM	COMPONENT or PARAMETER	DIMENSION (mm)	DIMENSION (in)
Receiver Cavity	Cavity Diameter	1778	70
	Cavity Length	2032	80
	Receiver OD	2184	86
	Total Receiver Length	2794	110
	Aperture Diameter	330	17
Heat Exchanger (HX)	HX/TES Tube Centerline Diameter	1575	62
	HX Tube OD	51	2
	Spud Tube OD	25	1
	HX Tube Wall Thickness	1.5	0.06
Corrugated TES Containment Tube	Wall Thickness	0.25	0.01
	Convolution OD	100	3.94
	Convolution ID	91	3.58
	Convolution Pitch	6.4	0.25

Figure 3-2: SDHRT Receiver Dimensions

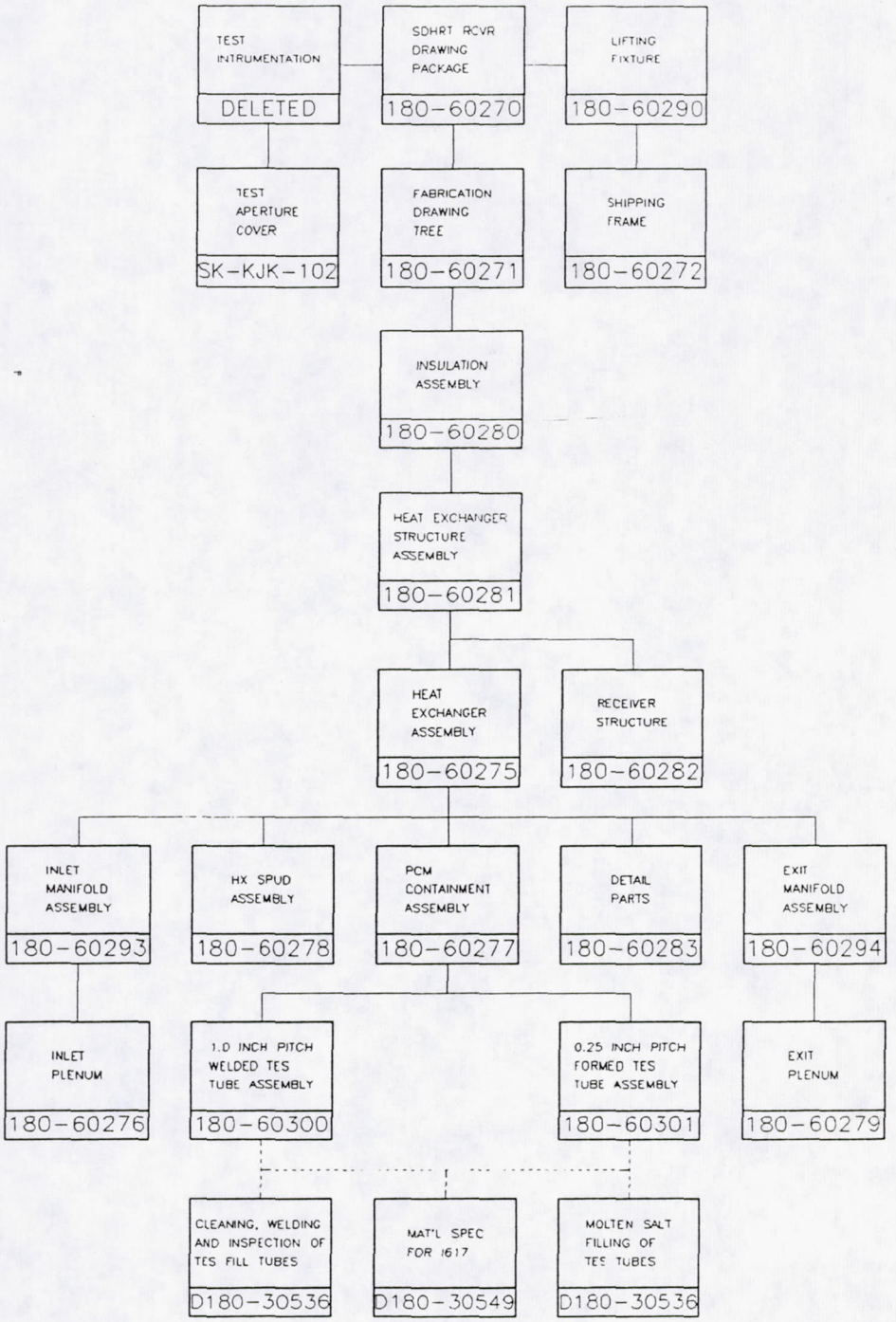

Figure 3-3: SDHRT Receiver Fabrication Drawing Tree

To circumvent these problems in the SDHRT test receiver, a nickel felt metal mesh is contained inside the TES annulus and is integral with the salt. Felt metal consists of a matrix of many small wires, which are rolled to a specified density and sintered together at high temperature. The sinter bonds develop where individual wires cross, forming small pores within the matrix.

Introduction of the nickel felt increases the effective thermal conductivity of the salt by roughly a factor of 3. Thus, more PCM can be contained within a given heat storage tube assembly reducing the number of components in the receiver. Felt metal also influences the distribution of voids in the solid phase and prevents gravitationally induced migration of molten salt by the surface tension force that occurs between the salt and felt metal.

The felt metal was chosen with an effective pore radius sufficiently small to suspend (wick) molten salt by a capillary force that develops with wetting of the felt metal surfaces. The felt metal used in the SDHRT receiver has a mean wire diameter of about 20 microns and has a porosity of about 80% (20% volumetric density). Wire surfaces must be kept very clean to ensure complete wetting by the salt (reference 11 and 19). When "wicking" of the salt is achieved, the force developed by surface tension is greater than the gravitational force, preventing gravitationally induced migration of liquid salt into void regions. The nickel felt metal was chosen to wick molten LiF-CaF_2 to a height approximately equal to the diameter of the heat storage tube assemblies (approximately 102 mm). Therefore, the receiver is tested in a near-horizontal orientation to obtain the full advantage of the felt metal and to obtain ground test data that is representative of space performance data.

Gravity-induced salt flow is prevented by the capillary force between the salt and the felt metal but this force causes another type of molten salt migration to occur during solidification of the salt. The capillary force is inversely proportional to an effective pore radius, initially that of the felt metal. As the salt solidifies inside the felt matrix, smaller pores are created in the salt itself thereby increasing the surface tension force in the region of the phase front. This causes molten salt to be drawn into the solidification voids (solidification wicking). Thus, as heat is removed from the inner HX tube, salt is drawn radially inward forming a very dense region of salt around the inner HX tube and a region on the outside of the TES containment that is primarily void of salt. A small amount of salt may concentrate on the inside surface of the TES containment tube because of heat losses but the amount of salt will be small because the losses are negligible compared to the rate of heat transfer to the gas during eclipse. Upon reacquisition of the sun (or heater power during ground testing), heat is transferred inward through the felt metal and, as the salt melts, it flows radially outward towards the heated surface. This phenomena will occur when operating in either a space or a 1-g environment. Thus, the goal to obtain usable ground test data is achieved, and correlation of the receiver thermal models allows a direct extrapolation of terrestrial test data to microgravity space operation.

The use of a fluoride salt compound as a heat storage material requires careful processing controls to ensure that no contaminants are introduced during filling or handling operations. Exposure testing of molten LiF-CaF_2 at 871°C (1600°F), Inconel 617, and the nickel felt have demonstrated compatibility between these materials if the system is kept very clean (reference 11). Therefore, contamination of the TES system before, during, or after filling with salt must be prevented. The felt metal allows the PCM to be contained in a single storage compartment per tube reducing the number of filling operations required to complete the fabrication process. The felt metal in the TES annulus requires that the heat storage tubes be filled with the salt in a molten state. Boeing developed a dedicated molten salt filling facility to fill the heat storage tubes (see section 4.2). The tubes are filled with molten salt at 927°C (1700°F) to ensure sufficient volume for the molten salt during all defined operating scenarios.

3.2 Heat Storage Tube Configuration

Thermal stresses are induced by temperature gradients within the tube assembly. The primary temperature gradient results from driving the thermal energy through the salt/felt metal composite to the HX tube and working fluid. The design temperature difference between the outer TES containment tubes and inner HX tubes is 83.3°C (150°F). Therefore, the outer tubes expands more than the inner tubes and, because the system is constrained by the end-caps, compressive stresses are induced in the tube assembly components. A second type of thermal stress results from a variation in the temperatures around the circumference and along the axis of the tube assembly. These "hot-spot" stresses are caused by the expansions of the material located in hot regions being constrained by the surrounding material in the cooler regions. Hot-spot temperature gradients result from the following effects:

1. Concentrator design characteristics and surface imperfections.
2. Blockage by receiver components and surface orientation.
3. Differences in the axial distance of receiver surfaces from the concentrator focal point at the aperture.
4. Differences in the working fluid temperature (rate of energy removed) along the length of the HX tube.

A corrugated TES containment tube is used to reduce the constrained stiffness of the outer tube and resulting in less stress being induced into heat storage tube components by the differential expansions. The corrugations act like a spring to accommodate deflections. A "formed" bellows is used as the corrugated tube. The convolutions are individually formed on a single length of cylindrical tubing. The entire corrugated tube is inserted over uniform-sized felt metal disks stacked onto the inner HX tube. A small gap results between the OD of the felt metal disks and the inner diameter (ID) of the corrugated containment tube. The convolution radius is kept small (about 1.6 mm) to minimize the volume of the gap, and the number of corrugations is increased to reduce the stress in the convolutions. The inside of the TES annulus showing the felt metal/salt composite and convolutions gaps is shown in Figure 3-4. This section was taken from one of the first test components and does not show a representative bellows to end-cap termination. Thermocouples can also be seen inside the annulus.

The ends of the convoluted tube are straight to facilitate connection and sealing to the end-caps. Two thick rings are interference-fitted to the outside and inside of the straight section ends of the convoluted tubes to increase the thickness for welding to the end-caps as shown in Figure 3-5. The tube ends are welded at 2 locations on the end-cap forming a redundant seal of the TES annulus. The first seal is provided by a full-penetration weld of the corrugated tube end-face to the outside faces of the end-caps. Fabrication experience showed that small cracks develop in the weld region and can extend between the inner and outer bands causing a leak path for the TES material. This is illustrated in Figure 3-6. Therefore, a 2nd seal is provided by a radial laser weld through the side of the corrugated tube end; through the outer weld band, the convoluted tube wall, the inner weld band, and into the side of the end-cap. This weld configuration has demonstrated a 100% acceptance by helium leak checking all of the seals made by this method. The weld seal of the bellows to the end-cap is also illustrated in Figure 3-7.

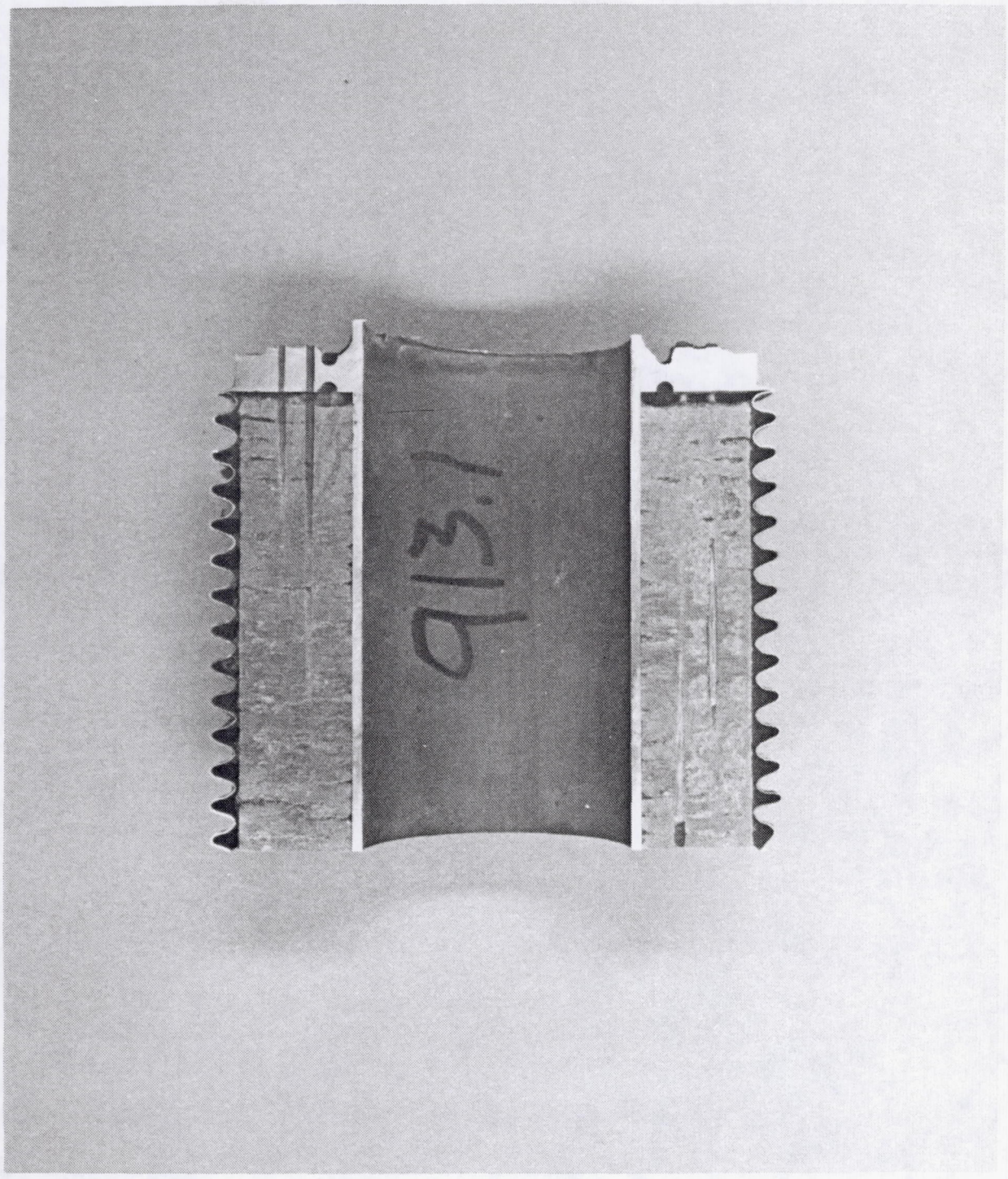

Figure 3-4: Salt/Felt Metal Composite Inside the TES Annulus of Test Canister TC4

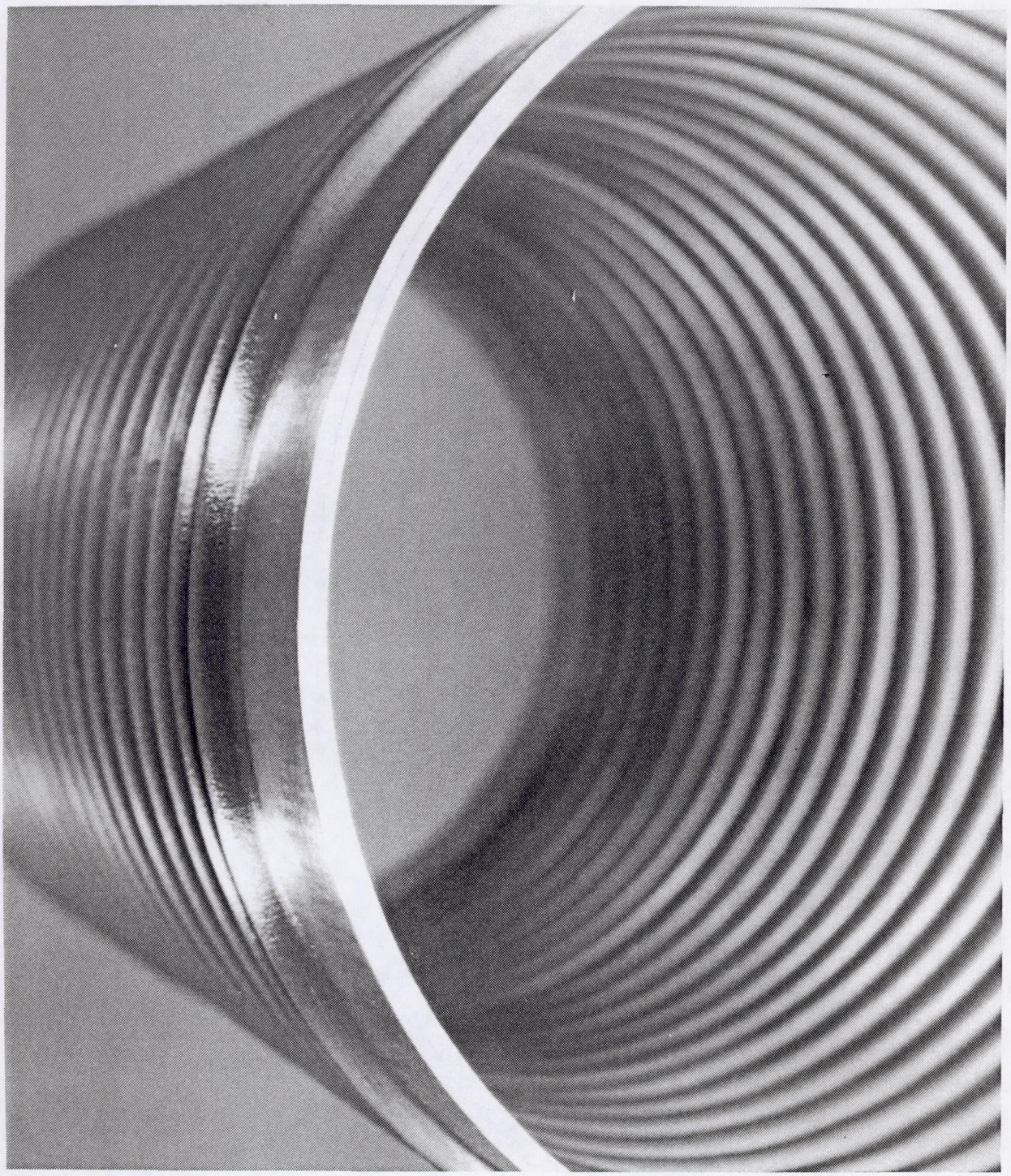

Figure 3-5: Inner and Outer Weld Rings Installed on the Straight Section of Bellows for Termination Weld to End-Caps

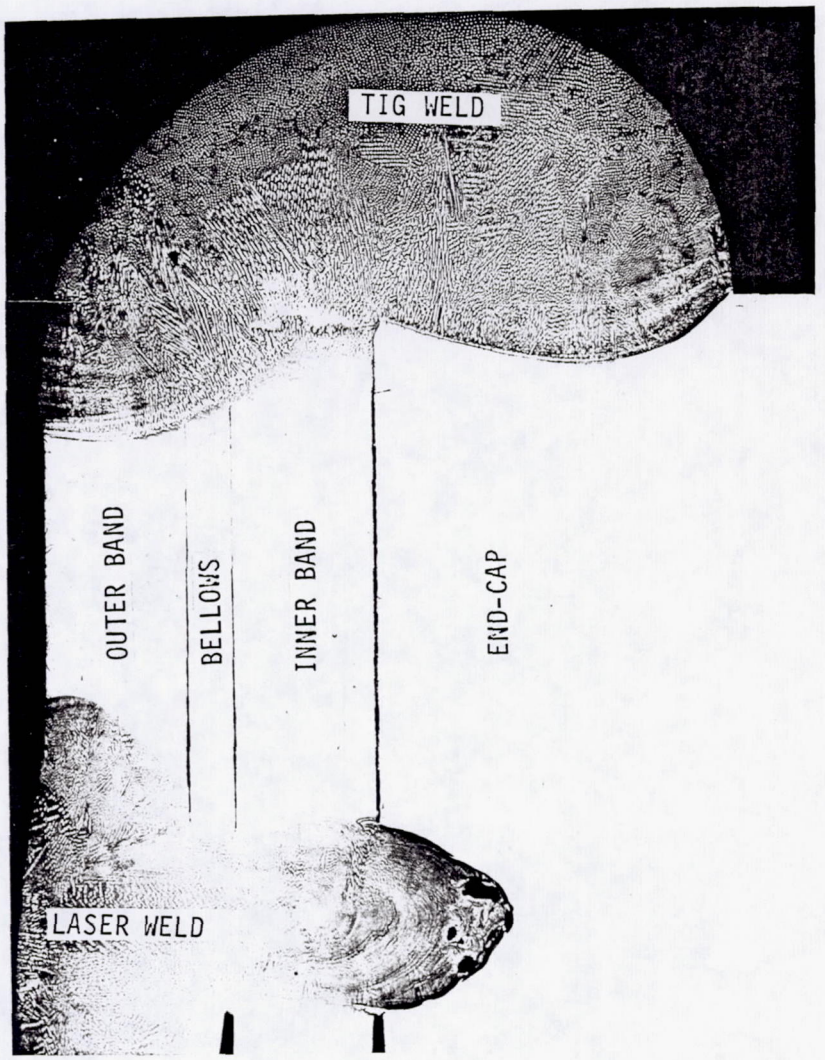

Figure 3-6: Bellows to End-Cap Termination Weld Configuration

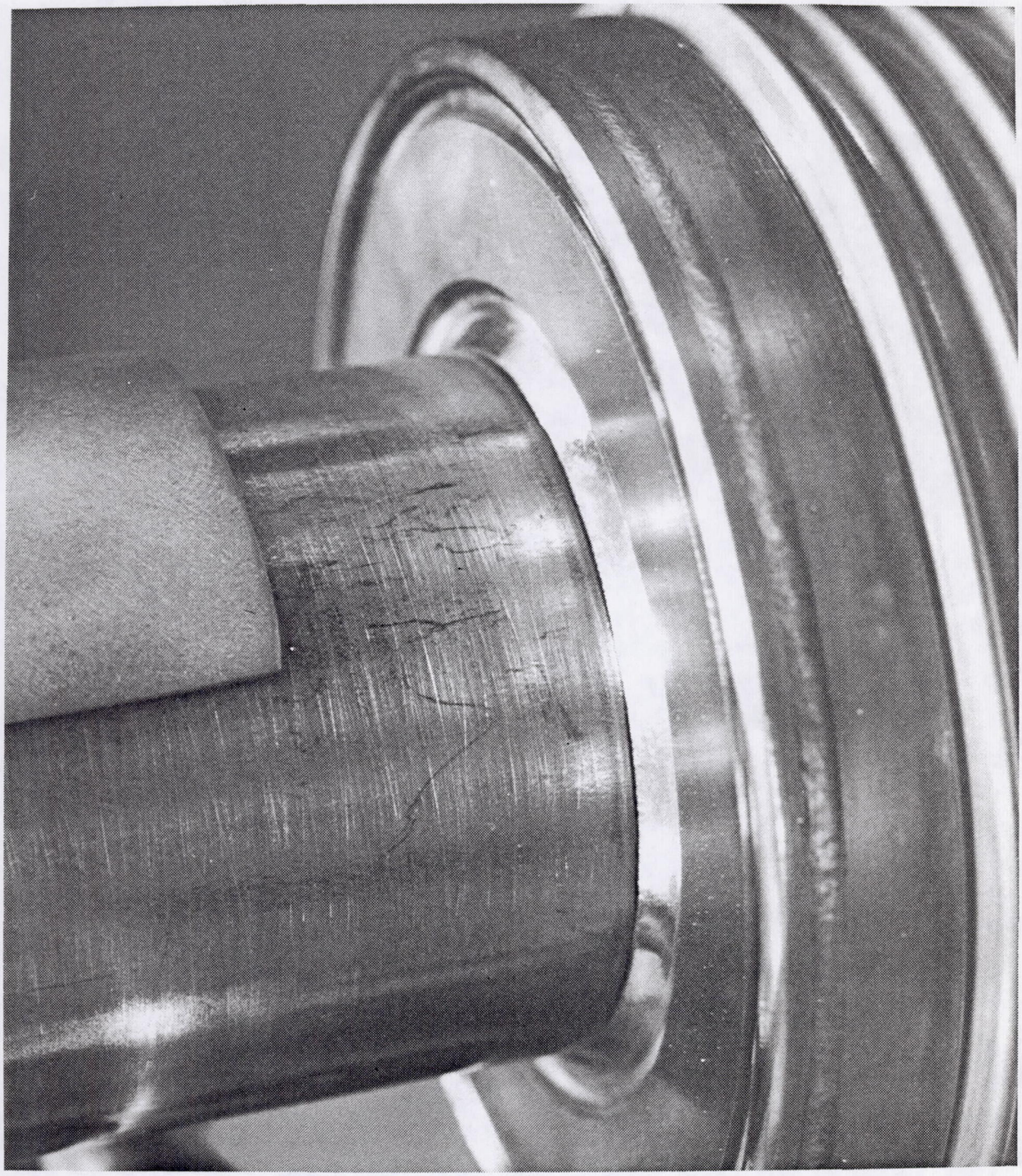

Figure 3-7: Close-up of Bellows to End-Cap Termination Weld Region on Test Canister TC9

The thermal and mechanical behavior of the convoluted tube assembly was demonstrated using small-scale canisters identical to the full-size heat storage tube assemblies except for length (1/6 scale). The canisters were cycled above and below the melt temperature of the salt (771°C) by 25°C (45°F) and 72°C (130°F) respectively. The objectives of these tests were to demonstrate (1) the felt metal void control and thermal conductivity enhancement and (2) the mechanical performance of the convoluted TES containment design including the seal at the end-caps. These tests are described in detail in reference 11. In all, 9 different canisters were tested. The symmetrical control of void distribution in the solid salt by the felt metal was confirmed by observing nearly identical thermal behavior at the top and bottom of the canisters (canisters tested in a horizontal orientation) and by obtaining nearly identical weights from sections obtained from both the top and bottom regions of the canisters. The measured temperature gradients matched prediction using the enhanced thermal properties of the salt/felt metal composite demonstrating the improvement in heat transfer characteristics through the felt metal/salt composite. The tests also demonstrated the reliability of the seals at the end-caps and as well as the EB weld seal of the PCM fill tubes. The last canister tested, TC9, is shown in Figure 3-8.

A large-diameter HX tube is used to support the entire length of the HX/TES tube assembly during ground testing. This eliminates the need for mechanical attachment along its actively heated length. The required rates of gas-side heat transfer are obtained by forming a flow annulus with a sealed "spud" assembly located in the center of the HX tube (see insert on Figure 3-1. The full-size spud and heat storage tube are shown in Figure 3-9. The reduced cross-sectional flow area increases gas velocities, and convective heat transfer is enhanced. Gas-side heat transfer significantly effects the peak surface temperature of the TES containment tube. Use of the flow spud allows "tuning" of the gas-side heat transfer without a complete redesign of the HX/TES tube assembly. The spud is cantilevered from the inlet end of the tube and is supported along its length by small standoffs. It does not support significant load and is, therefore, fabricated from 316 stainless steel. The spud assembly is sealed under vacuum to prevent contamination from being introduced during fabrication and hydrostatic testing.

3.3 Gas Distribution and Pressure Piping Network

Domed, cylindrical plenums are used to distribute the gas flow to and from the HX tubes. Pressure-drop variations in the plenum are expected to be small because flow velocities are low and should be mostly uniform. Slight differences between the lengths of piping that connect the HX tubes to the plenums do produce a small difference in pressure drop in these piping runs. However, analysis has shown that no flow orifices are required to regulate the gas flow between HX tubes. If testing shows a significant flow variation to exist, the large diameters of the plenums (102 mm at the inlet and 203 mm inside) allows flow orifices to be installed at a later date. This is a significant advantage over a torus type of flow distribution system. In addition, the domed plenums are much less expensive to fabricate than an equivalent torus system. The total pressure drop across the receiver is estimated to be only 2.5% of the inlet pressure at 634 kPa (92 psia).

Piping runs that connect the HX/TES tube assemblies with the inlet and exit plenums are located outside the active flux regions of the cavity and operating temperatures are lower than those experienced by the HX/TES assemblies. This is also true for the plenums. This allows 316 stainless steel pipe to be substituted for Inconel 617 in the SDHRT test receiver to significantly reduce cost by allowing off-the-shelf pipe fittings to be used. Schedule 40 piping components and schedule 80 plenum components are used to meet the ASME Boiler and Pressure Vessel Code requirements even though the SDHRT receiver will be tested for less than 1000 hours. Piping that connect the inlet gas plenum to the inlet of the HX tube is 25.4

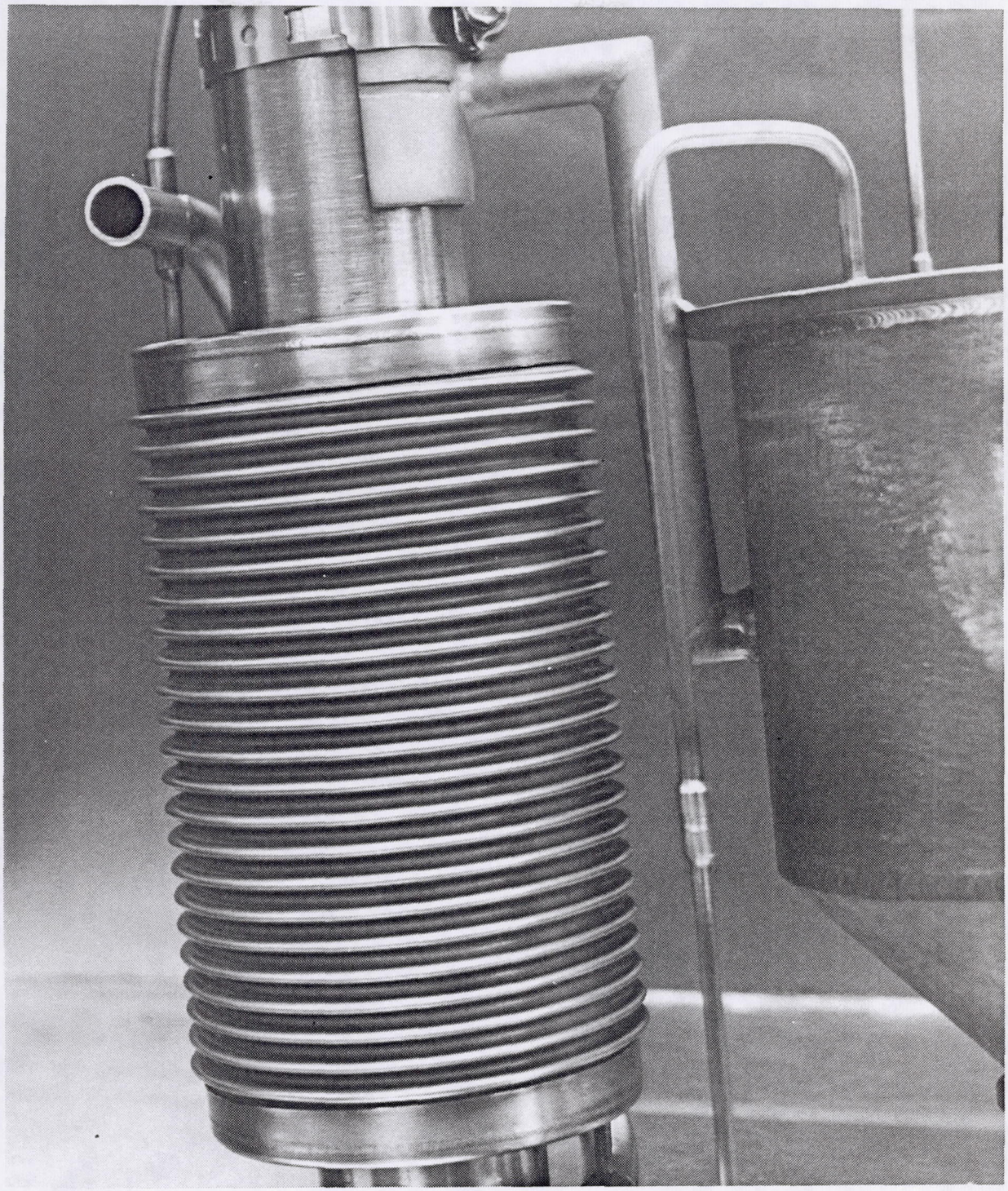

Figure 3-8: Test Canister TC9 Ready for Molten Salt Filling

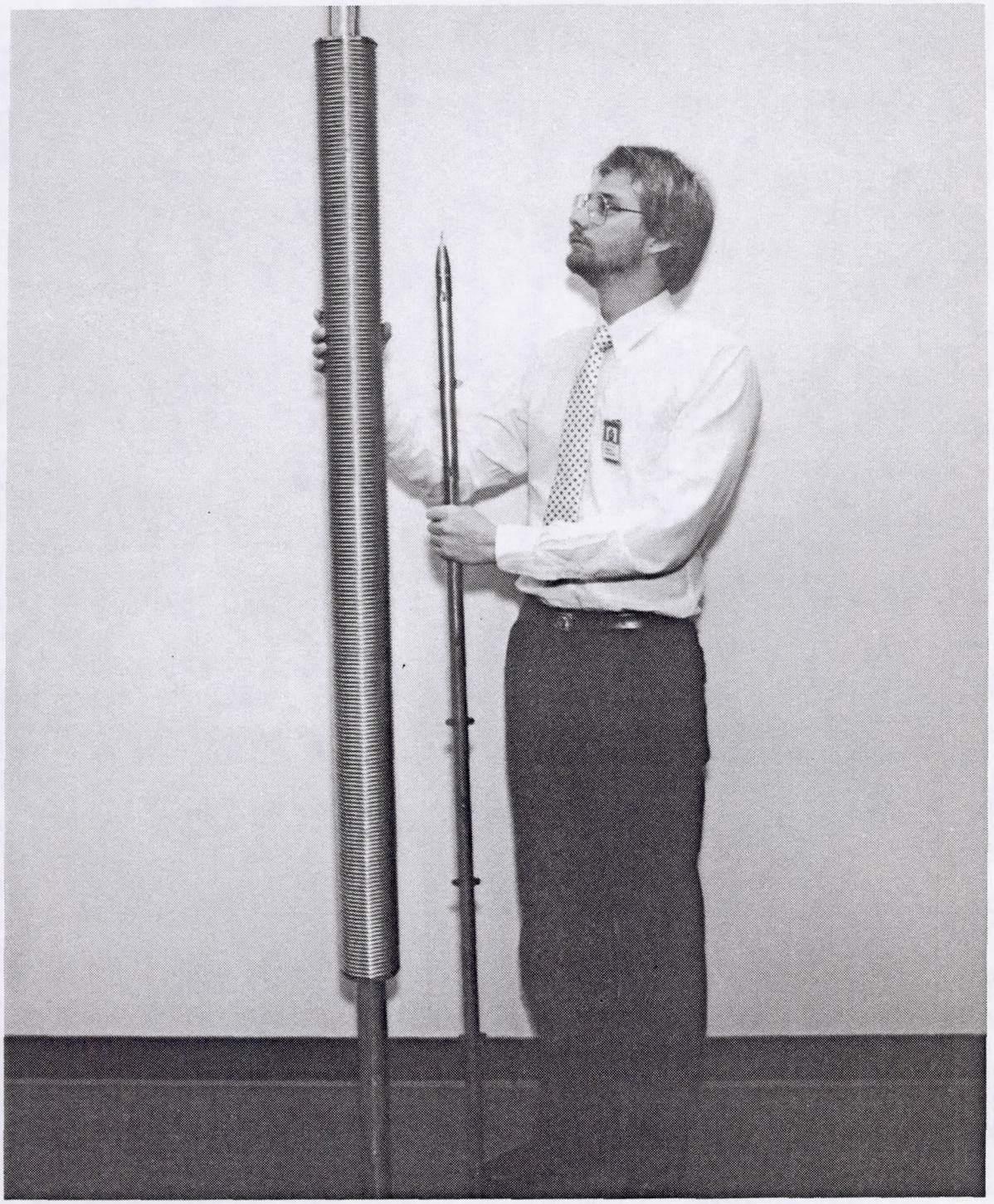

Figure 3-9: Full-Size Heat Storage Tube and Flow Spud Assemblies

mm (1 in) in diameter except for a short section that transitions between the 25.4 mm (1 in) diameter stainless steel pipe to the 51 mm (2 in) diameter Inconel 617 tube. The small diameter inlet pipe was used to allow them to be located between the inner cavity wall and outer structure of the receiver with minimal interference. The exit end of the HX tube transitions between 51 mm (2 in) diameter, Inconel 617 tube and 51 mm (2 in) diameter stainless steel pipe. The 51 mm (2 in) pipe runs are used to connect to the exit plenum because they require more strength at the higher gas temperatures. In a flight configured heat receiver, these plenums and the pressure piping system would be made of Inconel 617 which would significantly reduce the receiver weight.

3.4 Receiver Structure

All receiver components expand during heat-up from a cold soak condition. Constraint of this expansion must be avoided because it can cause excessive stress to develop in receiver components. The piping network of the receiver is structurally supported only at a front structural ring, allowing independent thermal growth of heat exchange and structure components with a minimum of constraint. The single support attachment of the heat exchange system not only reduces induced stress but improves receiver efficiency by reducing heat loss paths to the environment.

In addition to supporting the heat exchange system, the front support ring is also used for lifting the receiver (vertically or horizontally) and to support a "sun simulator" heater assembly for thermal vacuum testing. The support ring is formed from a 102 X 102 X 10 mm (4 X 4 X 3/8 in) rolled 316 stainless steel angle. Ring stiffness is increased by welding a 10 mm (3/8 in) thick rolled plate on the top side of the angle. Each of the 24 HX/TES tube assemblies attaches to the support ring by a saddle clamp structure (see Figure 4-21).

Additional support of the piping network is provided by three support straps, which attach the inlet and exit plenums to a rear support ring. These straps are only required during ground testing of the heat receiver and do not significantly constrain the axial displacement of the heat exchange system during heat-up. The rear support ring is formed from a 76 X 76 X 10 mm (3 X 3 X 3/8 in) rolled 304 stainless steel angle and is also used for lifting of the receiver (horizontally).

A structural shell is formed by connecting the front and rear structural rings with small 38 X 38 X 5 mm (1.5 X 1.5 X 3/16 in) angles. Additional stiffness is introduced by two mid-span rolled ring supports made from 51 X 51 X 6 mm (2 X 2 X 1/4 in) structural T sections.

All of the receiver outer structure is fabricated from 304 stainless steel to provide adequate structural strength to support the gravitational static weight loads at the higher temperatures, which would have resulted from the operation of the receiver in an uncooled vacuum chamber (ADRT testing will be conducted with a cold shroud). Therefore, a significant weight penalty exists that would not be present for a receiver designed for flight application. A flight design of the SDHRT receiver would use lighter weight materials such as aluminum for the outer structure, and the size and number of structural elements could be substantially reduced because launch and gravity loads will be supported at cool temperatures (high design allowables).

3.5 Receiver Insulation

An alumina-silica refractory fiber insulation, Manville Cerablanket, is used throughout the receiver. This insulation was chosen based upon cost, availability, and performance. It can be used in a vacuum chamber because it contains no organic binders and will not off-gas (other than water vapor) at the high temperatures. The insulation is sewn into a blanket using high-temperature quartz fabric backing and both quartz and stainless steel threads. The blanket

configuration simplifies assembly and provides the radiating cavity surface properties needed for redistribution of solar energy. Optimization of insulation type, density, and thickness has not been done for the SDHRT test receiver. Such an optimization would also reduce the weight of the SDHRT receiver in a flight configuration.

3.6 Receiver Performance Summary

A summary of the SDHRT receiver thermal performance in a flight environment is given in Figure 3-10. These data were derived from the results of the detailed thermal analyses described in reference 11. The calculation of receiver efficiency includes both thermal losses and an increased heat input required to compensate for sensible heat storage in the receiver.

Stress analysis of the HX/TES tube assemblies shows an operating life in excess of the required 10 years. Other receiver components, such as the plenums and connecting piping, are conservatively designed to greatly exceed a 1000-hr test life.

A weight summary of the SDHRT test receiver is given in Figure 3-11. The weight of an aperture protection assembly is not included. Weights shown for a flight configuration are preliminary estimates based upon design of the receiver for operation only in a microgravity environment.

Total Solar Input to Receiver:	184.9 kW
Minimum Receiver Efficiency:	91.3%
Maximum Receiver Thermal Loss	13.7 kW or 7.4% of total
Reflection	0.8 kW or 0.4% of total
Reradiation	9.0 kW or 4.9% of total
Conduction through insulation	3.9 kW or 2.1% of total
Sensible Energy Storage	2.4 kW or 1.3% of total
Temperatures (nominal quasi-steady operation)	
Control of Turbine Inlet Temperature	705°C (1300°F); -9°C (-15°F) +16°C (30°F)
Maximum TES Containment Temperature	896°C (1645°F)
Maximum TES Temperature Gradients	
Circumferential	72°C (162°F)
Axial	116°C (241°F)
Maximum Heat Exchanger Tube Temperature	822°C (1512°F)
Maximum Insulation Temperature	955°C (1751°F)
Pressures	
Pressure Loss	2% of Inlet
Maximum Variation Between HX Tubes	0.4%

Figure 3-10: Predicted SDHRT Heat Receiver Performance Summary (Flight)

RECEIVER SUBSYSTEM OR COMPONENT	SDHRT WEIGHT		FLIGHT WEIGHT	
	(kg)	(lbs)	(kg)	(lbs)
HX/TES Heat Storage Tubes:	759	1673	759	1673
PCM/LiF-CaF_2	319	703	319	703
Nickel Felt Metal Discs	298	657	298	657
TES Containment	46	101	46	101
HX Tubing	96	212	96	212
Receiver Insulation	454	1000	227	500
Heat Exchanger Tubing/Pipe	338	745	49	108
Inlet and Exit Plenums	82	181	82	90
Receiver Structure	545	1202	272	600
TOTAL RECEIVER WEIGHT	2178	4801	1389	2971

Figure 3-11: Predicted SDHRT Receiver Weight Summary

4.0 RECEIVER FABRICATION

The fabrication and assembly of the SDHRT solar heat receiver was performed to the requirements specified on the SDHRT drawing set, 180-60270, approved, in writing, by the NASA program manager. The procurement of raw materials, component fabrication, and assembly of the receiver were competitively bid and subcontracts were awarded based upon cost, technical competence, schedule, and reduction of risk. A list of the suppliers of receiver raw materials, components, and/or assemblies is given in Figure 4-1.

Quality assurance (QA) was maintained throughout the program using the Developmental Record System (DRS) as described in the revised SDHRT Quality Assurance Plan (reference 20). All QA inspections were performed by SDHRT engineering or by subcontractor QA personnel.

Drawings were prepared to Level I of MIL SPEC DOD-D-1000B (contract Mod 2, dated 13 Nov 85). Engineering maintained an ENGINEERING CONTROL COPY of all SDHRT drawings and red-line changes were maintained on this drawing set. All red-line changes were approved by the SDHRT program manager.

The red-line changes made to the ENGINEERING CONTROL COPIES of the drawings were used to revise and release the master drawing set for storage in the vault. Copies of the master red-lined drawings and the receiver developmental records (drawings which have no specific developmental record sheets are built per the requirements on the drawing and have no specific testing or inspection points) were delivered with the receiver to NASA-LeRC.

4.1 Heat Storage Tube Fabrication

The raw materials and components for the heat storage tubes were ordered by and received at Boeing. The 35 Inconel 617 corrugated tubes received from Tofle America were assigned serial numbers, helium leak checked, visually inspected for excessive tooling marks or flaws, and rated as to over-all quality. All of the corrugated tubes passed the helium leak check. The 30 best corrugated tubes were chosen for heat storage tube fabrication and shipped to Pacific Scientific in Daytona Beach, FL with the other raw materials and components for assembly of the heat storage tubes.

The heat storage tubes were carefully assembled to the requirements given on drawing 180-60301. A total of 30 heat storage tubes were ordered, 24 for the receiver cavity and 6 spares. The total number of tubes fabricated was set by the quantity of Inconel 617 plate purchased from existing stock. Two of the 30 heat storage tubes were ordered with internal thermocouples (noted as -20 parts on the drawing). An outline of the fabrication tasks used by Pacific Scientific to complete the 30 SDHRT heat storage tubes is given below.

4.1.1 Material Preparation and Component Fabrication

The following steps were completed to prepare the raw materials and fabricate the components needed for the 30 heat storage tubes:

1. Helium leak check the sheathed thermocouples to be used on the 2 instrumented heat storage tubes.
2. Trim the 51 mm (2 in) diameter HX tubes to a 2,159 mm (85 in) length. Mark the position of the exit end end-cap on one end of the HX tube.
3. Ream one end of 65 PCM fill tubes to a 2.7 mm (0.1065 in) ID for a 51 mm (2 in) length minimum. Mark the end opposite the reamed end for identification using a permanent black marker or scribe.

ITEM	QUANTITY	SUPPLIER
Raw Materials		
Inconel 617, 0.010 X 16 X L coil (corrugated tubes)	700 lbs	Metal Goods Seattle, WA
Inconel 617, 0.060 thk sheet (PCM fill tubes, HX tubes)	as req'd	Purchased by supplier of PCM & HX tubes.
Inconel 617, 36 X 120 X 0.030 sheet (corrugated tube weld bands)	1 sht	Metal Goods Seattle, WA
Inconel 617, 36 X 48 X 0.27 plate (end-caps)	1	Metal Goods Seattle, WA
Nickel felt, 23 X 30 X 0.125 X 80% porosity	375 shts	National Standard Corbin, KY
304 Stainless steel, angles, plate, pipes, elbows, etc.	as req'd	Lukas Machine Seattle, WA
Pure LiF salt (eutectic boost)	101 lbs	Cerac Inc. Milwaukee, WI
$79_a LiF\text{-}21_a CaF_2$ salt (eutectic)	1317 lbs	Cerac Inc. Milwaukee, WI
Components		
Corrugated tubes, 3.935 OD X 3.676 ID X 0.25 pitch X 62 length	35	Tofle America Exton, PA
PCM fill tubes, 0.15625 OD X 0.028 wall X 12 length	250	Valley Metals El Cajon, CA
HX tubes, 2 OD X 0.060 wall X 85 length	32	Valley Metals El Cajon, CA

Note: dimensions shown are in inches

Figure 4-1: Suppliers of Raw Materials, Components, and Assemblies for the SDHRT Heat Receiver

ITEM	QUANTITY	SUPPLIER
Heat Storage Tubes		
Assembly	30	Pacific Scientific Daytona Beach, FL
Corrugated tube end-cap seal laser welding	60	Boeing Seattle, WA
Molten salt filling	30	Boeing Seattle, WA
PCM fill tube seal EB-welding	60	Boeing Seattle, WA
Receiver Fabrication		
Structure/piping/plenums	as req'd	Lukas Machine Seattle, WA
Assembly	1	Lukas Machine Seattle, WA
Insulation	as req'd	John Manville Elkhart, IN

Figure 4-1 (con't): Suppliers of Raw Materials, Components, and Assemblies for the SDHRT Heat Receiver

4. True the ends of the 30 corrugated tubes to round. Measure the OD and ID of the straight end sections to determine the proper dimensions of the weld bands.
5. Form and weld the rings used for the bellows termination weld bands (note that 2 sizes are required; 1 each for the OD and ID weld bands).
6. Rough cut the end-caps from Inconel 617 plate maximizing the quantity of disks to be removed from plate (i.e., stagger cuts). Machine the inlet and exit end end-caps per drawing requirements. Prepare 2 inlet end and 2 exit end end-caps with holes for the sheathed thermocouples used in the instrumented heat storage tubes.
7. Stamp out the felt metal disks from the felt sheet with the proper inner and outer diameter (approximately 14,000 total required). Maximize the number obtained per sheet by proper staggering of cuts. White glove handle the felt metal at all times.
8. Develop tooling and punch the holes for the thermocouple penetrations in approximately 500 felt disks for the 2 instrumented heat storage tubes.
9. Section in half approximately 315 of the regular felt disks and 24 of the thermocouple prepared felt disks.
10. Heat the felt metal disks in a vacuum to 982±28°C (1800±25°F), with a maximum heating rate of 482°F/hr (900°F/hr), until a maximum chamber pressure of 1 X 10^{-5} torr is achieved. Hold for an additional 30 minutes at temperature. Remove felt disks from furnace, bag, and seal with desiccant.
11. Clean metallic components to BAC 5758 Type II or equivalent (except for felt metal). After cleaning operations of metallic components, all parts must be white glove handled and storage and assembly environment will meet the requirements of BAC 5703, Class 400,000 or be approved by Boeing engineering.

4.1.2 Heat Storage Tube Assembly Operations

The following steps were performed to assemble the 30 heat storage tubes for the SDHRT heat receiver.

1. Heat and shrink fit the outer bands to the corrugated tube OD ends. Cool and expansion fit the inner bands to the corrugated tube ID ends.
2. Vacuum braze the thermocouples to the 4 special end-caps for the 2 instrumented heat storage tubes.
3. Insert the reamed end (opposite the marked end) of the PCM tube into the end-caps and weld the PCM fill tubes to end-caps. Helium leak check the PCM tube to end-cap welds.
4. Weld the TES side of the exit end end-cap to HX tube. Weld the outside of the exit end end-cap to the HX tube but do not completely seal the weld so as to not entrain gases inside the weld region. Helium leak check the end-cap to HX tube weld.

5. Assign a HX tube to each of the 30 corrugated tubes to be used during heat storage tube build-up. Insert the corrugated tube over TES section of the HX tube and match up the end with the exit end end-cap. Mark the location of inlet end end-cap on HX tube (note: the lengths of the corrugated tubes vary by almost 13 mm). Remove the corrugated tube from the HX tube and store until needed.
6. Stack the felt disks over HX tube. Use tooling to snug disks together uniformly. Complete the stack to within 25-38 mm (1-1.5 in) of the inside surface of the inlet end end-cap (the position is marked on the HX tube). Leave the minimum length to complete a weld of the inside surface of the inlet end end-cap to the HX tube. Note that special care will be required on the 2 instrumented tubes to fit the felt disks over the sheathed thermocouples.
7. Weld the inside surface of the inlet end end-cap to HX tube. Weld the outside surface of the inlet end end-cap to the HX tube but do not complete the weld around the entire circumference to ensure no gases become entrained within the weld. Mark this end-cap as inlet on the outside surface of the end-cap.
8. Insert the sectioned felt metal disks to fill the void up to the inside surface of the inlet end end-cap. The location of the sectioned interface should be staggered around the circumference of the tube except on the two instrumented tubes which require the interface to be located in the plane of the thermocouples. Figure 4-2 shows a prototype tube with the nickel felt metal disks in place and the corrugated tube ready to be inserted over the disks.
9. Slowly insert the corrugated tube over the HX tube and felt metal disks. Weld the end face of the corrugated tube to the end-caps at the weld "preps" located on the OD of the end-cap.
10. Engrave the serial number on the end-cap using the part number 180-60301-# where the # is the serial number assigned to the corrugated TES containment tube used in the assembly.
11. Visually check the entire heat storage tube, especially the bellows for damage, flaws, etc. Helium leak check the tube assemblies and mark the location of any leaks at the weld of the corrugated tube to the end-cap. After leak checking is complete, purge the tube with dry argon or nitrogen and seal the PCM fill tubes with heat shrink Tygon tubing.
12. Bag each individual unit in plastic, backfill with dry argon or nitrogen gas with an enclosed desiccant.
13. Crate each tube assembly separately and ship to Boeing.

4.1.3 Laser Welding

After shipment to Boeing, the tube assemblies were uncrated and inspected for damage. No damage was found during the inspection of the tubes. The tubes were then installed, one-at-a-time, into the Boeing laser welding chamber and the laser weld was made to both end-caps. The tubes were removed and a helium leak check was performed being especially critical of any tubes which showed a leak before laser welding (only 2 of the 30 heat storage tubes leaked prior to laser welding). All of the 30 heat storage tubes passed a final helium leak check after laser welding was completed. The tube assemblies were now ready to be filled with molten salt.

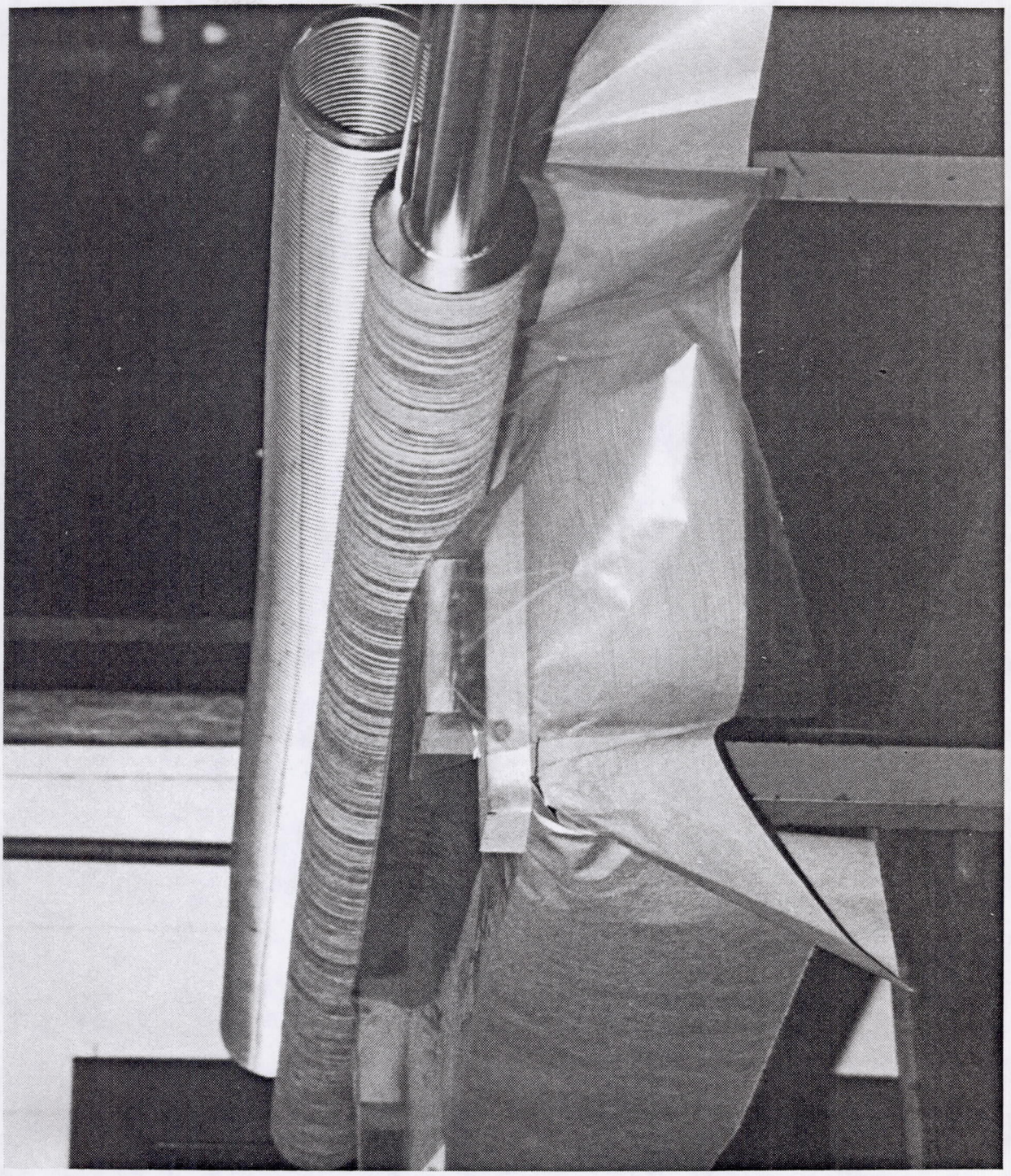

Figure 4-2: SDHRT Heat Storage Tube Showing Nickel Felt Installed on HX Tube and Corrugated TES Containment Tube Ready for Assembly

4.2 Molten Salt Filling

Boeing developed a dedicated, High-Temperature Thermal Energy Storage (HTTES) facility to cast molten salts into large containment vessels. The design, fabrication, and set-up of the HTTES facility was funded by Boeing but the actual fill operations to cast molten salt into the SDHRT receiver heat storage tubes was paid for by the SDHRT contract.

The design of the HTTES facility hardware was based upon research conducted at the Oak Ridge National Laboratory (ORNL) in the late 1960's (reference 21). ORNL demonstrated a facility capable of filling multiple heat storage tubes with molten LiF (849°C melt temperature). The design concept used in the ORNL facility was validated for SDHRT application by casting molten LiF-CaF_2 into subscale canisters during Task 4 (reference 11 and 22). The canister filling operations confirmed that a eutectic salt mixture could be cast as a liquid into TES containment components containing the nickel felt metal material.

4.2.1 Molten Salt Filling Requirements

The filling of TES containment hardware with molten salt is a time consuming process. Each fill operation requires refurbishment of the facility and the fill operation itself is conducted over several days to allow off-gasing to occur at acceptable rates. The large specific heat and poor thermal conductivity of the salt limit the rate of heat input and increases the time to reach its melt temperature. Upon melt, the thermal conductance improves slightly but, if left to conduction alone, the time required to input sufficient energy to melt all the salt can be significant. Furthermore, each fill operation poses a risk to the TES component(s) because of the possibility of failure of a facility component during the filling operation. The Boeing HTTES facility was designed to fill multiple TES containment components during a single fill operation to reduce the total number of fill operations, costs, and the risks of equipment failure.

Fluoride salt mixtures like LiF-CaF_2 are relatively inert in granular form at room temperature. However, strong oxidation reduction reactions will occur between the salt and its containment material if heated and melted in the presence of air or water vapor (reference 12). Other contaminates can either cause corrosive reactions or degrade performance. Therefore, the salt must be purchased in a highly purified state and must remain in this state during the filling operation. This is accomplished by maintaining the salt and all of its associated transfer lines, storage containers, and TES components in a high-vacuum environment during the entire fill operation. The salt (both LiF and LiF-CaF_2) is purchased to the following specification:

> The salt mixture shall be 55.5±1.0% LiF by weight (for the LiF-CaF_2 mixture) and shall be a minimum of 99.9% pure. A spectrographic analysis shall be performed to determine metallic impurities. An analysis shall be performed to determine the levels of nitrogen, oxygen, and carbon impurities. An analysis shall be done to determine the amount of silicon oxide (SiO_2) present as an impurity. The salts shall be supplied as fused, 3 mm (1/8 in) fines. The salts shall be packaged in sealed containers, back-filled with an ultra-high purity inert gas of either argon or nitrogen.

The exterior of the TES tubes must be maintained in a vacuum during filling to prevent excessive oxidation and preserve their radiation properties. In the receiver application, the exterior surfaces of the TES containment components must reflect and/or radiate energy. It is also important to eliminate natural convection inside the chamber to prevent asymmetric heating and cooling of the TES components. A minimum vacuum of at least 5×10^{-4} torr is required during the entire filling operation for the SDHRT receiver (note: a vacuum of at least 1×10^{-5} torr required to fill the tubes for a flight receiver).

The high melt temperatures of fluoride salt mixtures requires a facility capable of operation to temperatures in excess of 927°F (1700°F). Very few materials are available that have sufficient strength at these temperatures. Selected materials can be replaced after each fill operation to limit time at temperature and to allow welding of the TES components into the salt transfer system lines. Components will be designed for creep rupture with a factor of 4 for the operational life of the facility. After the operational life is exceeded, these components must be replaced.

Optimal operation of the SD heat receiver requires that the heat storage annulus be completely filled with the eutectic salt mixture at a temperature which exceeds the maximum expected nominal operating temperature of the heat storage tube assemblies. The maximum peak operating temperature of the TES during normal operation will be about 899°C (1650°F). Peak temperatures may exceed 927°C (1700°F) during certain off-design operational cases but the peak temperatures will be limited to a relatively small region of the tube surface. The average temperature of the TES containment tube will be less than 871°C (1600°F). Therefore, a 927°C (1700°F) is the required fill temperature to ensure sufficient volume for the molten salt during all hypothesized operating scenarios.

The heat storage tubes are filled in a vertical orientation for the following reasons: (1) all previous experience (ORNL and Boeing) filled the TES tubes or canisters in a vertical orientation; (2) a vertical chamber takes less laboratory space; (3) chamber support structure and interfaces are simpler; and (4) a complete fill is assured because the static pressure is constant at any cross-section of the tube assembly.

One of the functions of the felt metal disks inside the TES annulus is to suspend (wick) the molten salt and prevent the gravity force from moving it into voids in the lower regions of the containment volume. However, the felt metal can only wick molten salt to a height roughly equal to the OD of the heat storage tube (approximately 102 mm). The tubes are filled in the vertical orientation and, therefore, once filled, molten salt can flow down to the inlet end of the tube assembly if the salt is frozen first at the bottom of the heat storage tubes. This is unacceptable because most of the 30% void would then occur at the top of the TES annulus and the bottom region would be solid. This could cause problems during the first remelt of the salt during operation inside the heat receiver cavity. To prevent this from occurring, the tubes must be carefully cooled to freeze the salt radially outward and from the top of the TES annulus downward to the bottom.

The nickel felt metal will only control the salt void distribution if its surfaces are wetted by the salt. The degree of wetting by the salt is a strong function of the surface condition of the fibers including the degree of surface oxidation. The individual felt metal disks are heated in vacuum to 982°F (1800°F) prior to their assembly into the heat storage tube. However, a small surface oxide forms on the nickel fibers because they are assembled in air. Testing has shown that purging the felt with a 5% hydrogen-95% argon gas mixture reduces the surface oxides and promotes improved wetting of the fibers by the LiF-CaF_2 salt mixture (reference 19). Therefore, the heat storage tubes must be purged with a 5% hydrogen-argon gas mixture while at high temperature prior to filling the tubes with salt.

4.2.2 HTTES Fill Facility Configuration and Operation

A schematic of the final configuration of the HTTES facility is shown in Figure 4-3. The basic operation of the HTTES facility is simple and is only complicated by the high-temperature and vacuum requirements.

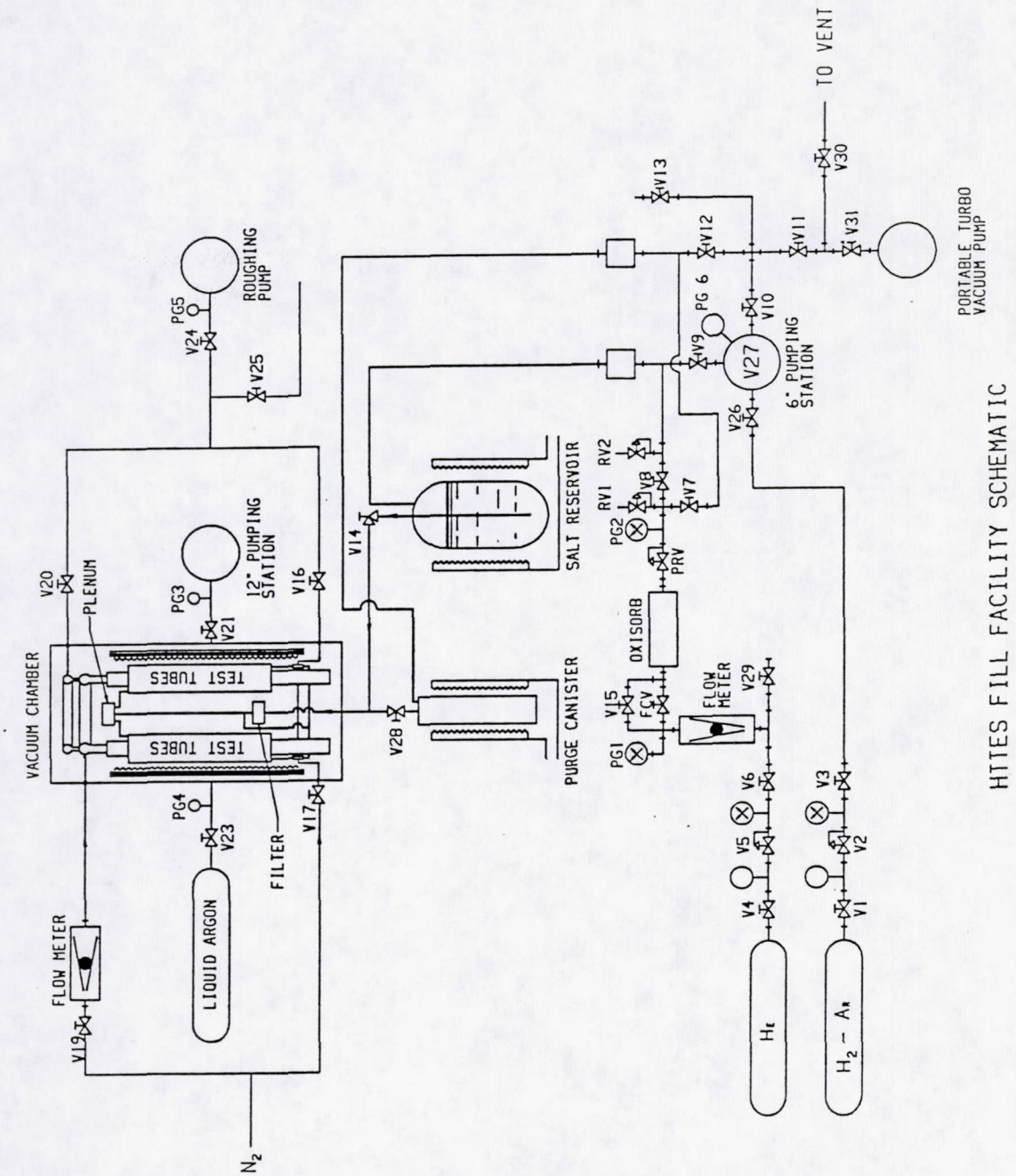

Figure 4-3: Final Configuration of the HTTES Molten Salt Fill Facility

Granulated salt is loaded into a salt reservoir where it is heated under vacuum. After it is melted, helium gas is introduced into the top of the reservoir forcing molten salt up a dip-leg, through the salt transfer line, and into salt manifolds that connect to both ends of the heat storage tubes. A filter is located upstream of manifolds to remove solid contaminants from the salt. Salt flows out of the reservoir through the transfer line, manifolds, and into the heat storage tubes until the TES annulus is full. When no more salt can flow into the heat storage tubes even with an increase in the static head on the salt reservoir, a complete fill is signaled by no more helium gas flow into the salt reservoir. The static pressure is increased and if no additional salt flow is observed, the tubes are considered full.

After a complete fill is achieved, the vacuum chamber heater is shut off and cooling gas is introduced into the freeze valve to solidify the salt in the lower PCM fill tubes. Gas is also introduced into a special bayonet HX to begin freezing the salt inside the TES annulus radially outward and from the top of the annulus downward. Static pressure is maintained on the system to prevent salt movement out of the heat storage tube until transfer line temperatures inside the vacuum chamber have cooled below the melt point of the salt. Excess salt remaining inside the salt reservoir is then cast into a throw-away purge canister allowing the reservoir to be filled with granulated salt for the next fill operation with no danger of rupture.

After the heat storage tubes have cooled to near ambient temperature, they are removed from the HTTES facility and the PCM fill tubes are sealed by an EB weld (reference 23). The HTTES facility is then refurbished by replacing all of the salt transfer line and manifold components.

4.2.3 HTTES Fill Facility Hardware Description

4.2.3.1 Salt Reservoir

The salt reservoir holds the salt charge during its heat-up and through the melt. The salt reservoir is formed from an Inconel 600 cylindrical shell, 356 mm (14 in) in diameter with 9.5 mm (3/8 in) thick walls. Hemispherical heads are used top and bottom for a total length of about 889 mm (35 in). The reservoir volume is sized to hold approximately 88 kg (194 lbs) of granular salt (110% of the salt required for one complete fill of six heat receiver tubes).

The major problem experienced during the ORNL filling operations resulted because the salt was processed in the reservoir prior to the filling operation. After an initial melt to purify the salt compound, the salt mixture was allowed to freeze naturally inside the salt reservoir. During the remelt of the salt during the fill operations, a nonuniform expansion of the salt created excessive forces on the dip-leg and thermocouple well causing their penetration welds at the top of the reservoir to rupture. The HTTES facility was designed to use an initial charge of granulated salt for each salt fill operation by including a system to remove excess salt from the reservoir after each filling operation is complete.

The salt is loaded through a 51 mm (2 in) diameter access port on the top of the reservoir. The access port is also fabricated from an Inconel 600 tube and fitted with a flange for connection to the pressurized gas supply and evacuation line. The port was designed to extend out of the reservoir furnace heated zone to prevent diffusion bonding across the flange seal interface. A set of four baffles extend into the access port from the connecting tube and act as radiation shields to prevent heat loss out of the reservoir and prevent transport of salt vapors towards the vacuum system.

The salt is obtained in a highly purified state as 3 mm (1/8 in) fine granules at a composition of 79_aLiF-$21_a$$CaF_2$. However, experience has shown that this composition is slightly off the true eutectic composition and is rich in CaF_2. The CaF_2 will remain solid and plug the transfer lines because its melt temperature exceeds 1205°C (2200°F). Therefore, prior to loading the eutectic salt mixture into the reservoir, a small amount 9.1 kg (20 lbs) of pure LiF is first loaded into the bottom of the reservoir. The remaining CaF_2-rich salt mixture is then loaded on top of it. During the initial melt of the salt mixture, the excess solid CaF_2 falls to the bottom of the reservoir because it is more dense than the eutectic mixture in the molten state. It settles onto the layer of solid LiF on the bottom surface and combines to form more eutectic with a small percentage of excess and solid LiF. However, as the eutectic salt mixture is superheated above its melt temperature of 771°C (1420°F), the melt temperature of LiF (849°C) is exceeded forcing all of the salt inside the reservoir to be molten. The final salt composition, 82_aLiF-$18_a$$CaF_2$ is now slightly rich in LiF and no excess CaF_2 will be present in the reservoir.

Two 304 stainless steel mixing propellers welded to an Inconel 600 shaft are used to actively stir the salt mixture during the superheat and active filling periods of the operation. The rotary motion is transmitted through a Ferrefluidic vacuum feed-through and the shaft is driven by a small AC motor. The mixing propellers are rotated at a speed of about 30 rpm. Active mixing speeds the melting process by transferring heat inward from the reservoir wall by convection rather than by conduction and ensures that any off-eutectic solid components of the salt mixture do not collect at the bottom of the reservoir.

The salt flows out of the reservoir through a 9.5 mm (3/8 in) diameter dip-leg line provided in the center of the reservoir. Next to the dip-leg is a 6 mm (1/4 in) diameter tube, sealed at the bottom, containing 3 thermocouples to measure the salt temperature near the top, middle and bottom of the reservoir. The dip-leg and thermocouple tubes extend to within 10 mm (0.4 in) of the center bottom of the reservoir.

The salt reservoir is enclosed in two half-shell Watlow heaters, 762 mm (30 in) long and 406 mm (16 in) in diameter with a rated capacity of 4.2 kW each. In addition, a single 275 watt, flat plate, ceramic heater is installed under the bottom of the reservoir. The furnace is insulated with 102 mm (4 in) of 2.7 kg (6 lb) Cerablanket insulation and is contained within a 9.5 mm (3/8 in) thick stainless steel drum. The stainless steel housing acts as backup containment in the event of a failure of the salt reservoir. The 2 large side heaters are controlled by the salt fill data acquisition and control system (DACS). The bottom heater is controlled manually by a large variac.

4.2.3.2 Salt Transfer Line

The salt transfer line connects the salt reservoir to the salt manifolds and purge reservoir. It begins at the top of the salt reservoir and terminates at the inlet of the salt manifold assembly inside the vacuum chamber and at the inlet of the purge reservoir located below the vacuum chamber. Two mechanical valves are located in the transfer line to control the direction of salt flow. The entire salt transfer line, including the 2 mechanical valves and tee fitting is heated by 17 clam-shell heater elements of various lengths and capacities. The outside surfaces of the clam-shell heaters are insulated.

The salt transfer line is fabricated from 9.5 mm (3/8 in) diameter Inconel 600 tubing. The tee section splitting the flow up to the manifolds and down to the purge reservoir valve is a 9.5 mm 304 stainless steel weld fitting. The entire length of the transfer line including the tee section and 2 mechanical valves are replaced after each filling operation. This reduces the risk of line rupture because of accumulated high-temperature creep damage and ensures an open and uncontaminated line for each fill operation.

The design of the transfer line allows the expansion of the tubing during its heat-up from room temperature to 927°C. Little or no constraints of the tubing allows the growth to occur without inducing significant thermal stress. The transfer lines between the salt reservoir and TES tube assembly are constrained only at the vacuum chamber feed-through weld and at the top of the salt reservoir. Thermal growth is accommodated by the two 90 degree bends in the lines. The clam shell heaters for the transfer lines have a large enough ID to accommodate radial motion of the line. The purge reservoir and insulation assembly are mounted on a counterbalance platform to permit 13 mm (0.5 in) of vertical axial growth.

Two mechanical valves are located in the transfer line; one at the 90° bend above the salt reservoir (V14) and one just above the purge reservoir (V28). Valve V14 isolates the transfer line and heat storage tubes from the salt reservoir during salt heat-up, melt, and superheat. Thus, salt vapors cannot migrate to colder areas in the system and it protects the heat storage tubes from damage in the event of a leak in the reservoir or transfer lines. Valve V14 is not opened until ready to fill so the heat storage tubes are only vulnerable for about 30 minutes of the total fill operation duration. Valve V28 prevents salt from entering the purge canister until ready to empty the salt reservoir at the end of the fill operation. Freeze valves used previously for these applications were not effective.

All of the transfer lines are enclosed in ceramic fiber, clam-shell heaters. The heaters are insulated with soft fibrous insulation wrapped around the heater sections and tied with wire. Detailed thermal analysis of the transfer line showed that the insulation must be carefully installed to prevent it from blocking any view of the transfer line surface to a heater. Any blockage of the transfer line surface can cause excessive temperature gradients and a temperature drop of sufficient magnitude to freeze the salt in a no or slow flow situation. When the salt is flowing at a reasonable flow rate, its enthalpy is usually sufficient to keep transfer line wall temperatures above the melt temperature of the eutectic salt mixture.

The transfer line penetrates the vacuum chamber through a specially designed feed-through. The vacuum chamber feed-through assembly is 457 mm (18 in) long and is heated by a pair of dedicated clam-shell heaters that are wrapped with 25 mm of fibrous insulation rolled in a stainless steel shell before inserting in the feed-through. This design is necessary to reduce the amount of heat transfer to the 406 mm (16 in) diameter vacuum flange bolted to the bottom of the vacuum chamber which uses a temperature sensitive o-ring seal. The length of the feed-through allows the lines to extend up into the heated zone and increases the conduction path to the flange. The feed-through is connected to the bottom of the vacuum flange with a high temperature, copper gasket seal.

4.2.3.3 Manifold Assembly

The manifold assembly consists of an inlet filter, lower torus manifold, and upper plenum manifold. The manifold assembly is replaced after each fill operation. The filter is made from a 25 mm (1 in) section of 102 mm (4 in) diameter, schedule 40, 304 stainless steel pipe. The filtering material is made up of 3 to 4 layers of 3 mm (0.125 in) thick nickel felt disks cut to fit to the inside diameter of the pipe. Plenums are formed at both the inlet and exit end of the filter by separation rings and the filter is completed by welding caps to both ends. The filter plenums ensure sufficient surface area is available to remove all particulates without clogging.

The lower torus manifold splits the flow of salt into the bottom PCM fill tube of each of the six heat storage tubes and is located in the heated zone of the vacuum furnace. The lower manifold is fabricated from Inconel 600. The torus body of the manifold is 9.5 mm (3/8 in) diameter X 0.9 mm (0.035 in) wall tubing and each of the six manifold legs are 6 mm (1/4 in) diameter X 1.24 mm (0.049 in) wall tubing.

A specially designed transition piece connects each of the manifold legs to the 4 mm (5/32 in) diameter PCM fill tubes on the heat storage tubes. The transition piece was needed to ensure an unobstructed flow path across the connecting weld. Originally, the 6 mm (1/4 in) manifold leg was welded directly to the thin-walled (0.7 mm) PCM fill tube. This weld was very difficult to make because the closure fillet weld burned through the thin-wall of the PCM fill tube. The weld was further complicated by the limited room between the PCM fill tube and the HX tube as illustrated in Figure 4-4. Flow testing and examination of the manifold attachments after one of the fill operations showed all of the welds had significant burn-through and blockage. One of the legs was completely blocked. The new transition allows the critical weld to the thin-walled PCM tube to be made while the tubes are lying on the bench. Thus the weld is fully inspectable for blockage (visually) and leakage (helium leak check). A small piece of 6 mm (1/4 in) tubing is reamed to fit over the OD of the PCM fill tube. The end cross-section is welded and inspected to ensure a clear flow path with no leaks. A small piece of 8 mm (5/16 in) diameter X 0.9 mm (0.035 in) wall tubing is then fillet welded to the thick-walled 6 mm piece of tube surrounding the PCM tube and leak checked. After the heat storage tubes are assembled, the 8 mm (5/16 in) piece of transition tubing is then inserted over the manifold legs and a closure fillet weld is made. The weld is still difficult due to the limited space but is much easier to make because the weld is onto a thick-walled tube. Testing of these welds has shown them to be repeatable and reliable.

The lower salt manifold has an integral freeze valve (upper toroidal tube shown on the manifold in Figure 4-4) to introduce cold gas around each of the 6 lower manifold legs after filling of the heat storage tubes is complete. The cold gas cools the surface of the 6 mm (1/4 in) diameter inlet tubes, freezing the salt, and forming a plug. The salt plugs prevents molten salt inside the TES annulus from flowing out back out into the manifold or transfer line.

The upper manifold is also located inside the heated zone of the vacuum chamber furnace. The manifold is similar in construction to the filter housing, using a 19 mm (0.75 in) length of the 102 mm (4 in) diameter stainless steel pipe. The bottom plate of the plenum manifold receives the inlet tubing from the filter and supplies the exit to extensions welded onto each of the 6 PCM tubes. The extensions are welded onto the tubes using transitions like those described on the bottom manifold. The extensions are welded from inside the top plenum before the top cap is welded onto the plenum manifold.

4.2.3.4 Chamber Assembly

The HTTES facility is designed to fill 6 tubes at-a-time. The tubes are assembled into a integral support and cooling fixture as shown in Figure 4-5. The tubes are evenly spaced around the 254 mm (10 in) diameter bottom torus shaped manifold and the bottom of the HX tubes rests on the base of the assembly. Bayonet cooling fingers run through the center of the tubes and maintain the assembly position concentric to the vacuum furnace assembly. The 38 mm (1.5 in) of axial growth is accommodated by not constraining the cooling fingers at the bottom base of the assembly. The cooling fingers connect to inlet and exit gas manifolds at the top of the assembly. The cooling finger bayonet HX is made from 5 mm (3/16 in) diameter tubes sealed inside 9.5 mm (3/8 in) diameter tubes. During cooling, gaseous nitrogen is distributed to each of the six cooling fingers by an inlet cooling manifold. The gas flows down the length of the assembly in the annular area between the two tubes and then flows back up through the 5 mm tube. It exits through a manifold at the top of the assembly.

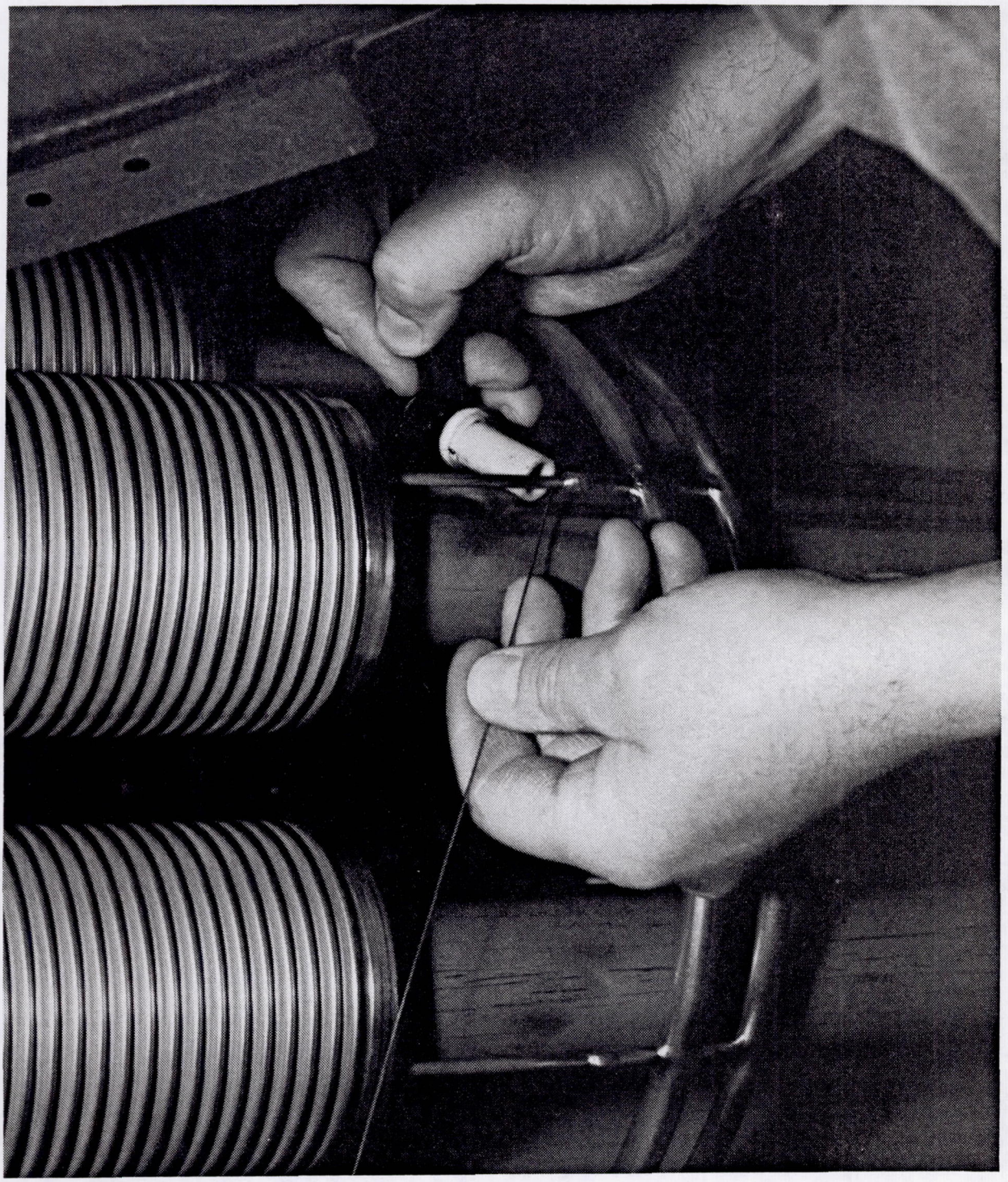

Figure 4-4: Welding Lower Salt Manifold to Heat Storage Tubes

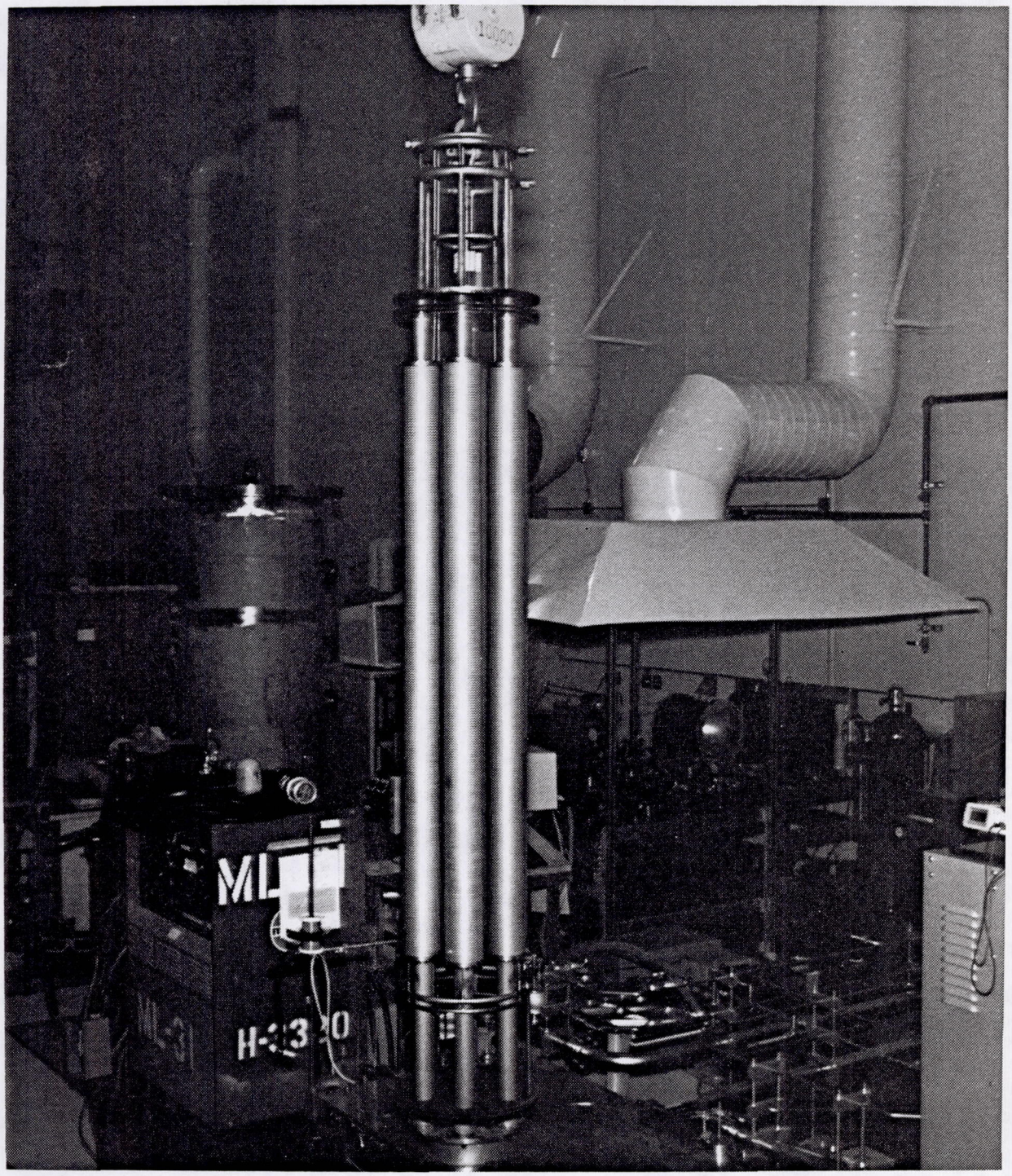

Figure 4-5: Configuration of the 6 SDHRT Heat Storage Tubes for Multiple Tube Molten Salt Fill Operation

The cooling fingers provide slow radiant cooling of the heat storage tubes from the inside HX surface and from the top to the bottom of the heat storage tube. Thus, the salt at the top of the TES annulus solidifies first and the phase front progresses down toward the bottom of the heat storage tube. This design ensures an even distribution of salt along the length of the annulus in preparation for the first melt inside the heat receiver. The bayonet design eliminates the need to weld manifolds at top and bottom between each fill and allows the hardware to be reused. The cooling rods are also used for clamping the tube assembly during handling. The attachment of the PCM fill tubes to the upper and lower salt manifolds was discussed previously.

4.2.3.5 Pressurized Gas Supply and Vacuum System

Vacuum is maintained inside the salt reservoir, transfer line, upper and lower manifolds, and heat storage tubes during most of the fill operation. A Cooke portable pumping station using a 152 mm (6 in) diffusion pump maintains the salt-side vacuum to approximately 1 X 10^{-5} torr. The salt-side vacuum and gas pressurization system can be seen in Figure 4-6.

The pressurized gas supply system has two separate inlets to control the flow of either a research grade helium or a 5% hydrogen-argon gas mixture. Helium is used to pressurize the salt reservoir to establish salt flow into the heat storage tubes. The hydrogen-argon gas mixture is used to conduct a hydrogen purge operation prior to melting the salt in the reservoir to precondition and clean the felt metal fibers. The reservoir, transfer line, and heat storage tubes are at 649°C (1200°F) during the hydrogen purge. The 5% hydrogen reduces, by reaction, a thin oxide layer on the felt metal fibers. This operation has been shown to improve the wetting of the felt metal fibers by the molten salt (reference 11 and 19). Vacuum is reestablished after the hydrogen purge and maintained for 2 hours before proceeding with the heat-up to melt.

The gas supply system includes an oxygen "getter" to remove traces of oxygen from either gas supply. The rate of gas flow is controlled by a fine metering flow control valve that can be bypassed by a second valve for rapid pressurization of the reservoir. Downstream system pressure is regulated to subatmospheric pressure with a negative pressure regulating valve. The fill process is performed at a static pressure of 205 kPa (15 psig).

Evacuation lines are provided between the portable pumping station and both the salt reservoir and purge canister allowing the entire salt side of the system to be evacuated prior to filling. This also removes residual moisture, oxygen, and nitrogen from the system during heat up, and the hydrogen gas mixture after the hydrogen purge operation. Cold traps in these lines capture the contaminants and protect the vacuum pump from molten salt and salt vapors. The fittings used in these lines are primarily VCR fittings with flange metal gasket seals. These seals were selected because they have been proven for use in leak-tight systems.

4.2.3.6 Vacuum Chamber and Furnace

The TES tube assembly is placed in the vacuum chamber during the fill process. The chamber is a 914 mm (36 in) in diameter, 2,743 mm (9 ft) high, and has a 305 mm (12 in) diameter port for the vacuum pump connection. A large flange at the bottom of the chamber houses twenty, 70 mm (2.75 in) flange flanges for instrumentation and power. It also has the special 406 mm (16 in) diameter vacuum flange for penetration for the high temperature transfer line.

The vacuum furnace elements are fabricated from standard, Watlow, fiber heaters. The vacuum furnace assembly is composed of 6 half-shell heaters, 610 mm (24 in) long and 406 mm (16 in) in diameter. Each of the heaters has a rated power of 7 kW for a total furnace capacity of 42 kW. The maximum steady state operating temperature of the heaters is 1094°C (2000°F). Three layers of radiation baffled shielding are provided between the back side of the heater and the vacuum chamber to reduce heat loss to the chamber (see Figure 4-6). The heater

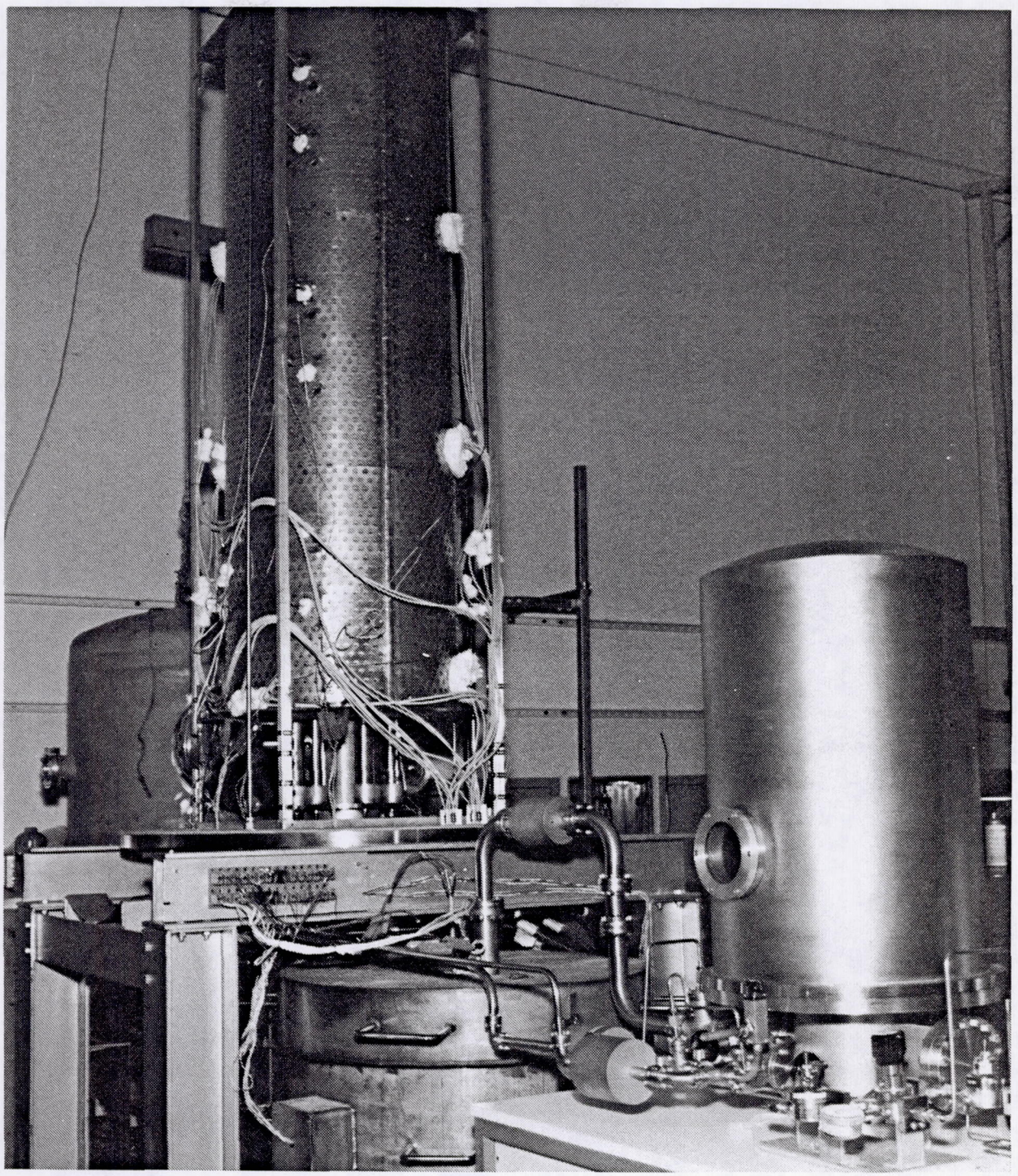

Figure 4-6: HTTES Facility Vacuum Chamber Heater and Salt Reservoir Gas Pressurization System

sections are controlled separately to adjust for variations in the heat losses along the lengths of the heat storage tubes. There are two thermocouples installed in each of the heaters to monitor temperatures and maintain symmetric heating of the heat receiver tubes.

4.2.3.7 Purge Reservoir

The HTTES facility was designed to use an initial charge of granulated salt and a provision was made to remove excess salt from the reservoir after each filling operation is complete. After the TES components inside the vacuum chamber have been completely filled with salt, the excess salt remaining in the transfer line and inside the salt reservoir is cast into a throw-away purge reservoir. This leaves the reservoir empty and allows a fresh charge of granulated salt to be loaded for the next fill operation without a re-work of the salt reservoir.

The purge reservoir is 127 mm (5 in) in diameter and 737 mm (29 in) long. The cylindrical canister is sized to hold the excess salt loaded into the reservoir for contingencies and not transferred into the heat storage tubes. The canister and inlet line are heated for a very short period of time and are disposable so they are made of 304 stainless steel. They connect with the salt transfer line just below valve V28. Flow is initiated into the purge canister by opening V28. Flow is so quick and enthalpy of the molten salt so large, no active heating of the canister is required.

4.2.3.8 Instrumentation and Power Control

The system is fully instrumented with thermocouples as shown in Figure 4-7 and all temperatures are recorded by a Hewlett Packard DACS. In addition, the DACS is used to control many of the heater powers to provide flexibility in adjusting system temperatures and assure even heating in all zones. The operator sets the maximum temperature and specifies an SCR voltage for each heater. All heater zones are shown schematically in Figure 4-8. Heaters not controlled by the DACS are identified on Figure 4-8 as "VAR" which denotes variac manual control of the heater voltage. If a temperature is exceeded, an alarm sounds for the operator to check the system. It is up to the operator to shut off the heater or reduce the SCR voltage.

4.2.4 Molten Salt Fill Operations Summary

Several fill operations were conducted to demonstrate the HTTES facility operation prior to filling contract hardware with the eutectic salt mixture. A demonstration fill was considered mandatory because the SDHRT program originally only fabricated 4 spare heat storage tubes and, therefore, a failure during a fill operation that damaged six tubes could potentially end the program.

The costs of the heat storage tubes and the eutectic salt mixture are high. Therefore, the planned initial demonstration used a single heat storage tube fabricated from 304 stainless steel. The salt annulus contained the felt metal disks just like the contract hardware. The first attempt to fill a single heat storage tube failed but after facility modifications, a second attempt was successful in completely filling a single full-size heat storage tube. The facility was then assumed to be capable of filling the SDHRT heat storage tubes but 2 attempts to fill the first six full-size SDHRT storage tubes were unsuccessful.

Extensive investigations of these 2 failures showed that the salt composition was slightly rich in CaF_2. The CaF_2 was separating inside the salt reservoir during the initial melting of the salts. At the initiation of the fill, solid CaF_2 was then being drawn up into the salt transfer line with the eutectic and clogging at constrictions and/or cold spots. Several design changes were made to correct this problem including: (1) boosting the salt composition to the LiF-rich side of the eutectic by adding pure LiF to the bottom of the reservoir; (2) adding a mechanical stirrer

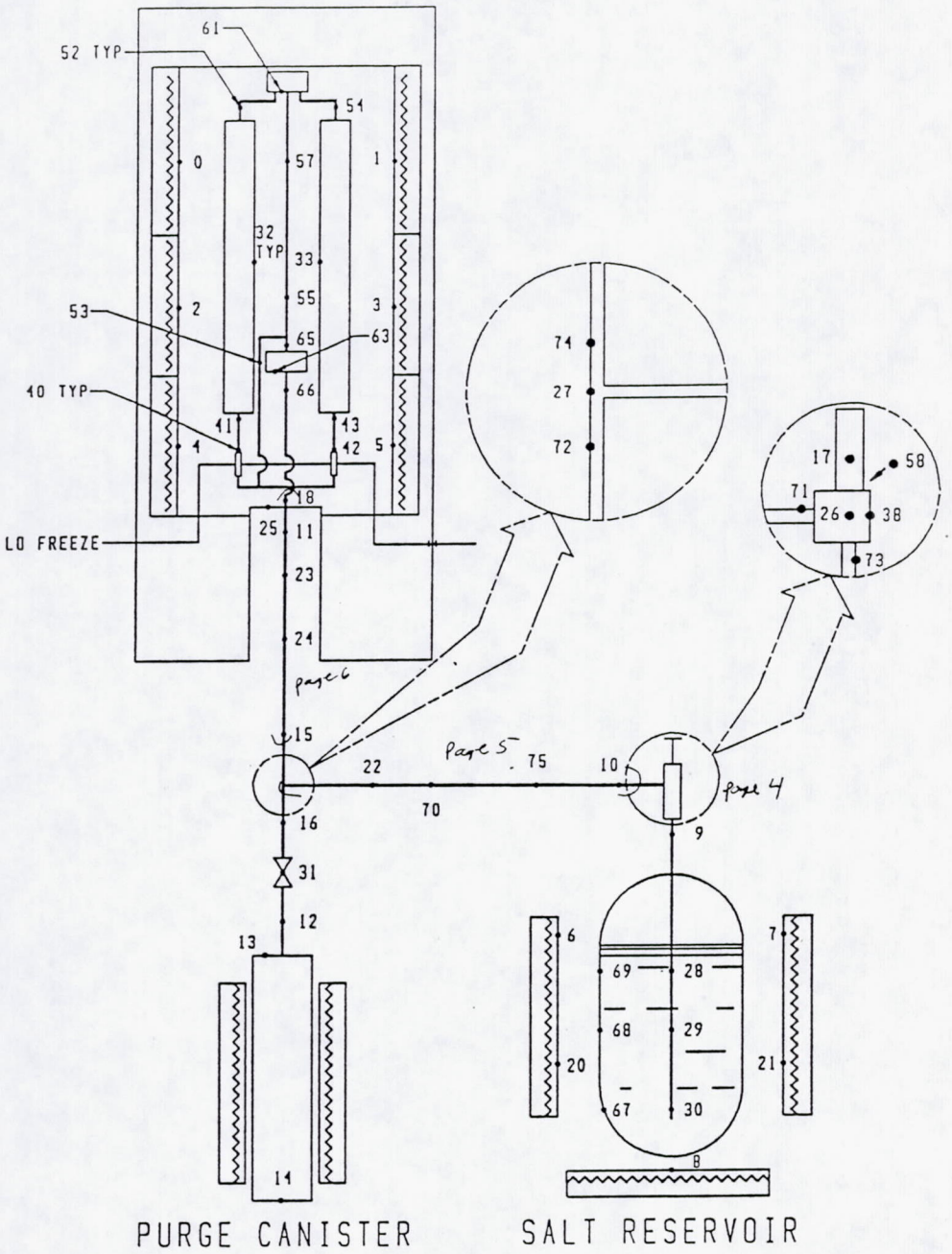

Figure 4-7: HTTES Facility Thermocouple Locations

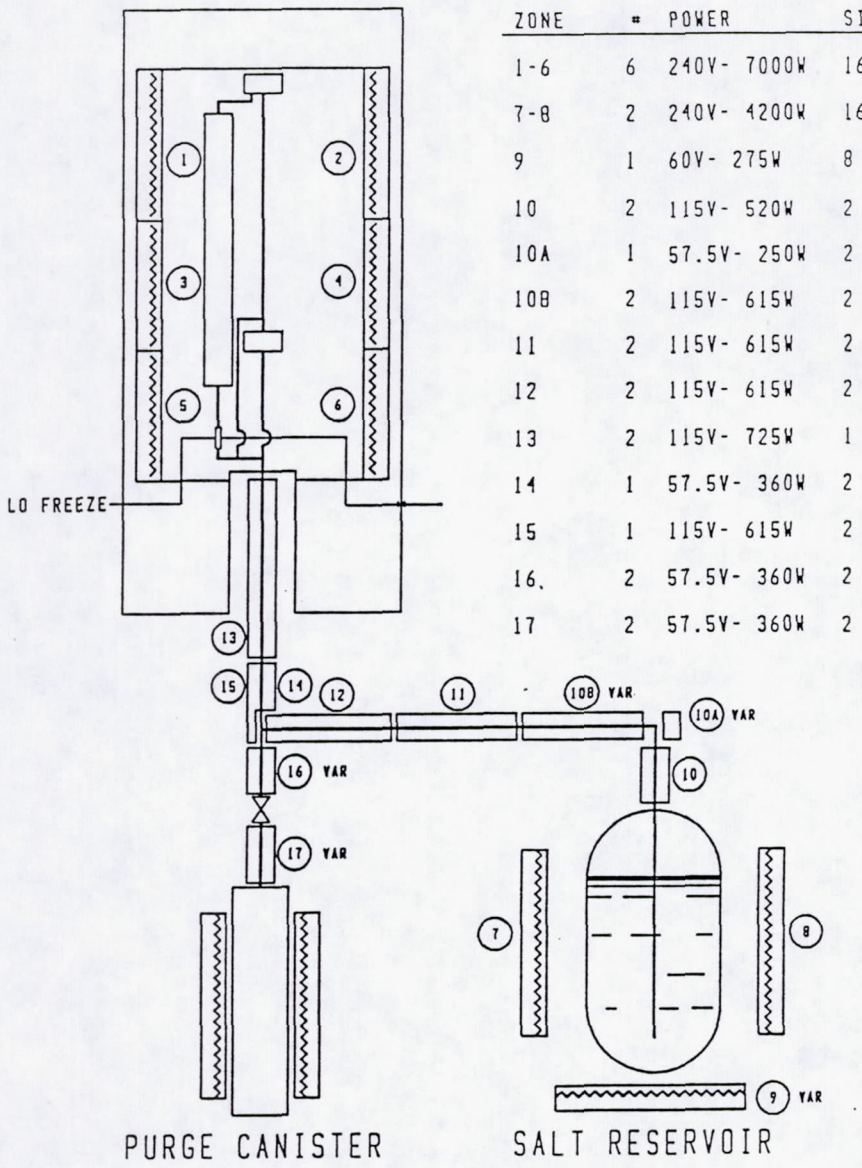

ZONE	#	POWER	SIZE (INCHES)
1-6	6	240V- 7000W	16 X 20 X 30
7-8	2	240V- 4200W	16 X 20 X 24
9	1	60V- 275W	8 X 10 X 2
10	2	115V- 520W	2 3/8 X 3 1/4 X 6
10A	1	57.5V- 250W	2 3/8 X 3 1/4 X 2 1/2
10B	2	115V- 615W	2 3/8 X 3 1/4 X 8
11	2	115V- 615W	2 3/8 X 3 1/4 X 8
12	2	115V- 615W	2 3/8 X 3 1/4 X 8
13	2	115V- 725W	1 1/4 X 2 1/16 X 18
14	1	57.5V- 360W	2 3/8 X 3 1/4 X 4
15	1	115V- 615W	2 3/8 X 3 1/4 X 8
16	2	57.5V- 360W	2 3/8 X 3 1/4 X 4
17	2	57.5V- 360W	2 3/8 X 3 1/4 X 4

Figure 4-8: HTTES Heater Element Locations

to mix the molten salt inside the reservoir; (3) adding a mechanical valve to the transfer line to isolate the salt reservoir from the heat storage tubes and prevent distillation of the LiF from the salt mixture; and (4) procedural changes to reduce the heat storage tube time at temperature to the minimum to ensure a clean and complete fill.

The 2 attempts to fill the first 6 SDHRT heat storage tubes resulted in damage to the felt metal inside the TES annulus. The tubes were at temperature for a period exceeding 57 hours and caused the nickel felt to sinter and compress to the bottom of the tube assembly (since the tubes are filled vertically). Two additional heat storage tubes were ordered by Boeing and manufactured by Pacific Scientific from the remaining raw materials leaving no more spares for the program. The 6 damaged tubes were then used in a 6-tube demonstration fill to ensure that the modifications to the facility had corrected the problems prior to filling any more receiver tube assemblies. The 6-tube demonstration fill operation was successful in completely filling the 6 damaged tube assemblies. Therefore, the filling operations for the remaining 24 receiver tubes continued.

The next 3 fill operations only completed the filling 12 of the 18 heat storage tubes. Further analyses of the facility showed the incomplete filling of some tubes was due to blockage by small metallic contaminants present in the salt. Additional salt analysis showed the metallic contaminants were present in the as-received salt in trace quantities. These were never a problem in the small canister fills because the quantity of salt used was small. However, in a full-scale fill, 88 kg (194 lbs) of salt produced something on the order of 91 g (0.2 lbs) of contaminants and because the inlets of the heat storage tubes are essentially a filter, salt flow was blocked. The system of salt manifolds were changed to the current configuration to fill from both the bottom and top of the heat storage tube and a filter was added upstream of the manifolds to remove the particulates from the salt prior to entering the heat storage tubes. This was the configuration described previously.

The next 2 fill operations completed filling all 12 tubes with salt within about 5 minutes after the initiation of the pressurizing gas to the salt reservoir. All problems with the molten salt HTTES facility were finally corrected. A summary of the results of all HTTES fill operations is given in Appendix A.

4.3 PCM Tube Sealing Operations

After cool down, the tubes were removed from the HTTES facility and the inlet and exit end PCM tubes were cut to a 19 mm (0.75 in) length. The solid salt was then reamed from the entire tube length to just past the end-cap. A small piece of tygon tubing is used to evacuate the PCM tubes and provides a temporary seal until they are sealed permanently by welding. The tubes were then boxed and shipped to the Boeing EB-Weld facility.

The PCM tubes are sealed by an EB weld in a vacuum chamber. Figure 4-9 shows a small test canister loaded inside the EB facility. Welding in a vacuum provides a sealed tube with no entrainment of air to react with the salt once it is molten. The complete EB weld process is described in references 11 and 23. A brief description of the process follows:

1. The heat storage tube is removed from the shipping crate and mounted into the weld fixture. The tygon tube is removed and the PCM tube is cleaned.
2. Inconel 617 weld wire, 0.9 mm (0.035 in) in diameter, is also cleaned and cut into 25.4 mm (1 in) lengths.
3. After cleaning, several strands of weld wire are inserted into and trimmed even with the end of the fill tube.

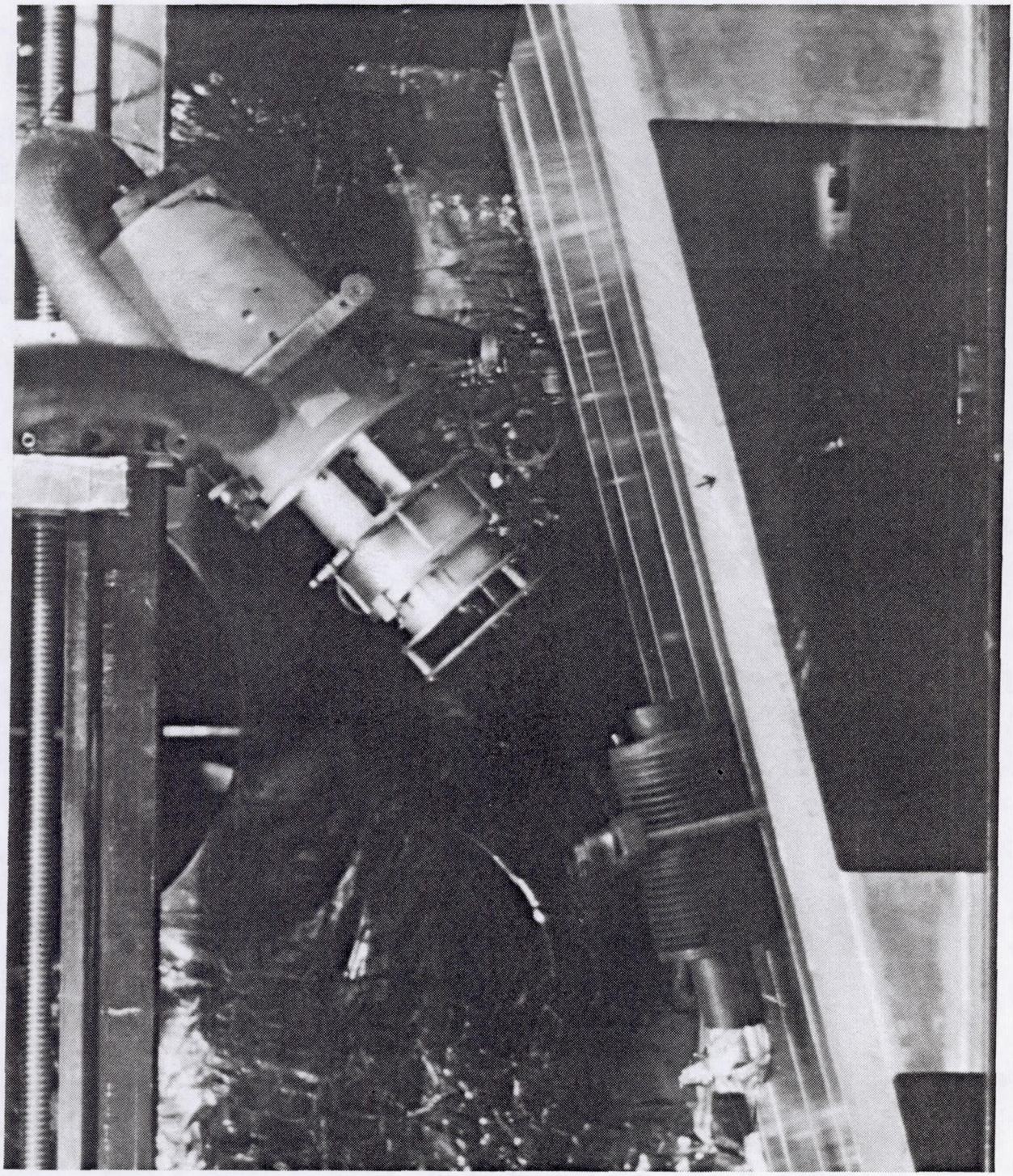

Figure 4-9: EB Welding PCM Fill Tube Seal on a SDHRT Test Canister

4. The tube is inserted into the EB vacuum chamber mounted in a special fixture and the electron beam is aligned at roughly a 45° angle to the axis of the tube.
5. The chamber is pumped down to a pressure of at least 1 X 10^{-4} torr.
6. Final alignment of the beam is performed at low power level by focusing it to the center of the cross-sectional area (seen by heating of the surface).
7. The beam is then defocused to cover the entire cross-sectional area of the tube. This ensures even heating of the weld wire and tube walls causing them to melt at the same time.
8. Power is applied and the weld is made in short, approximately 1-2 second bursts.
9. The tube was then removed from the chamber, turned 180°, and the process is repeated for the other end. The heat storage tube is removed from the chamber.
10. The center of the weld "ball" is filed flat to remove contaminants that collect in this region during solidification.
11. The weld is dye-penetrant inspected. If the weld shows porosity, the fill tube is cut back past the weld and the process is repeated until a good weld is achieved.

Almost all of the EB weld operations went smoothly. However, the weld attempt on the inlet end PCM tube on heat storage tube serial #6 was unsuccessful and several attempts to reweld caused the PCM tube to be shorten to where further welding could have damaged the end-cap. Therefore, a decision was made to replace the fill tube and begin the weld process over again.

The repair was made by Lukas Machine by a clever modification of a carbide end-mill tool for machining and preparing the surface of the end-cap enabling a full-penetration weld to be made on a replacement fill tube on the assembly. The sealing operation on the new PCM proceeded without incident. No cause was found to explain the problem encountered during the first attempt to EB weld the PCM tube.

4.4 Heat Storage Tube Status

The 24 SDHRT heat storage tubes were delivered to Lukas Machine for assembly into the heat receiver after completion of the EB welding. An inspection of the tubes showed some minor damage to several of the tubes during all of the handling operations. Figure 4-10 shows the most serious damage which is a rather sharp dent to the peak convolution near the middle of heat storage tube serial #6. It was intended to choose the best 24 heat storage tubes from the original 28 made but only 24 were completed due to the loss of 6 tubes during the molten salt fill operations. However, none of the damage observed is believed to be serious enough to cause a compromise of the TES containment during operation of the receiver. A summary of all 30 heat storage tubes fabricated under the SDHRT contract is given in Figure 4-11. Cavity position indicates where tubes were assigned for installation into the heat receiver at Lukas is illustrated in Figure 4-12.

4.5 Receiver Structure, Plenums, Piping, and Assembly

The receiver structure, gas plenums, and gas piping sections were fabricated by Lukas Machine in Seattle, WA. Lukas also assembled the heat storage tubes into the receiver cavity. Lukas Machine was chosen to build this hardware because (1) the Lukas welders are qualified to ANSI B31.1, 6-g position pipe welding (2) they have in-house helium leak checking capabilities; and (3) they bid the lowest cost to perform the work.

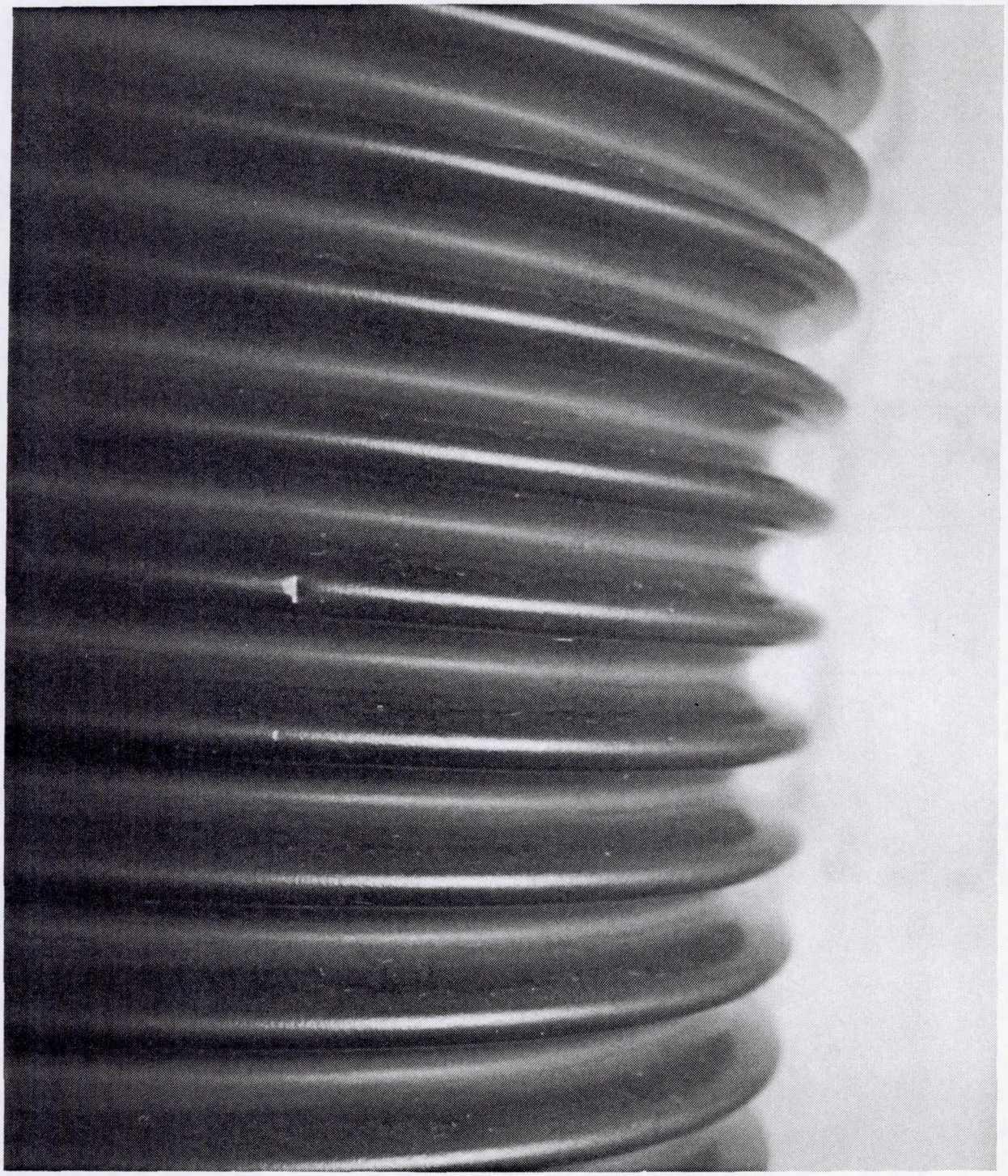

Figure 4-10: Damage to Mid-Length Convolution on Heat Storage Tube Serial #6

HX/TES Tube Assemblies
Status Summary

Tube #	Serial #	Fill #	Salt Wt (lbs)	Active Length (in)	C.G.	Cavity Pos.	Status
1	1	3	30.5	60.781	28.1	18	installed into rcvr
2	2	6tD	31.5	-	-	-	damaged felt, in TCPS lab, scrapped
3	3	3	29.5	60.750	27.6	6	installed into rcvr
4	4	5	30.5	60.563	27.6	2	installed into rcvr
5	5	5,7	31.0	60.750	26.9	1	installed into rcvr
6	6	3	30.5	60.719	27.8	3	installed into rcvr, small dent on peak convolution near mid pt @ 180°, source unknown
7	7	3	30.5	60.750	28.0	24	installed into rcvr
8	8	3	29.5	60.594	27.8	15	installed into rcvr
9	9	1,2	0	-	-	-	sectioned to examine condition of felt metal
10	10	3,7	30.5	60.781	27.8	20	installed into rcvr
11	11	4,7	31.0	60.906	27.8	7	installed into rcvr
12	12	6	31.0	60.875	27.7	4	repaired fill tube, installed into rcvr, instrumented with surface T/C's
13	16	6	31.0	60.625	27.6	10	installed into rcvr
14	17	6	31.5	60.906	27.8	16	installed into rcvr
15	18	6	30.5	60.969	27.8	13	installed into rcvr
16	19	5,7	31.0	60.563	27.8	12	outer TES T/C inlet end broke during fill, installed into rcvr, instrumented with surface T/C's
17	20	5,7	31.5	60.781	28.2	23	installed into rcvr

Figure 4-11: SDHRT Heat Storage Tube Status

Tube #	Serial #	Fill #	Salt Wt (lbs)	Active Length (in)	C.G.	Cavity Pos.	Status
18	21	4	30.5	60.719	28.2	11	installed into rcvr
19	22	6	31.0	60.750	28.0	14	installed into rcvr
20	23	4	30.0	60.750	27.1	21	installed into rcvr
21	24	6tD	31.0	-	-	-	damaged felt, at Lukas, scrapped
22	26	6tD	31.0	-	-	-	damaged felt, in TCPS lab, scrapped
23	27	6tD	31.5	-	-	-	damaged felt, in TCPS lab, scrapped
24	29	4	30.0	60.688	27.6	9	installed into rcvr
25	30	4	30.5	61.063	27.1	5	installed into rcvr
26	31	5,7	31.5	60.719	26.9	17	installed into rcvr
27	32	4	31.0	60.844	27.3	8	installed into rcvr
28	33	6tD	30.5	-	-	-	damaged felt, in TCPS lab, scrapped
29	34	6	31.0	60.813	27.8	22	installed into rcvr
30	35	5	30.5	60.688	28.5	19	outer inlet end TES T/C broken during EB sealing, installed into rcvr, instrumented with surface T/C's, small dent on peak convolution approx mid pt @ 0°, source Belfab

Notes:

1 6tD refers to 6 tube demo fill operation
2 Active length is measured from outside of opposite end end-caps
3 C.G. is measured from the outside of the exit end end-cap
4 Cavity position 1 begins at top of receiver, facing aperture, 7.5°-off centerline, and increments clockwise

Figure 4-11 (con't): SDHRT Heat Storage Tube Status

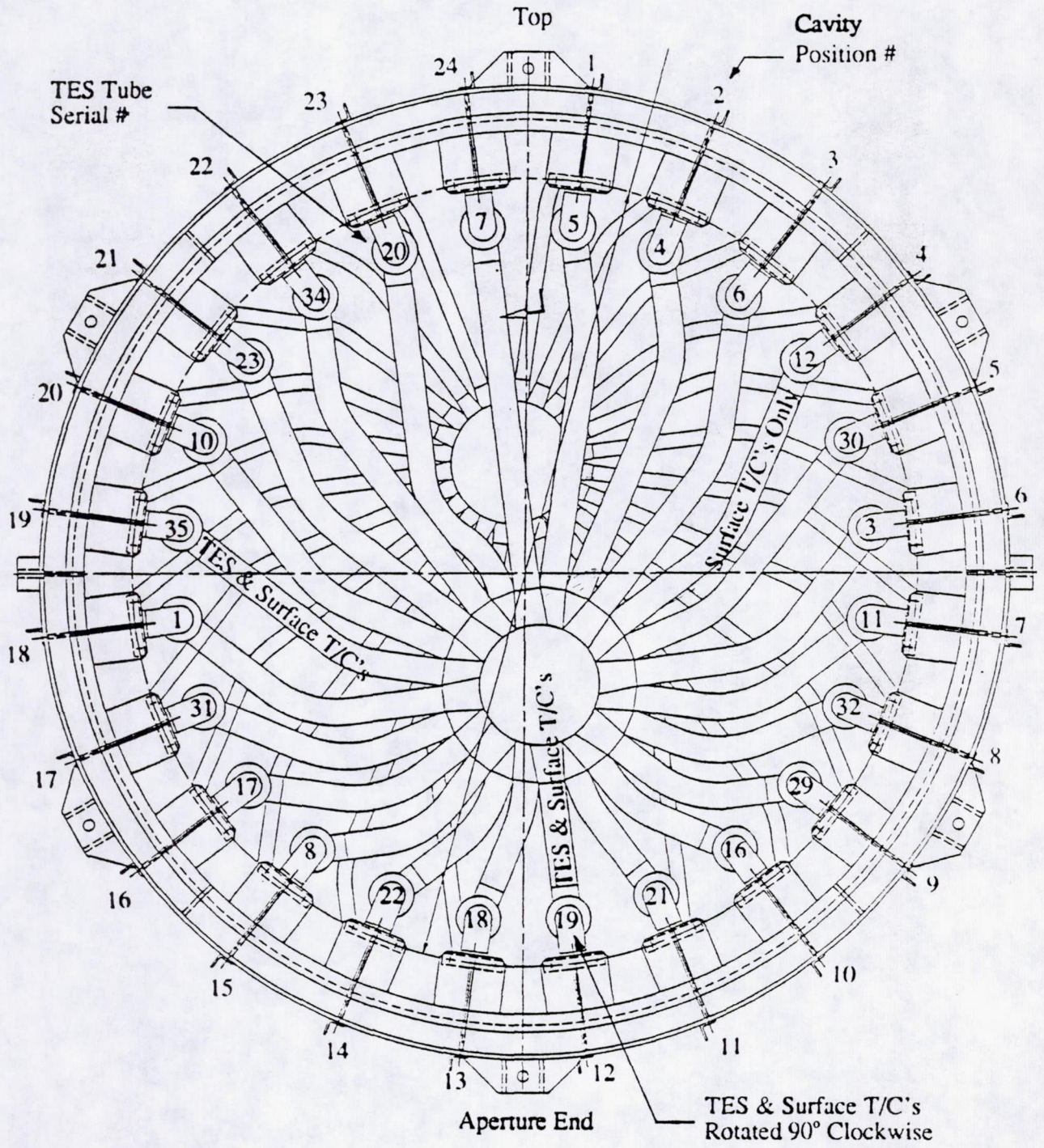

Figure 4-12: Location of SDHRT HX/TES Tube Assemblies in Receiver Cavity

A 1-1/2 year delay in the program schedule was encountered during the assembly of the receiver because of problems encountered here at Boeing during the salt casting operation. After these problems were corrected and the fill operation was completed, we delivered the heat storage tubes to Lukas. They then accelerated their work to reduce the impact of this delay on the overall program schedule. The quality of their work is excellent as demonstrated by a 99 percent acceptance rate on the nearly 350 of x-ray and helium leak check inspectable welds made in completing the fabrication of the receiver. Therefore, re-work was limited to just 3 welds on the entire assembly. A number of red-line changes were made during the assembly process and Lukas personnel worked closely with us to eliminate any increases in the cost of the overall effort. Therefore, the heat receiver was completed on-time (per the modified schedule) and without any increased cost even though the work was performed 1-1/2 years later than scheduled. In addition, all our materials and subassemblies were carefully stored during this delay without additional charge.

The receiver structure is made from 304 stainless steel. Welding of the support angles to the front and rear structural rings caused some distortion of the structural assembly but otherwise no problems were encountered. The structure was straighten after welding was completed but still shows a small amount of residual distortion. This distortion had no effect on the alignment of the internal components or the support of the receiver in a support structure for testing.

All pressure piping components, including the plenums, piping sections, and HX tube connections were welded and inspected to the requirements of ANSI B31.1 including full radiograph and helium leak checking. Consumable inserts were used to weld the piping elements. The inserts produced a very repeatable and reliable weld and resulted in an almost 100 percent acceptance of the weld joints in the pressure piping network.

Figures 4-13 and 4-14 show the inlet and exit plenums during buildup. The plenums are made from off-the-shelf pipe components (caps, pipe, and reducers). The inlet components are schedule 40, 304 stainless steel and the exit components are schedule 80, 304 stainless steel. The plenums were radiographed and helium leak checked before further buildup. Both plenums successfully passed the inspections.

After completion of both the inlet and exit plenums, the radial extension sections and elbows were welded to the plenums. Figure 4-15 shows the inlet plenum with the radial extension sections after welding. These assemblies were then radiographed and helium leak checked. All welds passed inspections. A large layout board was used to position the elbows before and after welding as illustrated in Figure 4-16. Again, weld distortion caused a slight misalignment of the tubes with a maximum deviation of about 6 mm (1/4 in) after straightening. The 2 plenums were then secured into position (relative to each other) by using U-bolt clamps as shown in Figure 4-16.

The assembly of the heat receiver was completed inside the structural cage. The inlet and exit plenums were hung inside the cage using a system of turnbuckles for vertical positioning as shown in Figure 4-17. The "U" shaped sections that transition the inlet 25.4 mm (1 in) diameter stainless pipes to the 51 mm (2 in) diameter Inconel 617 tubing were welded to the inlet ends of the heat storage tubes, holding the dimensions shown in the fabrication drawing. This process is shown in Figure 4-18. The tubes were rotated to ensure that the longitudinal weld seam on the bellows faced the cavity side wall. Plastic pipe sections were secured around the TES containment tubes to protect the convolutions during all handling operations (until after the receiver was insulated). A close-up of the 51 mm (2 in) stainless pipe to 51 mm (2 in) Inconel 617 tube reducer section is shown in Figure 4-19. The tube assemblies were then inserted inside the cage and the exit end HX tubes were scribed for cutting to their proper

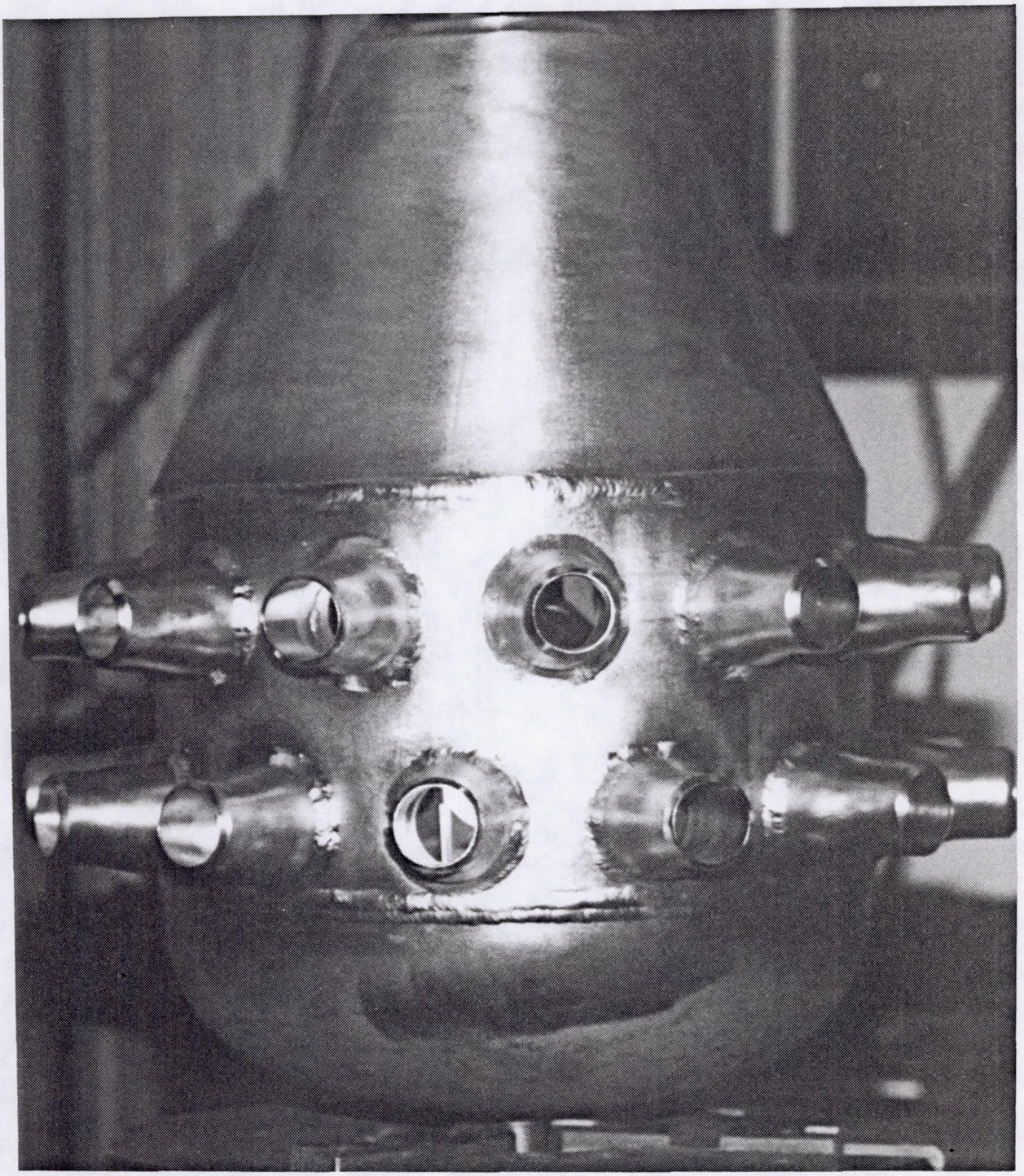

Figure 4-13: Inlet Gas Plenum During Buildup

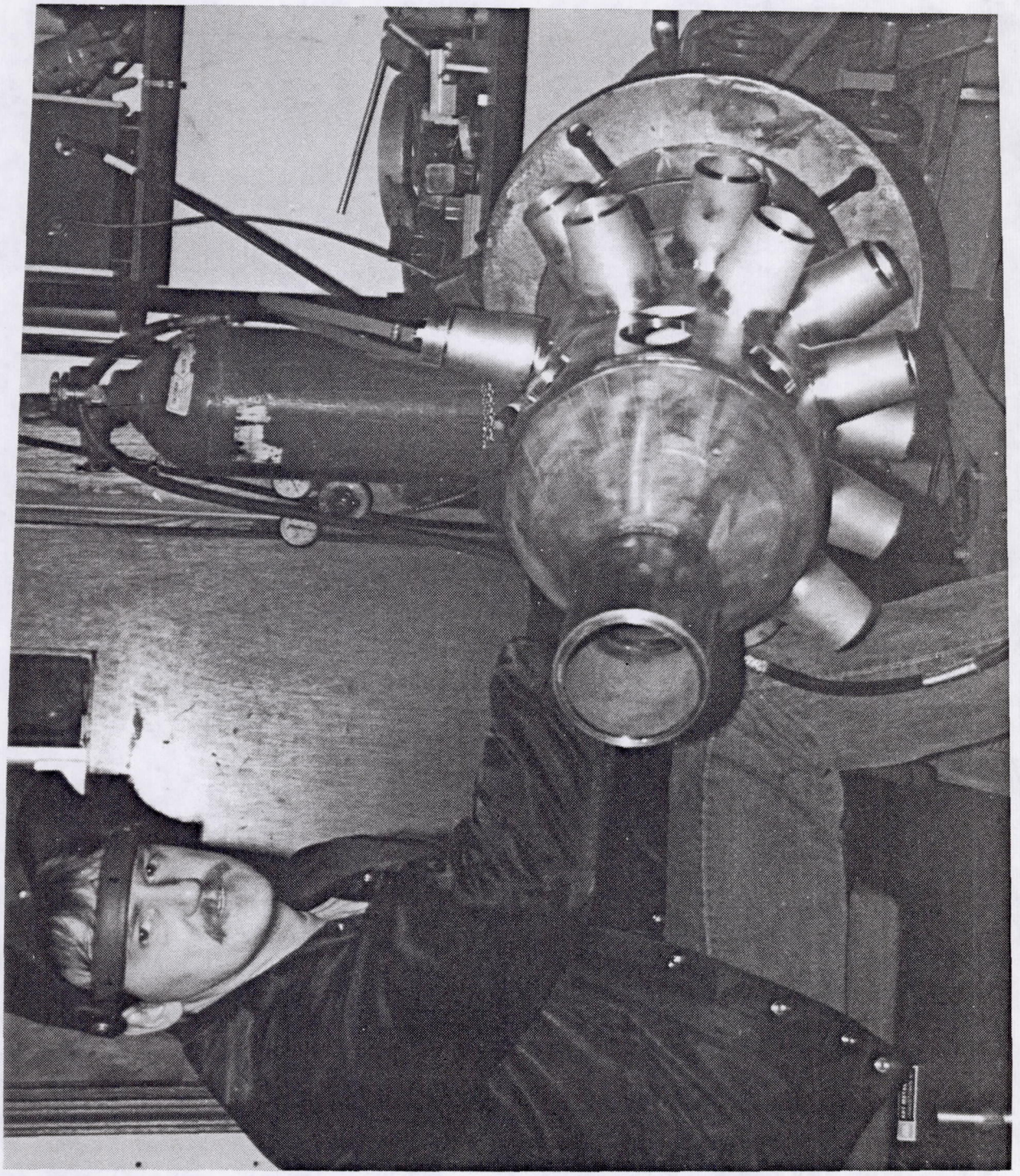

Figure 4-14: Exit Gas Plenum During Buildup

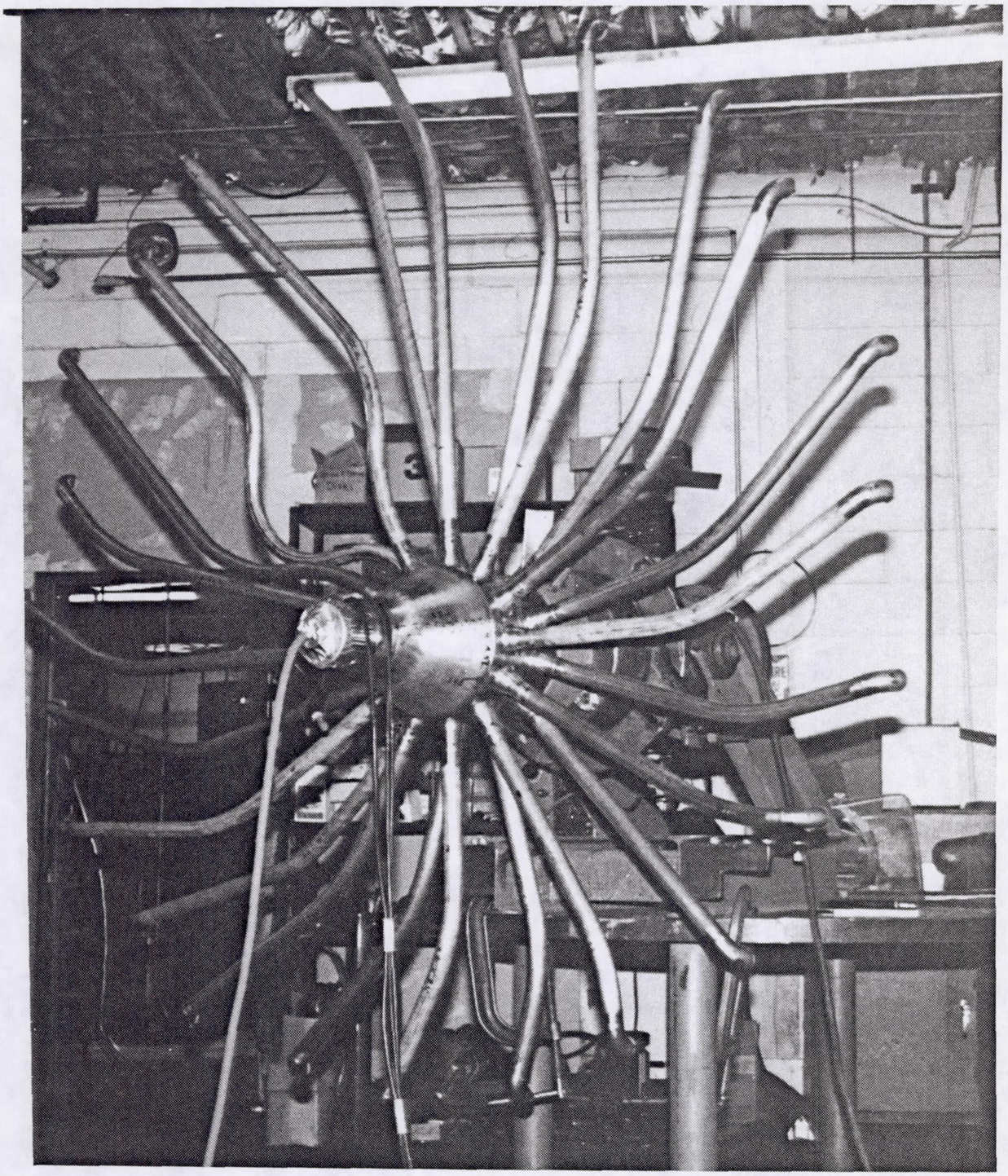

Figure 4-15: Inlet Plenum With Radial Extension Arms and Elbows

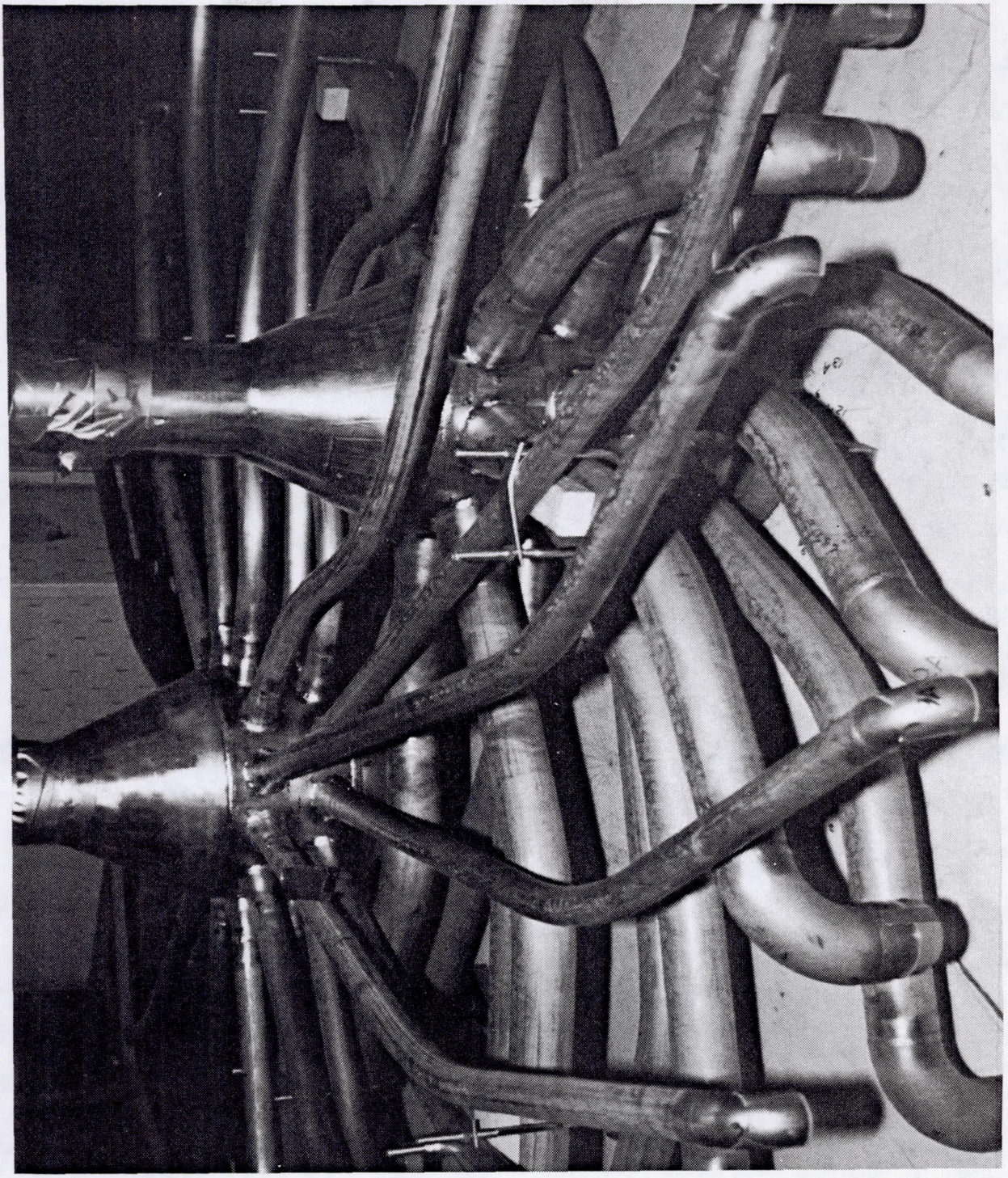

Figure 4-16: Layout Board Used to Align Radial Extension Arms on Plenums

Figure 4-17: Plenum Positioning Inside Structural Cage for Final Assembly of Heat storage Tubes Inside Receiver Cavity

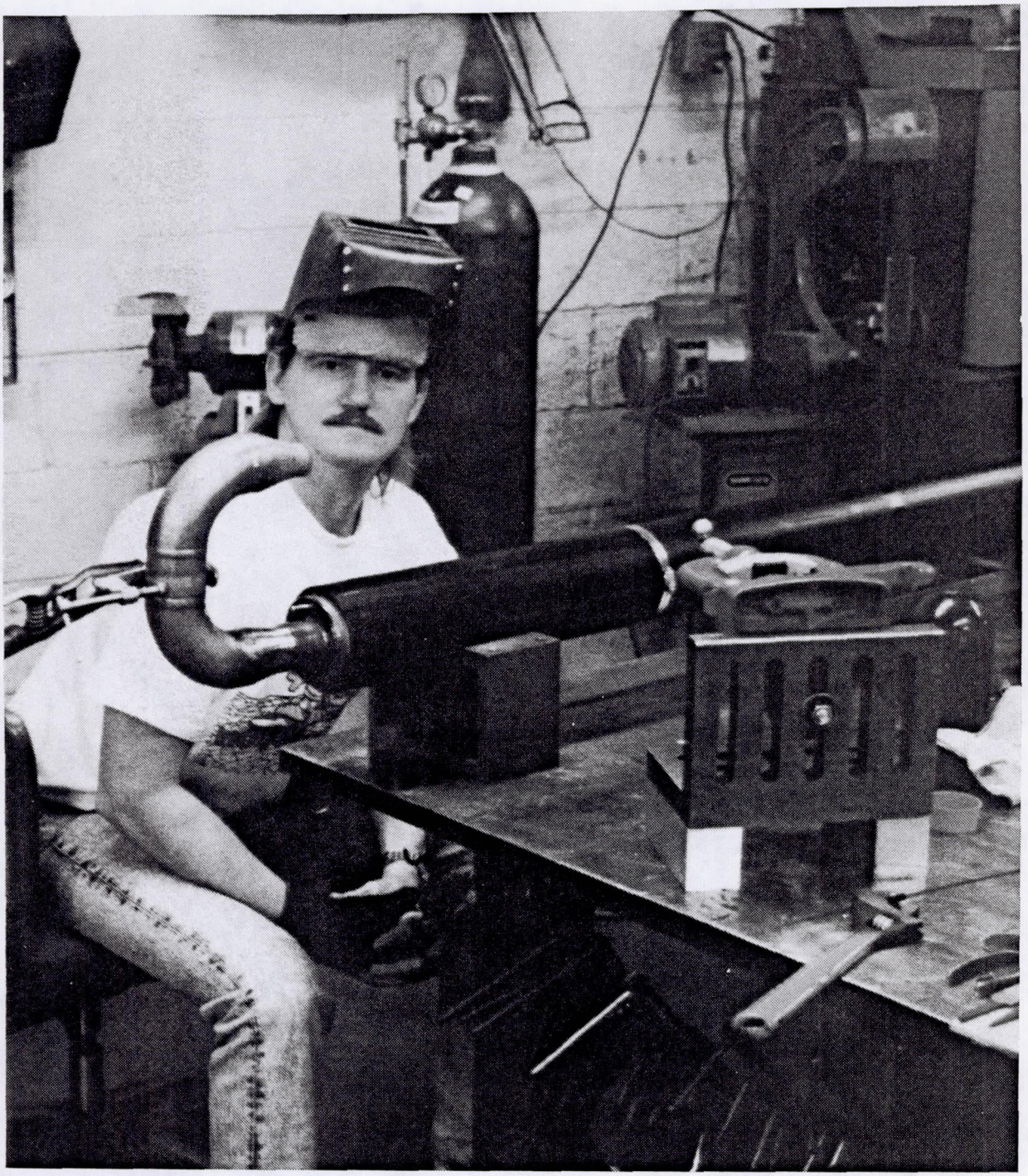

Figure 4-18: Welding the Pipe to Tube "U" Transition Section to the Inlet End of the Heat Storage Tubes

Figure 4-19: Close-up of the Stainless Pipe to Inconel 617 Tube Reducer Section Welds

length as shown in Figure 4-20. After removing the tube assemblies and cutting the exit end HX tubes to their proper lengths, they were inserted back through the structural cage and welded into place (connecting the exit end of the tubes to the exit plenums). The inlet and exit end welds were radiographed at the end of each day of work.

After all 24 tubes were welded into place, the inlet, 25.4 mm (1 in) diameter, straight tube sections, connecting the inlet plenum to the "U" transitions, were measured in place, cut, and welded at both ends. A close-up photograph showing the clamping arrangement of the heat storage tube assemblies to the front support ring plates and the initial root pass of the 25.4 mm (1 in) inlet pipe to the U-transition is shown in Figure 4-21. These welds were also radiographed at the end of each day of work.

Figures 4-22 and 4-23 show the receiver viewed from the front and rear respectively after all of the welding was completed. Note that the plenum support straps were not attached until after all of the receiver insulation was installed. A hydrostatic proof pressure test was conducted on the pressure piping network by filling the HX tubes, pressure piping, and plenums with distilled, deionized water and capping the plenums with high-pressure plugs. A port on one of the plugs was then used to introduce nitrogen gas to a pressure of 4 mPa (600 psig) and held at that pressure for 10 minutes. The proof pressure test was conducted with the receiver in a vertical position. The gas pressure was bled off from the plenums and the receiver was rotated 180° to drain the water from the system. A high-temperature (66±28°C) air blower was then used to dry out the tubing. The receiver was rotated to a horizontal position to conduct a helium leak check of the receiver pressure piping loop after completion of the hydrostatic test (Figure 4-24). The vacuum environment ensured no water remained inside the piping system. No leaks were detected.

4.6 Receiver Insulation

Receiver insulation was supplied and installed by John Manville. Boeing technicians assisted in the installation. The insulation was installed beginning at the back (plenum) end. The side-wall insulation was then installed beginning at the front (aperture) end of the cavity working back toward the back (plenum) end of the receiver. The front, aperture support insulation was installed last.

Sectional pieces were prepared at the factory and included the stitching of the cavity and exterior side quartz and E-glass fabrics. Sections were cut to fit during installation (Figure 4-25). Internal insulation, .i.e, non-lined Cerablanket, was supplied either cut to size (back end) or on rolls (cavity side walls). Figure 4-26 shows the cavity back-wall section after installation. The insulation was secured by stitching it to either pressure piping components on interior sections or to the outer structure. Both quartz and stainless steel thread were used to provide redundant support. Figure 4-27 shows a close up of the thread looped around the radial extension arms of the exit plenum for the sections that formed the cavity back-wall. Figure 4-28 shows the 2 gaps formed by the insulation between the inlet and exit plenum radial extensions arms.

The cylindrical cavity sections were installed in a similar fashion. The inner pieces were stitched to the 25.4 mm (1 in) diameter inlet tubes while the outer sections were stitched through to the inside cavity, around the 25.4 mm (1 in) tubes, and back out to the outer structure as shown in Figure 4-29. Small, aluminized tabs were used to protect the thread from the coarse surface of the structural support angles. Figure 4-30 shows the technicians feeding the needles through to a single technician on the inside. The completed inside cavity side and back walls

Figure 4-20: Marking the Exit End of Heat Storage Tube for Cut-to-Fit At An Assigned Location

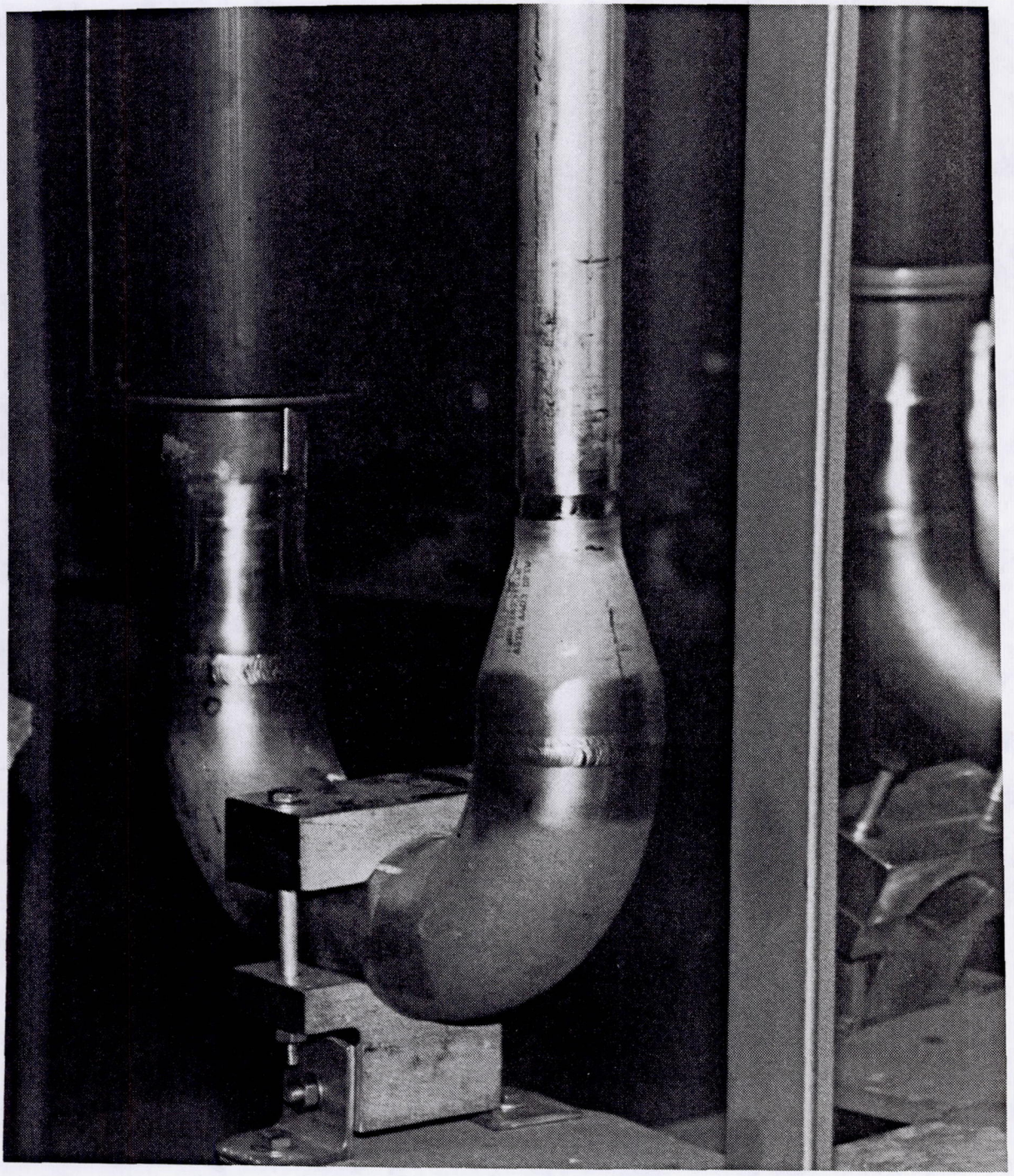

Figure 4-21: Close-up of the Front Brackets and Inlet Pipe Weld to Reducer Transition Section

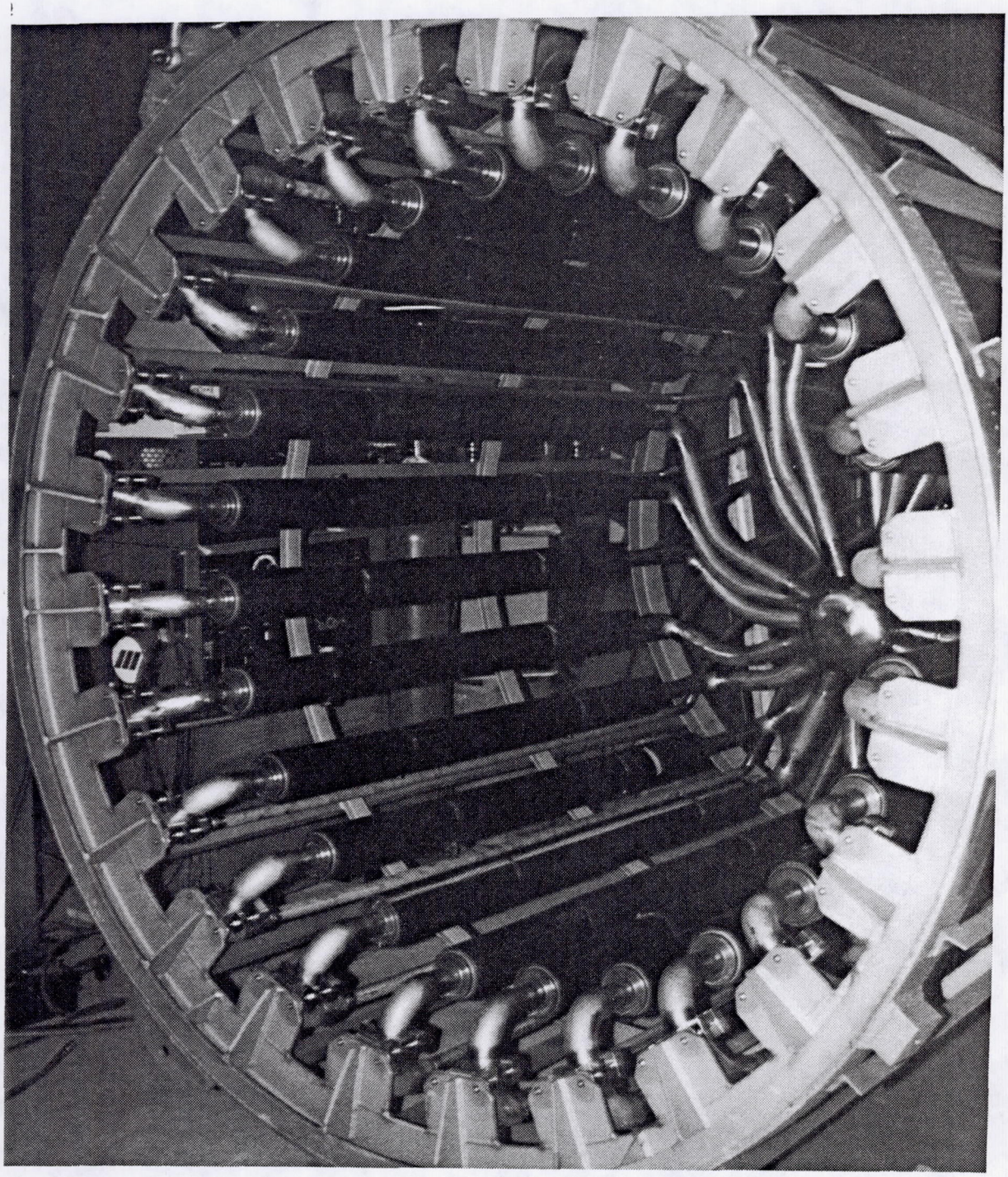

Figure 4-22: Front View of SDHRT Heat Receiver Prior to Installation of Insulation

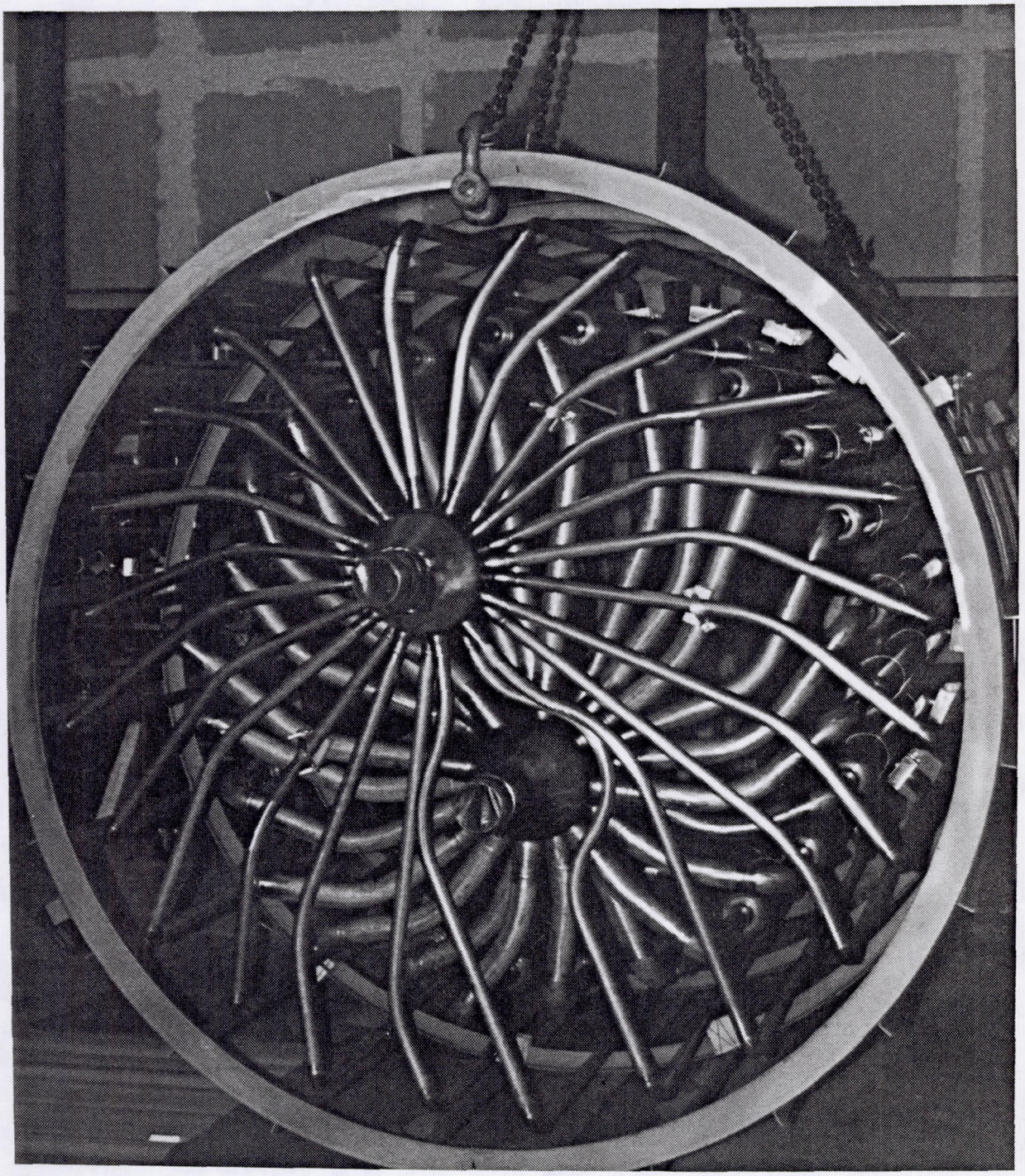

Figure 4-23: Rear View of SDHRT Heat Receiver Prior to Installation of Insulation

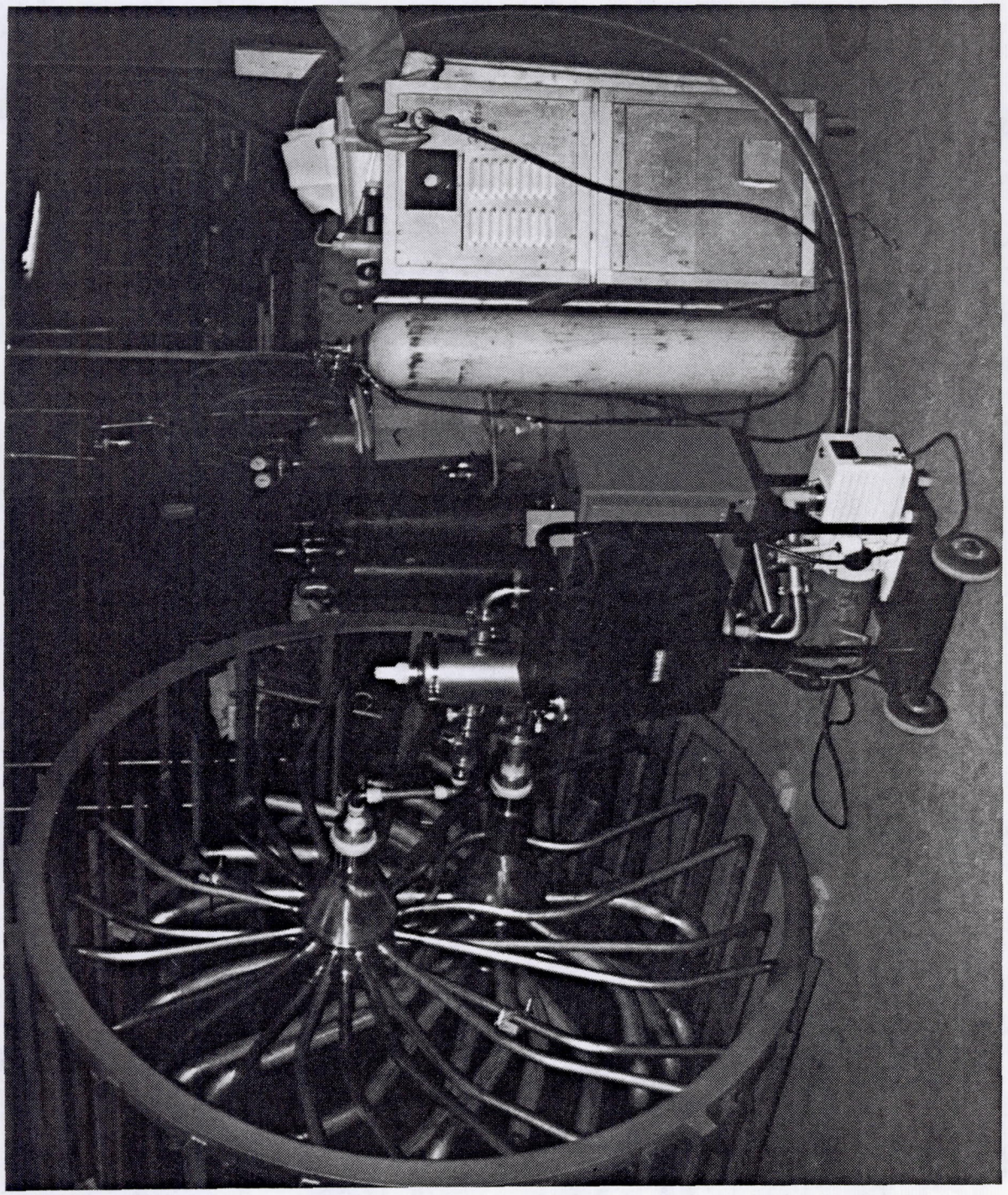

Figure 4-24: Final Helium Leak Check of SDHRT Receiver After Hydrostatic Proof Pressure Test

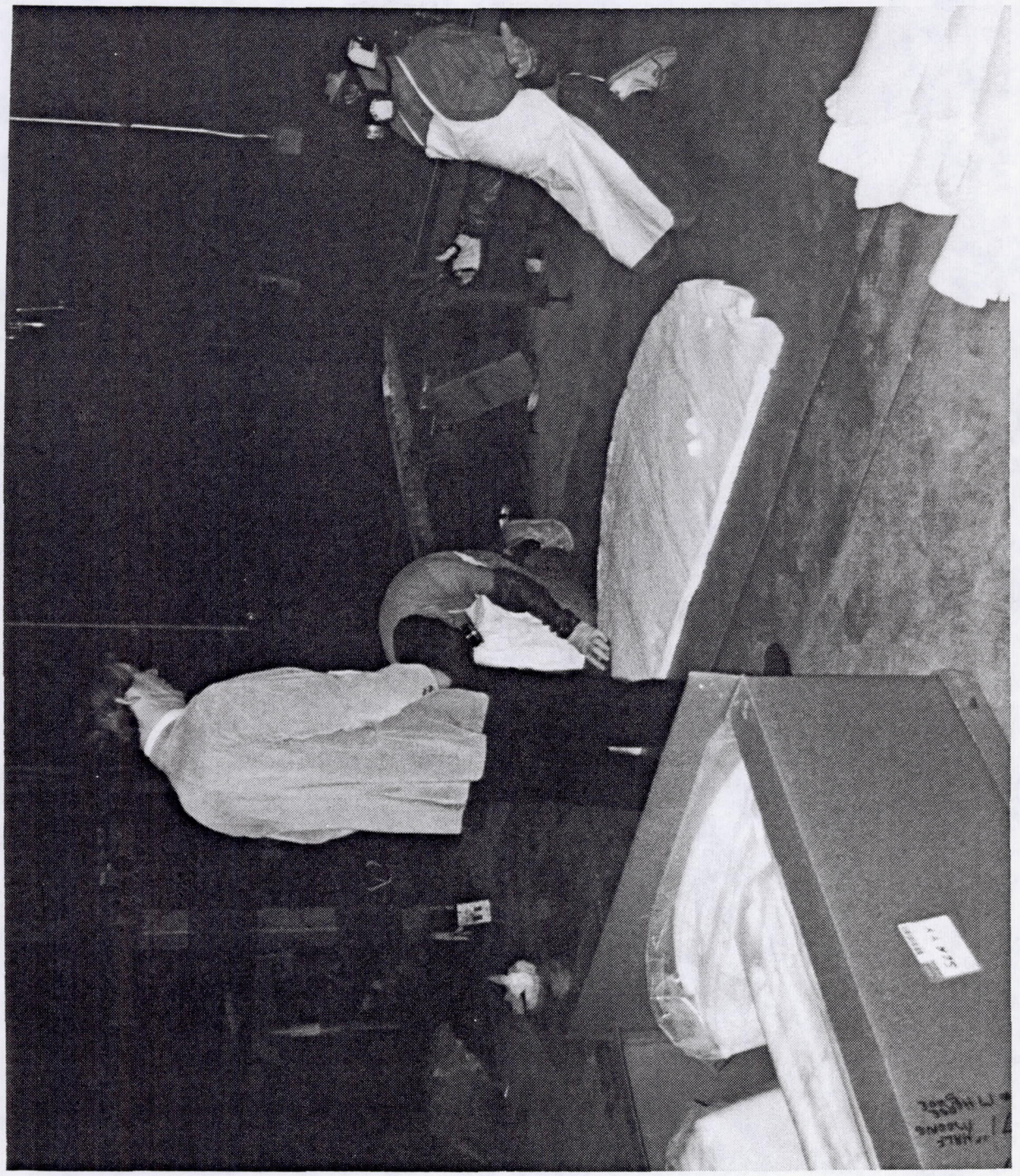

Figure 4-25: Preparing Insulation for Installation in the Receiver

Figure 4-26: Completed Inner Cavity Back Wall Insulation

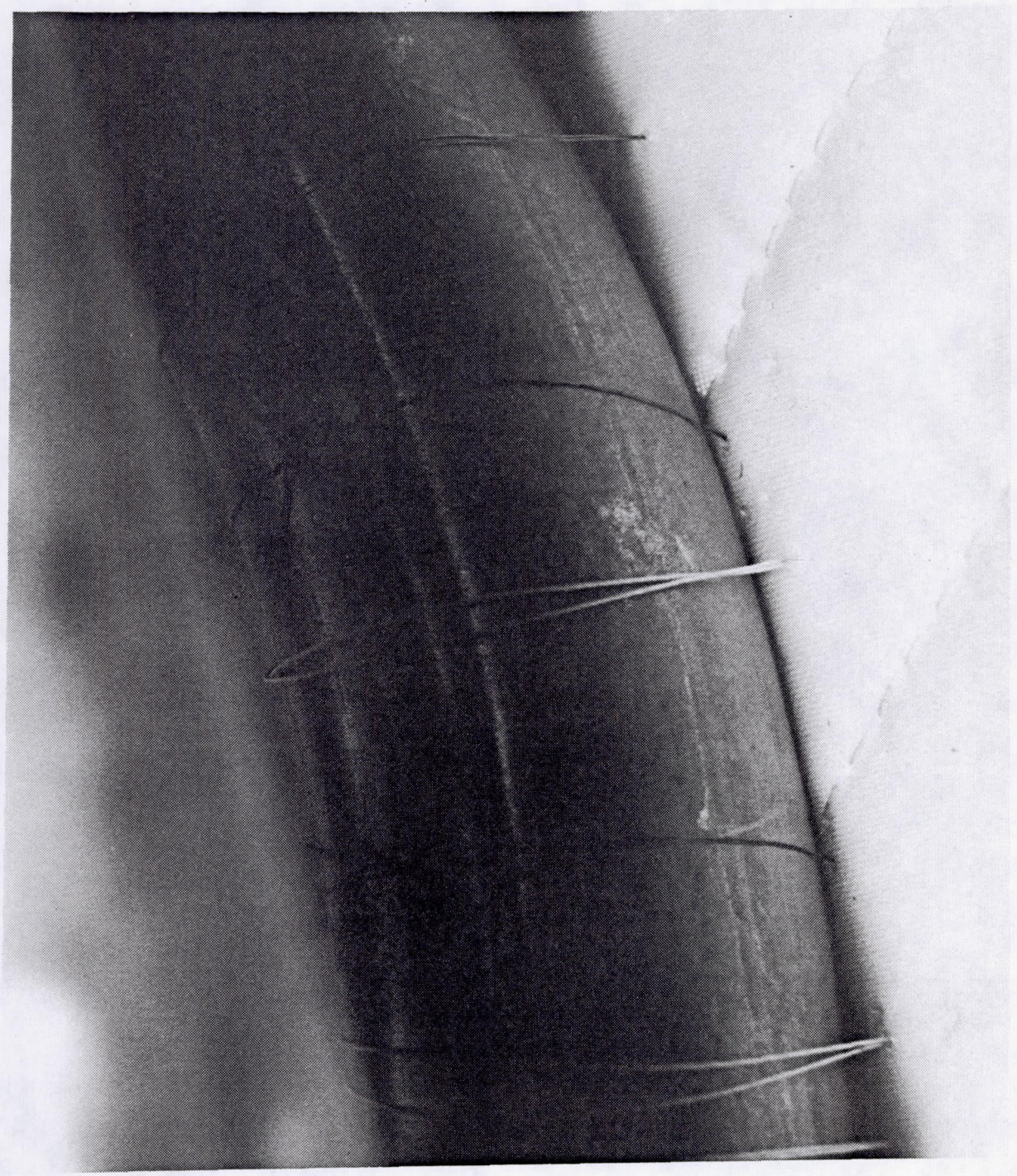

Figure 4-27: Threaded Attachment of Cavity Back Wall Insulation to the Radial Extension Piping Arms on the Exit Gas Plenum

Figure 4-28: Gaps Formed in the Regions Containing the Radial Extension Piping Arms of the Inlet and Exit Gas Plenums

Figure 4-29: Installation of the Cylindrical Side Wall Insulation

Figure 4-30: Technicians Feeding Needles Through the Insulation To Secure the Cerablanket To the Inside Piping and Cavity Walls

of insulation are shown in Figure 4-31. A close inspection of Figure 4-31 shows the stitching pattern of the back wall insulation to the exit plenum radial extension arm tubes. Instrumentation shown in the picture will be described in the ADRT Test Report when complete.

All of the front end insulation sections were cut to fit around the HX tubing, tube support brackets, and the gussett plates on the front structural ring. The pieces are secured by stitching to the HX tube and/or exterior structure. Figure 4-32 shows the front section of insulation for the receiver (shown without the aperture plug installed). The wires seen attached to the heat storage tubes are sheathed thermocouples installed for testing.

After installation of the insulation, the plenum support straps were connected to the plenums and rear structural ring and the pressure piping was back filled with argon to 136 kPa (5 psig). The straps and pressurizing valve are shown in Figure 4-33. The completed receiver is shown in Figure 4-34 ready for loading into the shipping container for delivery to the test site. Wires shown tied to the outside structure are the thermocouple leads for the internal thermocouples.

4.7 Shipment

The receiver was packaged for shipment in accordance with commercial practice and in a manner to protect it from corrosion, deterioration, and physical damage during shipment. The packaging conforms to interstate carrier regulations. The shipping container dimensions are 2,642 mm wide X 2,642 mm deep X 3,505 mm high (104 X 104 X 138 in) and the total shipping weight is approximately 2,724 kg (6000 lbs). The receiver is shipped in a vertical orientation, bolted to a floating pallet as shown in Figure 4-35. It is wrapped in plastic but openings were cut in the side to prevent condensation. An over-box crate is then built up around the receiver as shown in Figure 4-36. The outside crate is treated with a water-proof coating. The point of delivery and acceptance of the SDHRT receiver by NASA-LeRC is as follows:

Boeing Tulalip Test Site
Area 5
11224 34th Ave N.E.
Marysville, WA 98270

At the time of delivery, a Material Inspection and Receiving Report (DD Form 250) was prepared and delivered under separate cover to the NASA Contracting Officer, Mr. Curt Brocone, at NASA-LeRC in Cleveland, OH. Figure 4-37 shows the receiver after delivery to the Tulalip test site and ready for installation in the test facility. The receiver was delivered in June 1990.

Figure 4-31: Completed Cavity Side and Back Wall Insulation

Figure 4-32: Front Aperture End Insulation (shown without aperture plug)

Figure 4-33: Rear Plenum Support Straps and Pressure Piping System Purge With Dry Argon

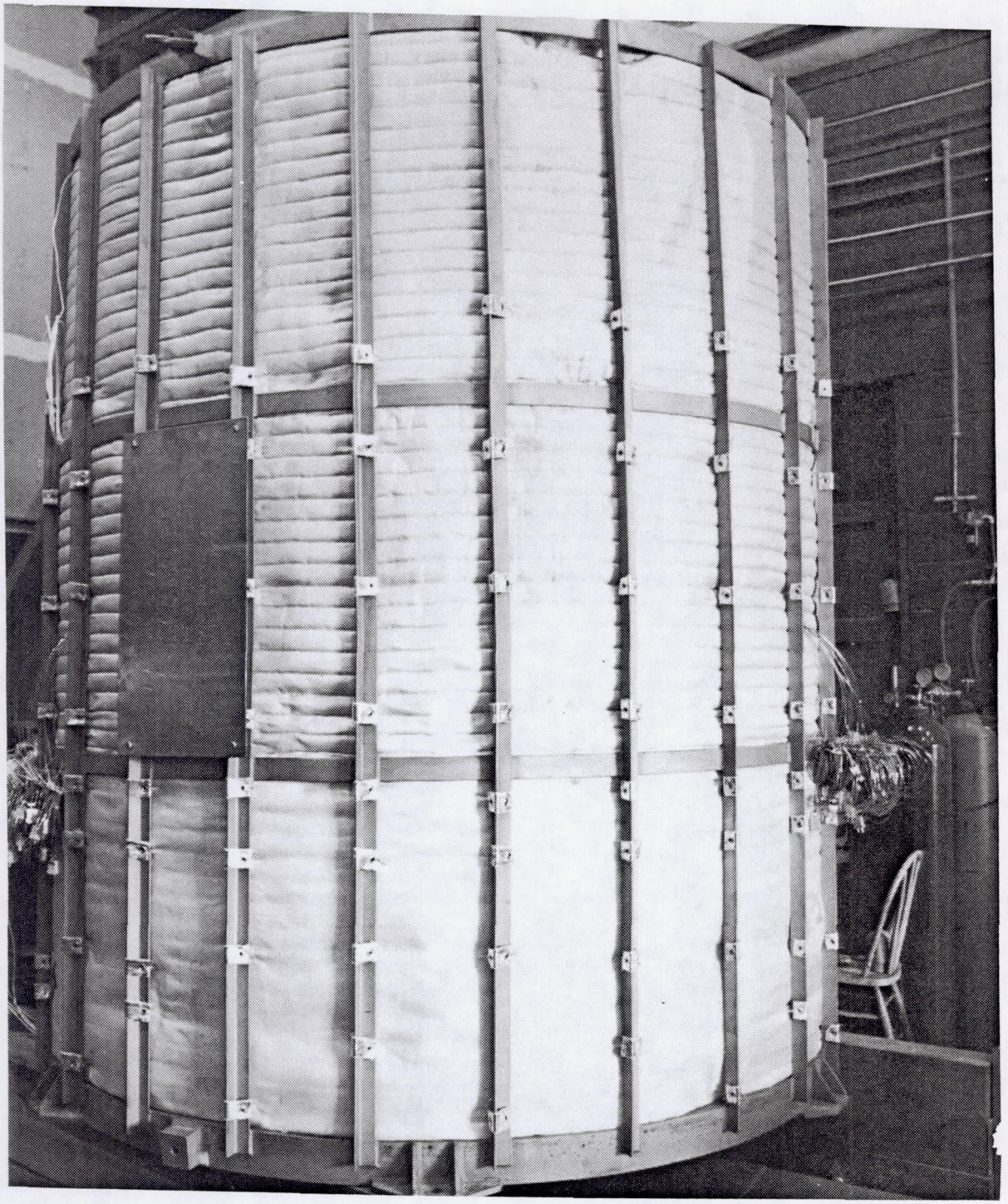

Figure 4-34: Completed SDHRT SD Heat Receiver

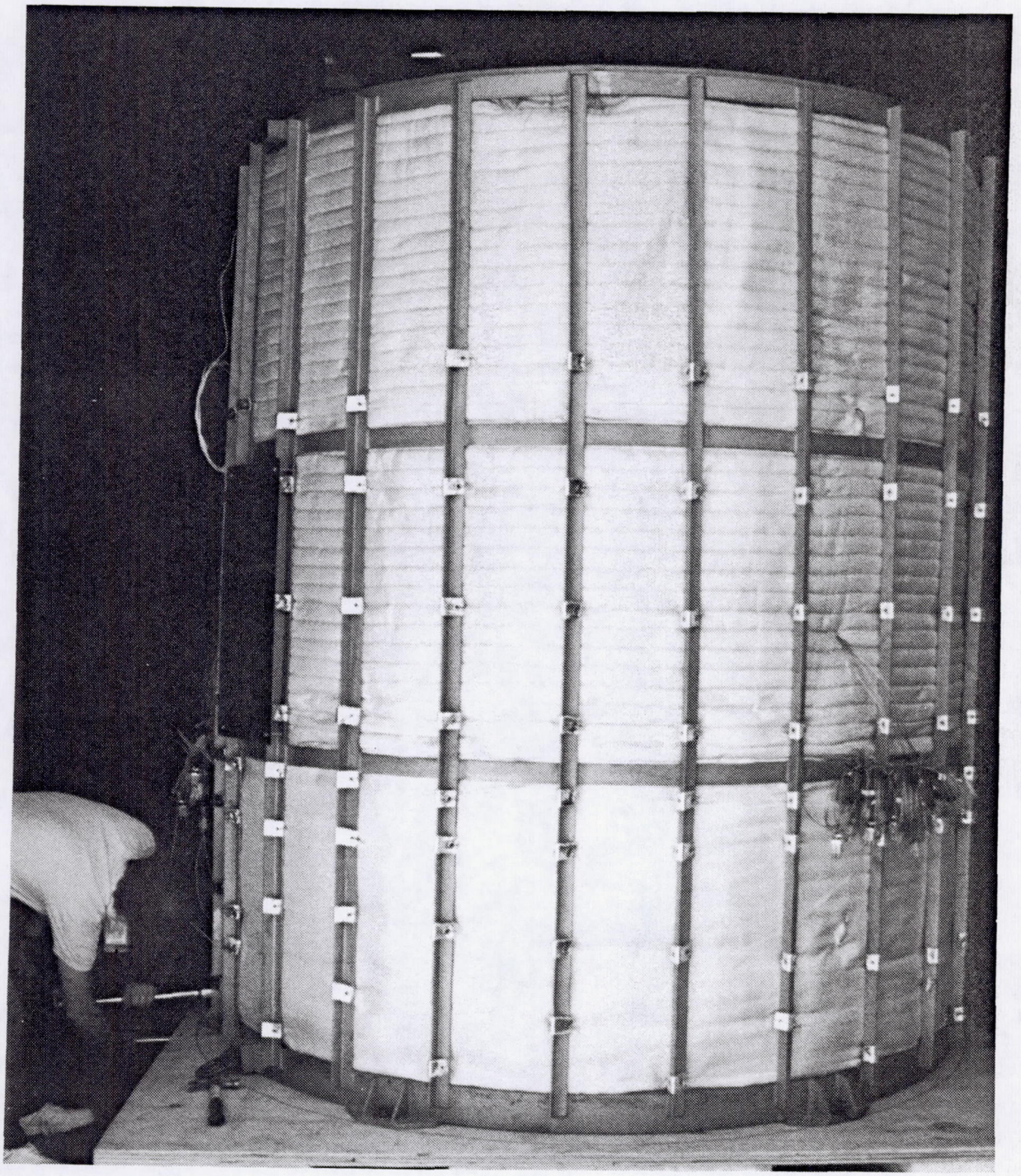

Figure 4-35: Securing the SDHRT Heat Receiver to a Floating Pallet During Packaging for Shipment to Test Site

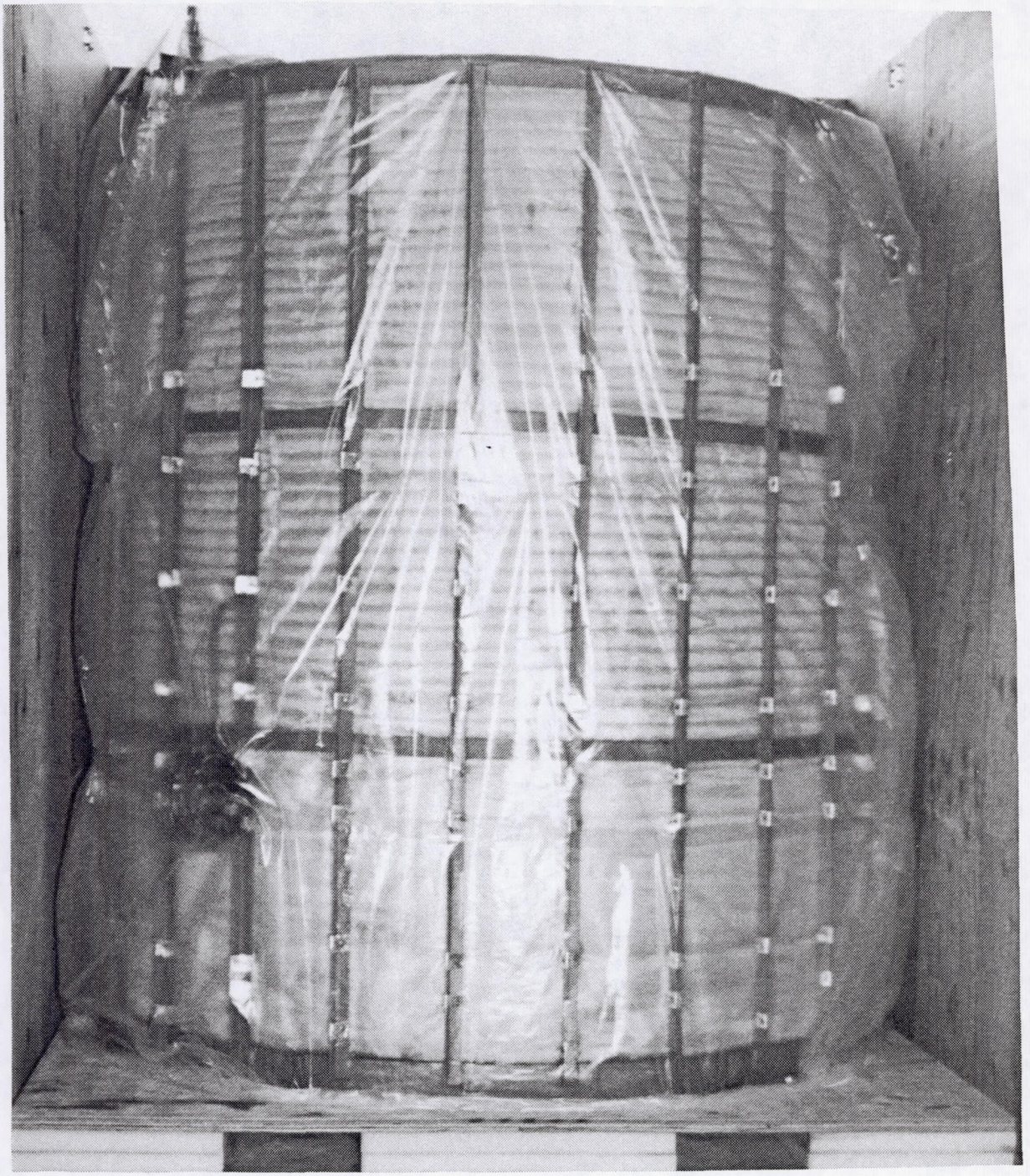

Figure 4-36: Build-up of the Over-Box Around the SDHRT Heat Receiver During Packaging for Shipment to Test Site

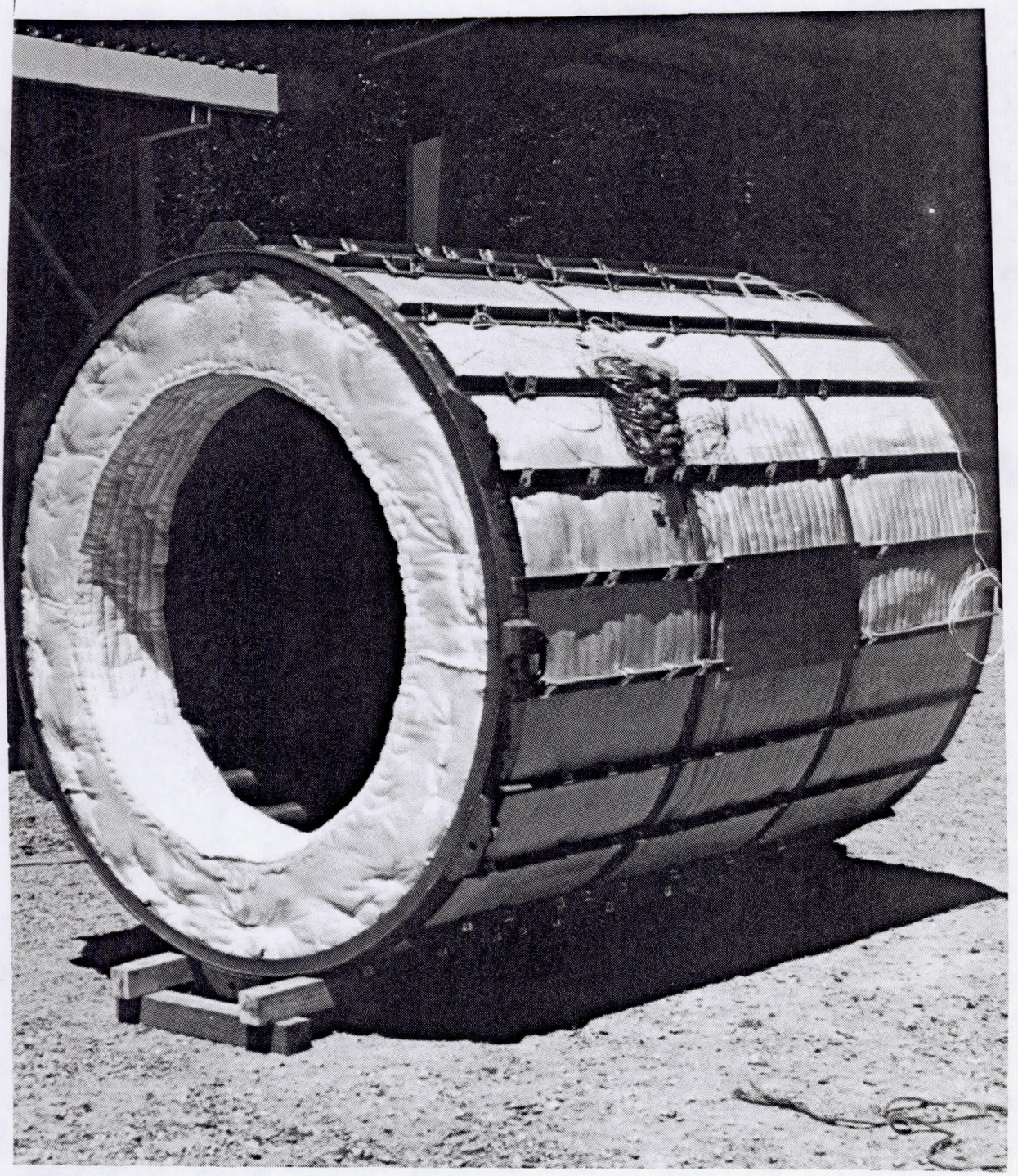

Figure 4-37: SDHRT SD Heat Receiver After Deliver to NASA-LeRC At the Tulalip Test Site

5.0 TEST SUPPORT HARDWARE

TSE required to test the SDHRT receiver were designed and fabricated as part of the SDHRT program. These hardware items were delivered to NASA with the heat receiver on a DD-250 report at the test facility. They were then supplied to Boeing as Government Furnished Property (GFP) for verification testing during execution of the ADRT contract. The following hardware were developed and fabricated as part of the SDHRT contract: (1) a CBC engine simulator; (2) a 30 zone quartz lamp heater; (3) a support cart for the receiver; and (4) an aperture plug for the front end of the receiver. These items are described in the sections to follow.

5.1 CBC Engine Simulator

The CBC engine simulator flows a gas mixture of 72% helium and 28% xenon (molecular) through the receiver at required test flow rates, pressures, and temperatures during all defined test modes. Figure 5-1 shows a schematic of the CBC engine simulator. A single-stage rotary lobe blower pressurizes and moves the working fluid through the piping network. The working static pressure of the gas at the inlet of the receiver is about 90 psia. A pulse damper is located between the blower outlet and a vortex shedding flow meter to smooth the pulsations inherent in the blower. Flow through the receiver is controlled manually using a blower by-pass valve. He-Xe gas returning from the receiver is cooled to an acceptable blower inlet temperature by first passing through a regenerative HX and then through a water cooled HX. The hot water exiting the HX is cooled by spraying it through a series of "misters" prior to its discharge into the environment. The gas is repressurized and slightly heated by the blower and preheated prior to entering the receiver by the regenerative HX.

Temperature control of the receiver inlet is achieved using a regenerative HX by-pass system consisting of two flow control valves in parallel. A large, coarse control valve is set manually to obtain an inlet temperature close to the desired value. A smaller, fine metering control valve with a temperature feedback loop then controls the gas inlet temperature to within ±5.6°C (±10°F) of the desired set point. The temperature feed-back electronics are supplied by Boeing and are not supplied with the CBC simulator after testing is completed. The fine control valve is designed to fail full open (fail-safe) to prevent over-heating of the receiver if an air pressure failure occurs. Temperatures and pressures are monitored throughout the CBC engine simulator to provide required receiver operating parameters.

If the leak-tight lines in the CBC gas loop need to be opened for an unplanned shut down of the system, a gas reclamation system is used to recover most of the expensive He-Xe gas from the CBC test loop. A two-stage metal bellows pump is used to reclaim the gas mixture and is capable of producing 791 kPa (100 psig) outlet pressure with a 48 kPa (7 psia) inlet pressure. The gas is pumped into a storage tank for later recharge of the system.

The gas reclamation system is also used to control the inlet pressure of the receiver. Initially, the CBC gas loop is filled with a premixed, high pressure bottle of He-Xe to a predetermined pressure. The CBC system will then be started up and brought to a condition of steady-state temperature and flow rate. If the receiver inlet pressure is too low, more gas is introduced into the system. If the receiver inlet pressure is too high, gas in the loop is then pumped into the gas reclamation storage tank using the reclamation system.

A He-Xe sampling port is included to allow the gas mixture composition to be monitored. A mass spectrometer, supplied by Boeing, will be used to determine the He-Xe mixture ratio. If the gas is deficient in helium, which is the most likely case, the amount of pure helium required to bring the mixture back into specification will be added from a high-pressure source.

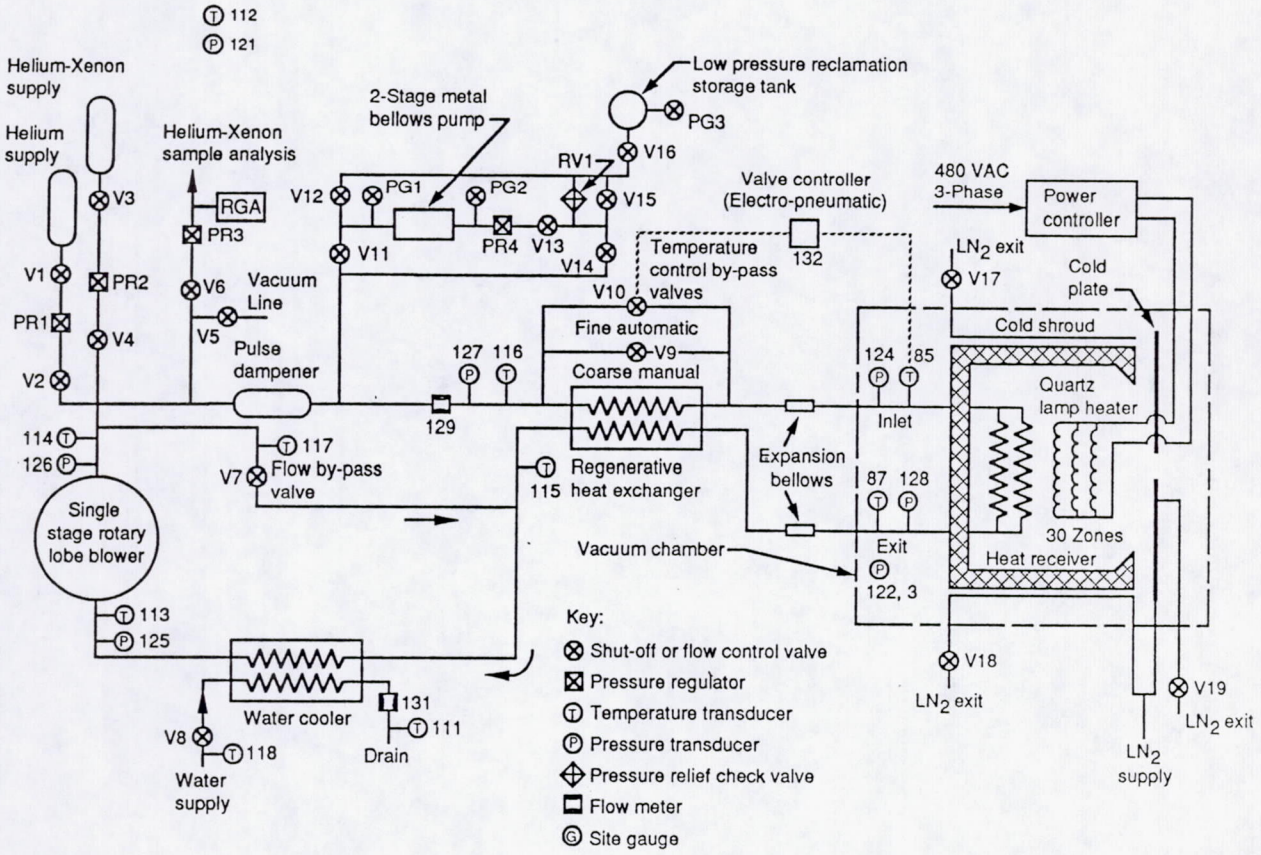

Figure 5-1: CBC Engine Simulator Schematic

The CBC engine simulator was fabricated at Lukas Machine in Seattle, WA. All components were individually helium leak checked prior to installation onto the simulator and each weld was leak checked in place. A final helium leak check was made of the simulator after it was completed and no leaks were detected. The CBC engine simulator was operated open loop with air prior to delivery to the Tulalip test site to ensure proper operation of the blower, valves, and flow meter. The simulator components are mounted on a steel pallet that is 2.4 m (8 ft) wide and 6 m (20 ft) long and it weighs roughly 4,540 kg (10,000 lbs). Figure 5-2 shows the CBC simulator after installation at the Tulalip test site. Figure 5-3 shows the piping runs and expansion bellows used to connect the CBC engine simulator with the receiver inside the vacuum chamber.

5.2 Receiver Support Structure

The receiver is suspended in the vacuum chamber by a receiver support structure. This structure also supports the back end of the quartz lamp array and the aperture cold plate. It is designed to roll in and out of the vacuum chamber on special tracked wheels. This allows the receiver and quartz lamp heater array to be assembled and mated while the assembly is outside the vacuum chamber. The entire assembly is then rolled into the vacuum chamber on tracks which already exist inside and outside the vacuum chamber. The rolled support of the receiver also allows the receiver to roll forward as the inlet and exit pipes connecting the receiver to the CBC engine simulator grow in length during operation.

The SDHRT heat receiver is shipped inside its shipping container in a vertical orientation. It is then unloaded from the shipping crate and tilted on a simple tilting stand to a horizontal orientation. The receiver is lifted in the horizontal orientation and placed inside the receiver support structure using a large fork lift. The support structure cables are secured to the receiver and the receiver weight is slowly transferred to the support structure. Figure 5-4 shows the receiver mounted inside the support cart. The tilting operations were conducted as part of the ADRT program.

5.3 Quartz-Lamp Heater Array and Aperture Plug Assembly

An infrared quartz lamp array is provided by the SDHRT program to heat the cavity of the receiver during the ADRT verification testing. The heat is supplied by quartz lamps (General Electric part number QH1000T3/CL/HT) which are rated at 1000 watts each at 220 volts. The lamps are configured and controlled in zones to produce an absorbed power profile along the length and around the circumference of the heat storage tubes that matches that which would be obtained if the receiver were operated using an on-axis, parabolic concentrator. Matching absorbed power profiles rather than incident flux eliminates the differences that are caused by the characteristic radiation wavelength and blockage by the heater structure and lamps (reference 11). The electrical power supplied to each zone can be varied to study the effects of off-design flux profiles.

The heater assembly is described in the SDHRT heater drawing package SK-LSS-101. The structure of the lamp array will exceed 982°C (1800°F) during operation so the choice of lamp structural materials was limited. A colombium alloy, C-103, is used as the primary structural material because of its improved creep characteristics when compared with those of superalloys like Inconel 617 (the lamp structure operates at higher temperature than does the heat storage tubes).

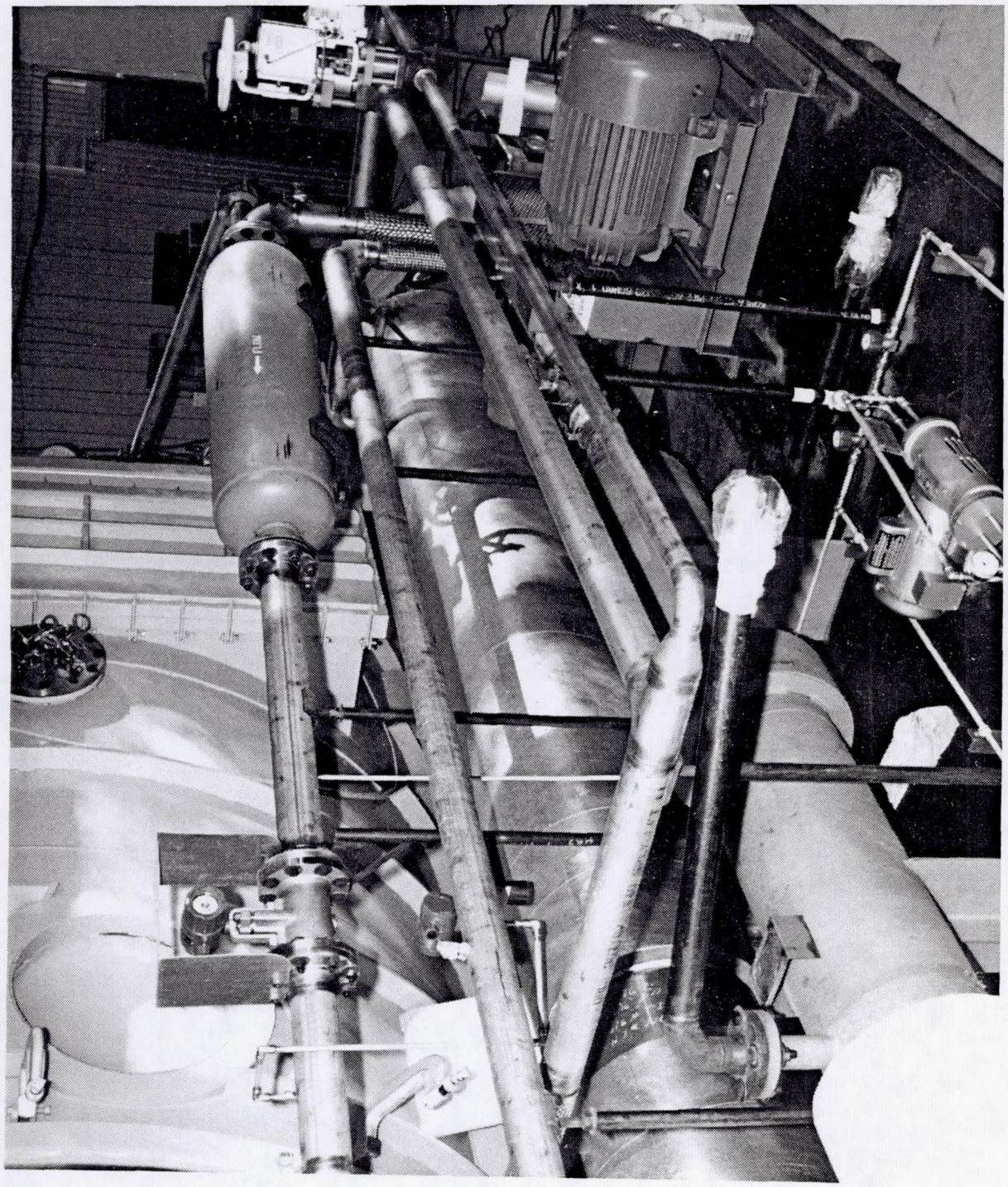

Figure 5-2: CBC Engine Simulator at Test Site

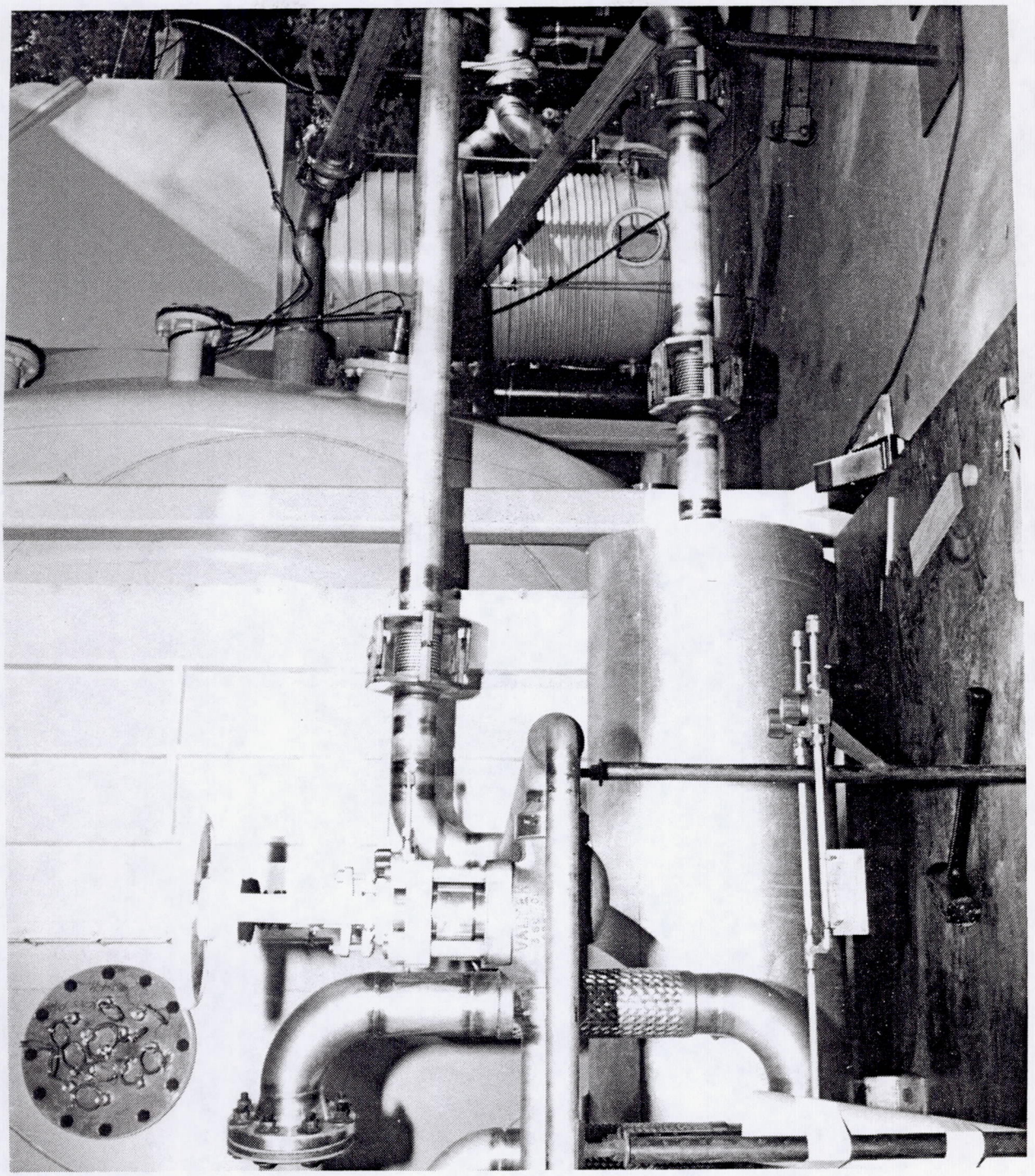

Figure 5-3: Piping Runs and Expansion Bellows Used to Connect the CBC Engine Simulator With the Heat Receiver Inside the Vacuum Chamber

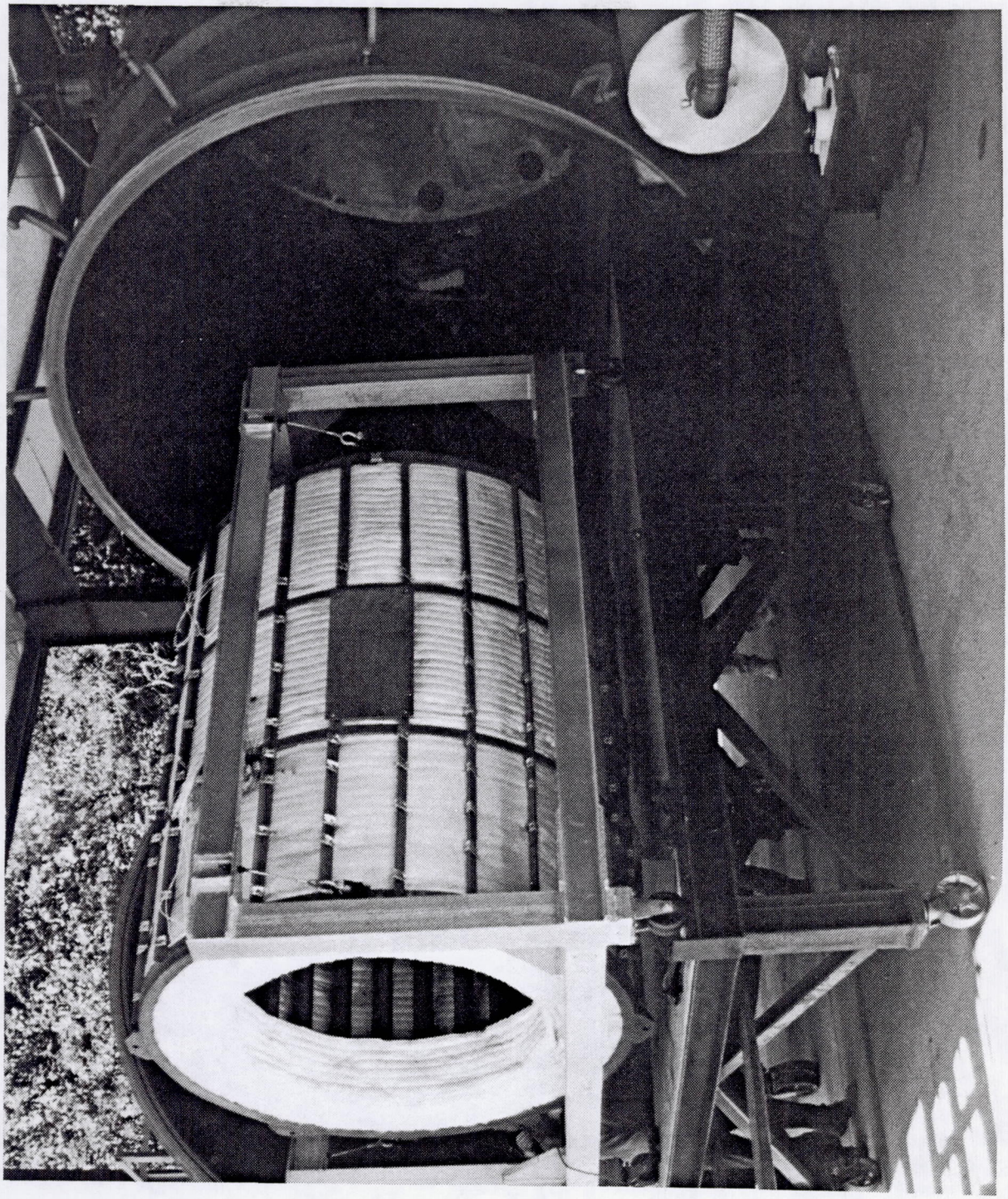

Figure 5-4: Receiver Mounted Inside Support Structure On Rails In Front of the Tulalip Vacuum Chamber

The primary structural support for the heater is provided by a single C-103 box beam. The box beam extends through the entire cavity length and supports 48 triangular C-103 plates. The plates conduct electrical power to the lamps and support the lamps in a near circular configuration with a nominal 1,219 mm (48 in) diameter. The quartz lamp array is shown prior to it's installation into the receiver cavity in Figures 5-5 and 5-6. Six plates form the positive and negative ends of each heater zone as shown in the figures. The plates attach to one another at their ends using alumina ceramic insulators that provide electrical isolation as shown in Figure 5-7. Ceramic insulators also attach the top plate to the box beam. A close-up of this attachment is shown in Figure 5-8. The total weight of the entire quartz lamp heater assembly (including the quartz lamps) is about 136 kg (300 lbs).

The heater is configured into 5 axial and 6 circumferential zones (formed by the 6 plates). The first two (highest flux) axial zones have 120 lamps per axial zone (20 lamps per plate) and the other three have 72 lamps per axial zone (12 lamps per plate) for a total array of 456 quartz lamps. The large number of lamps allows running each lamp at approximately one-half power during nominal baseline conditions to prolong lamp life. The 30 independently controllable zones allow reasonable variations in axial and circumferential flux distributions to be simulated.

The quartz lamps set into the notches cut into the plates and the quartz envelopes are secured to the plates using 0.4 mm (0.015 in) diameter molybdenum wire (mechanical support is required for the lamps on the bottom half of the lamp structure but all of the lamps are wired). The quartz lamps have pure nickel leads. Solid nickel ring terminals are crimped onto each lamp lead to increase reliability and to ease the installation of the lead onto molybdenum studs. A detail showing the placement of the lamp in the plate and the attachment of one of its leads to the plate is shown in Figure 5-9. The lugs are secured to the stud using molybdenum nuts (also visible in Figure 5-9). The use of molybdenum studs results in a junction that tightens during heating from room temperature (due to differing thermal coefficients of expansion). Molybdenum studs are also used to back up the ceramic supports between lamp plates and between the box beam and top plate supports (see Figures 5-7 and 5-8).

Electrical power is provided to the lamp plates through pure columbium bus rods. The positive and negative bus rods are 6.4 mm (1/4 in) and 9.5 mm (3/8 in) in diameter respectively. The electrical connection between the bus rods and lamp plates are made by threading the ends and attaching them to the plates with molybdenum nuts. The negative bus rods are threaded over their entire length to allow multiple connections to common grounded plate zones. The rods are insulated from plates where no connection is made using a ceramic insulator positioned by molybdenum nuts as shown in Figure 5-10.

The assembly of the heater structure is performed in two steps. Assembly of the six circumferential zones is performed in the dust-free environment of a clean room. The assemblies are then shipped to the test site where they are installed on the box beam and pinned together to form the complete structure. Preliminary assembly of the circumferential zones was completed under the SDHRT contract and is described below. Final assembly at the test site was performed as part of the ADRT contract and will be documented in the Final Test Report.

The initial assembly of the 6 circumferential heater sections was performed by Boeing technicians at our Thermal/Contamination/Propulsion Systems (TCPS) laboratory located in Kent, WA. All heater components and tooling were cleaned prior to assembly. Metallic items except the box beam were cleaned in a freon degreaser. Items with visible evidence of oils were first washed in detergent. The box beam was steam cleaned, wiped with acetone, and wiped with

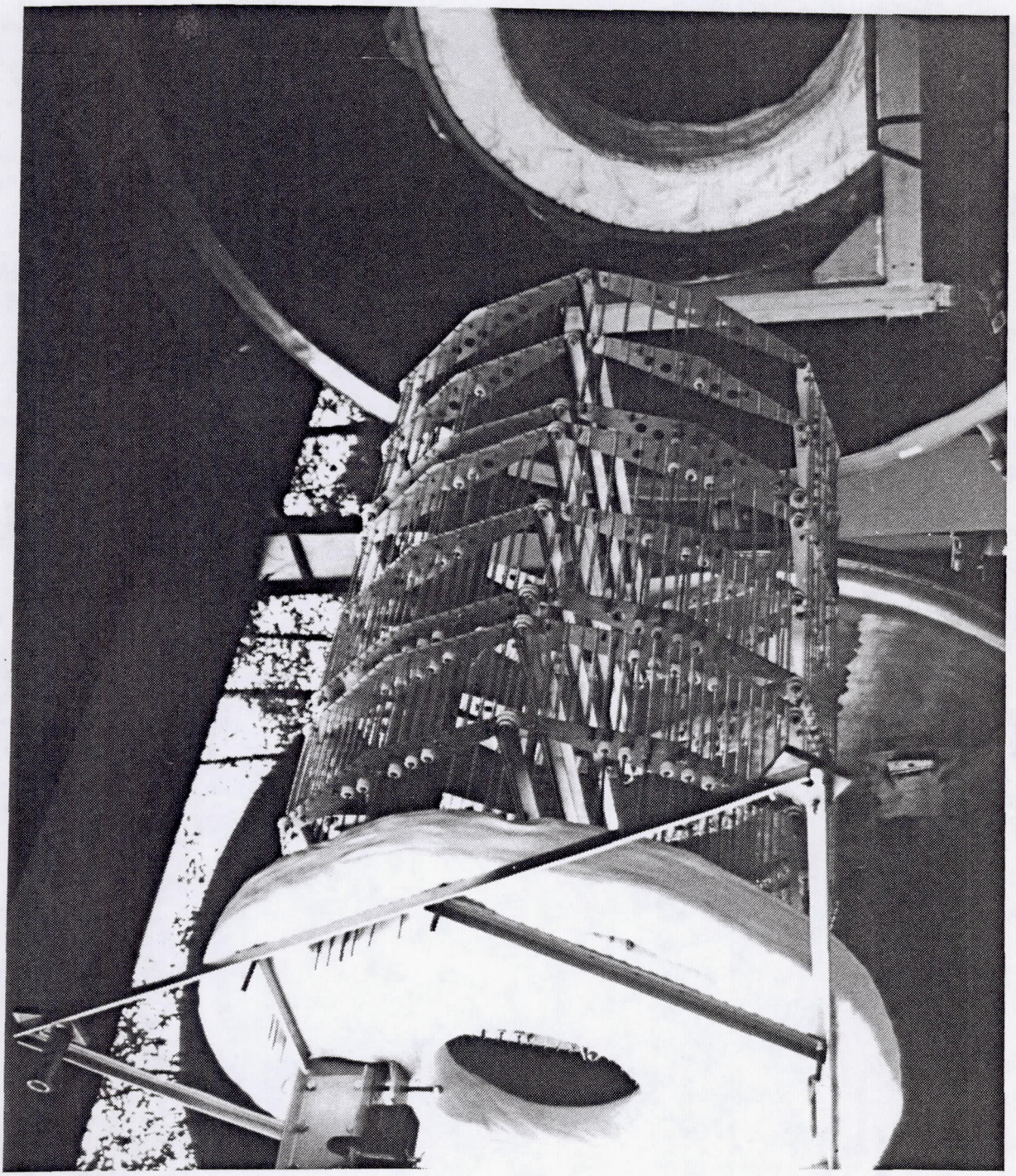

Figure 5-5: The 30 Zone Quartz Lamp Heater (With Aperture Plug) Prior To Installation Into Receiver Cavity

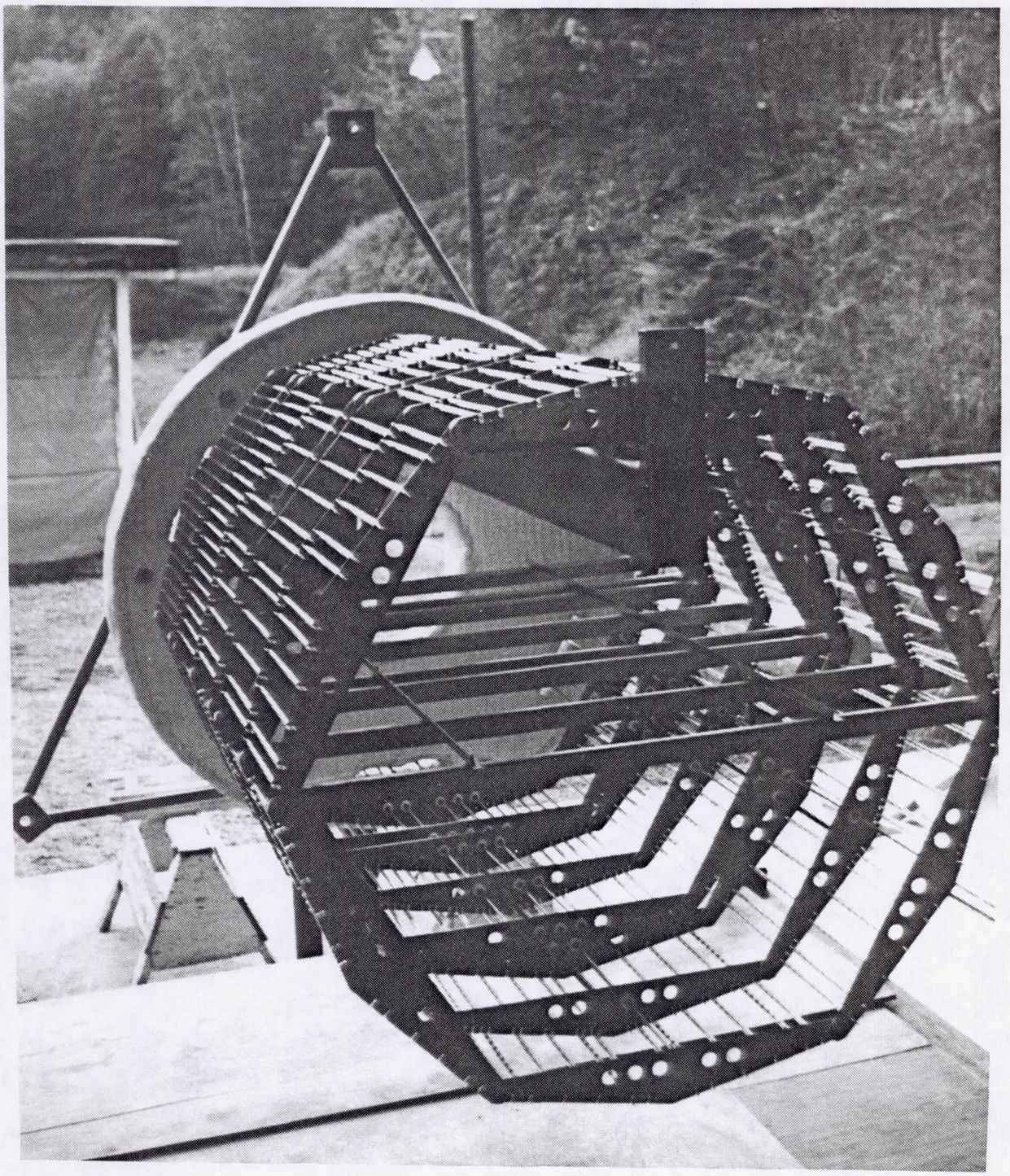

Figure 5-6: Rear View of the Assembled 30 Zone Quartz Lamp Heater (With Aperture Plug) Prior To Installation Into Receiver Cavity

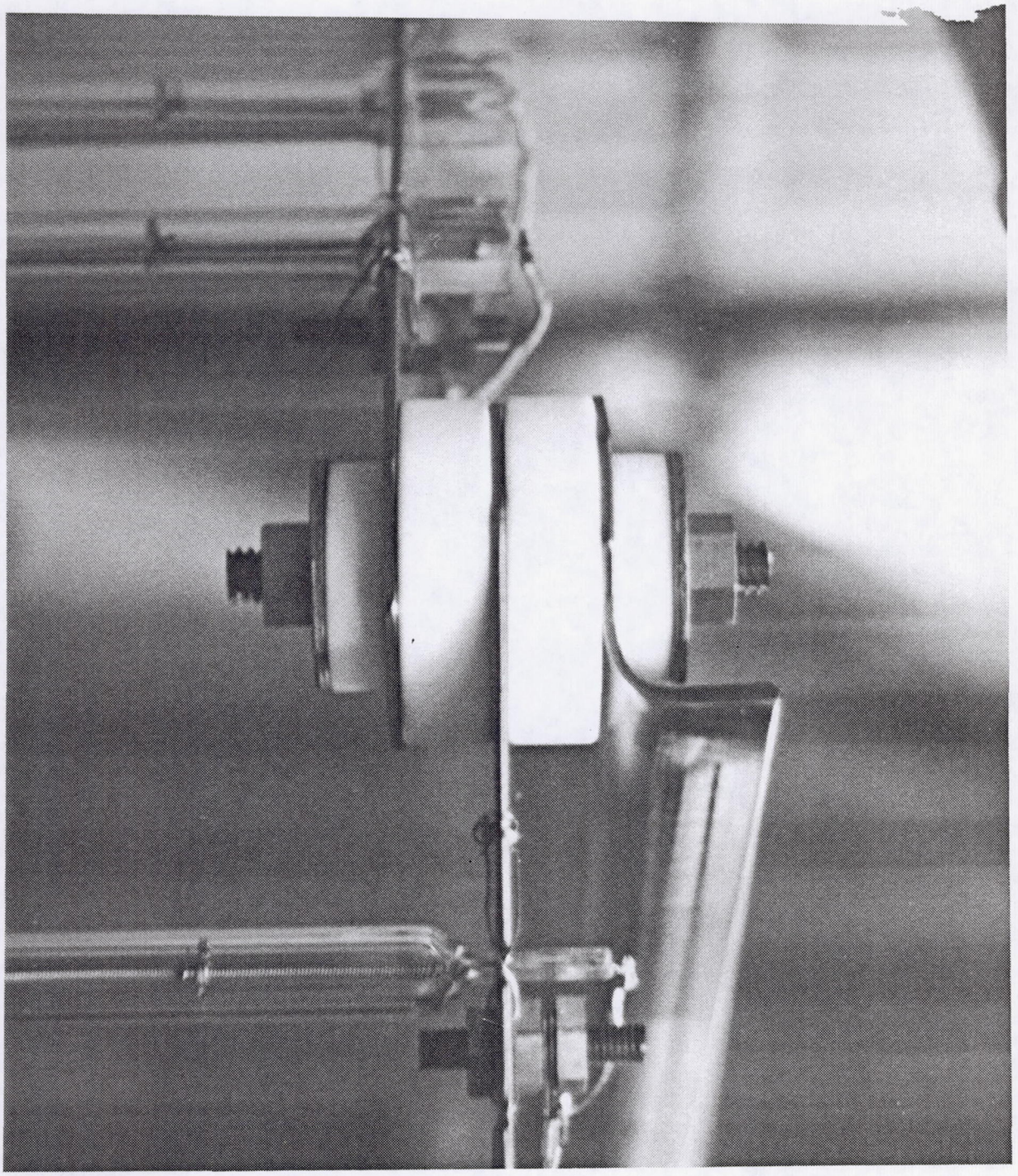

Figure 5-7: Ceramic Insulators and Molybdenum Stud Used To Connect Lamp Bus Plates At Ends

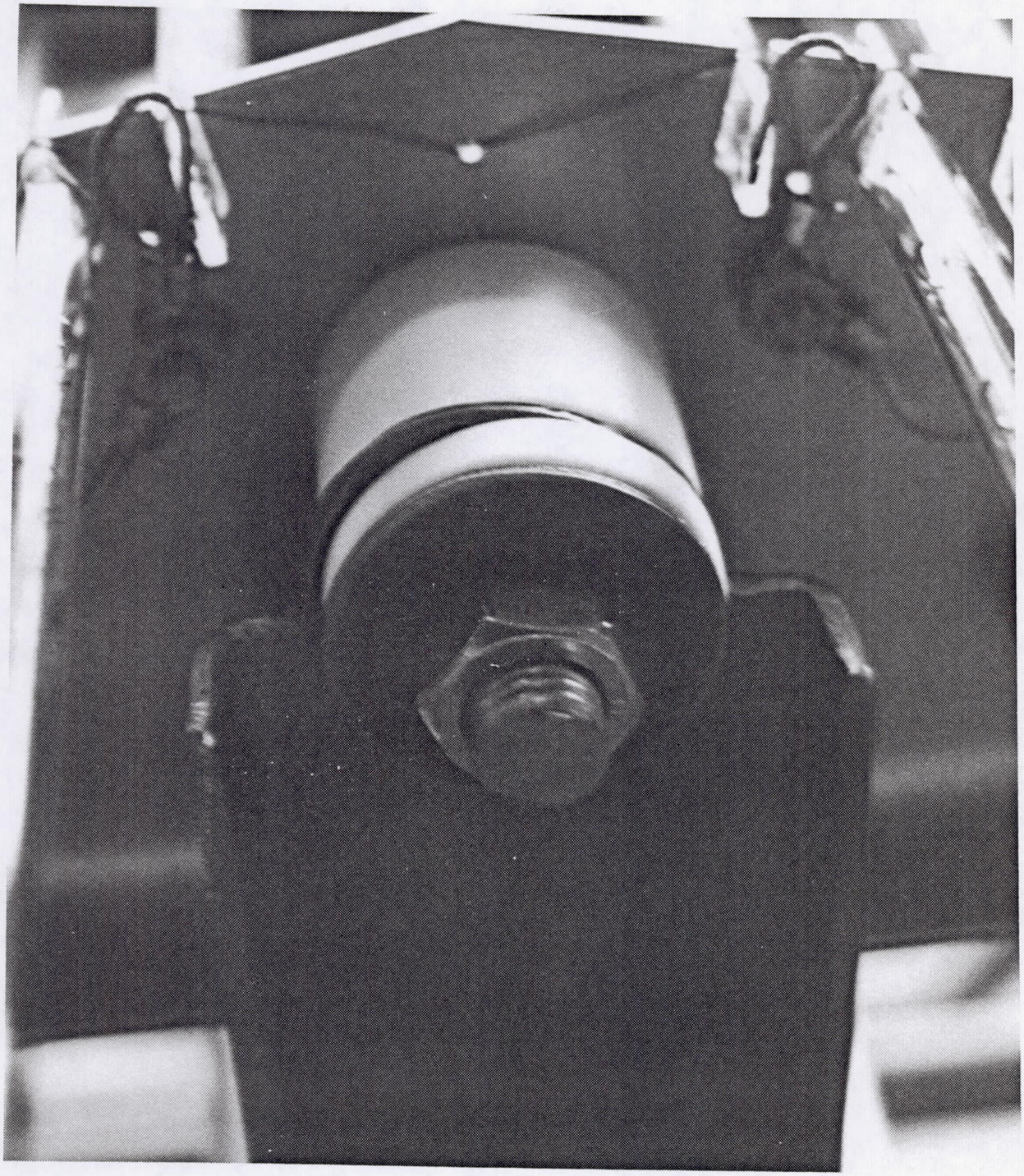

Figure 5-8: Ceramic Insulators and Molybdenum Stud Used To Connect Top Lamp Bus Plates To Box Beam Brackets

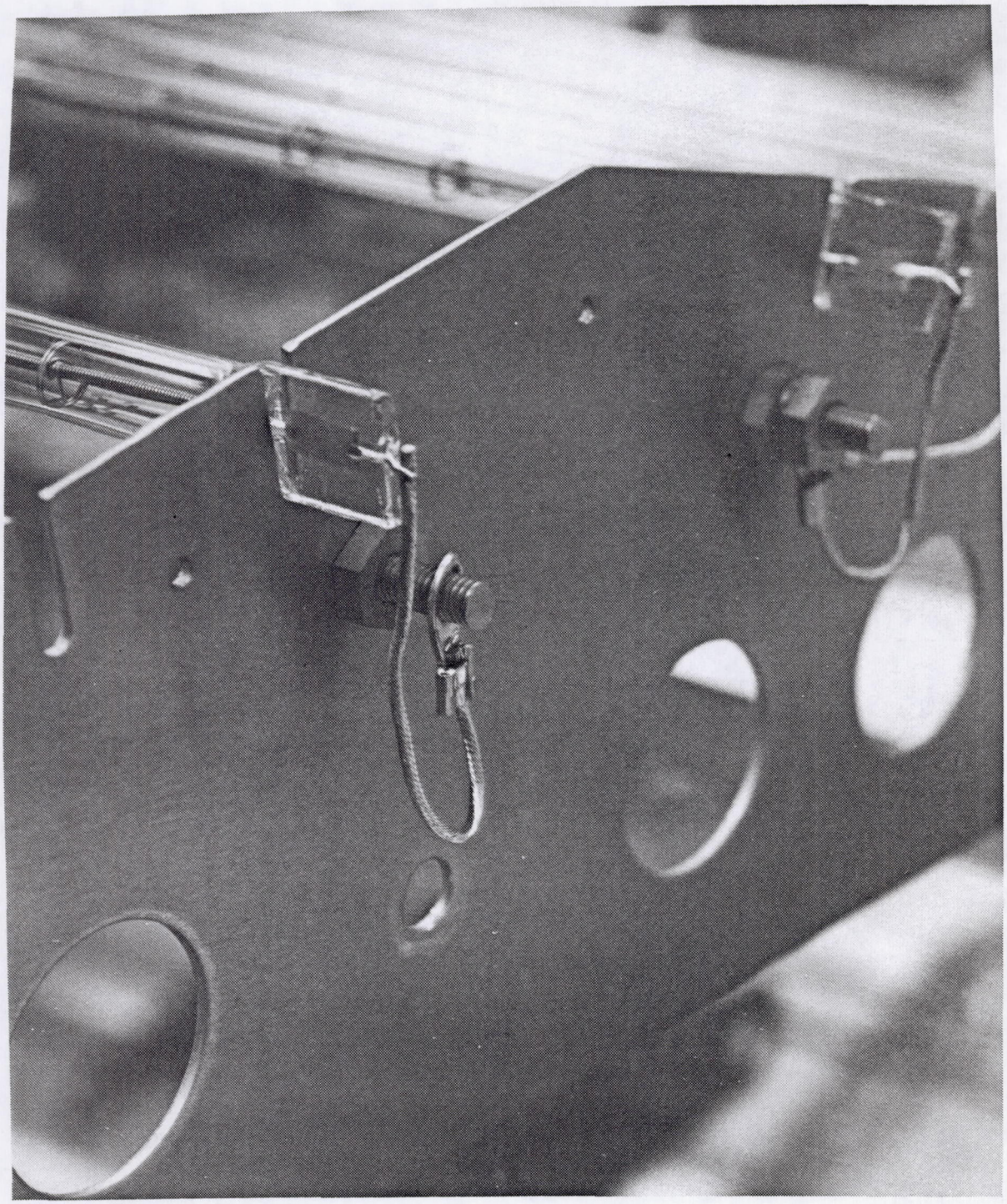

Figure 5-9: Quartz Lamp Lead Attachment To Molybdenum Studs on Lamp Bus Plates

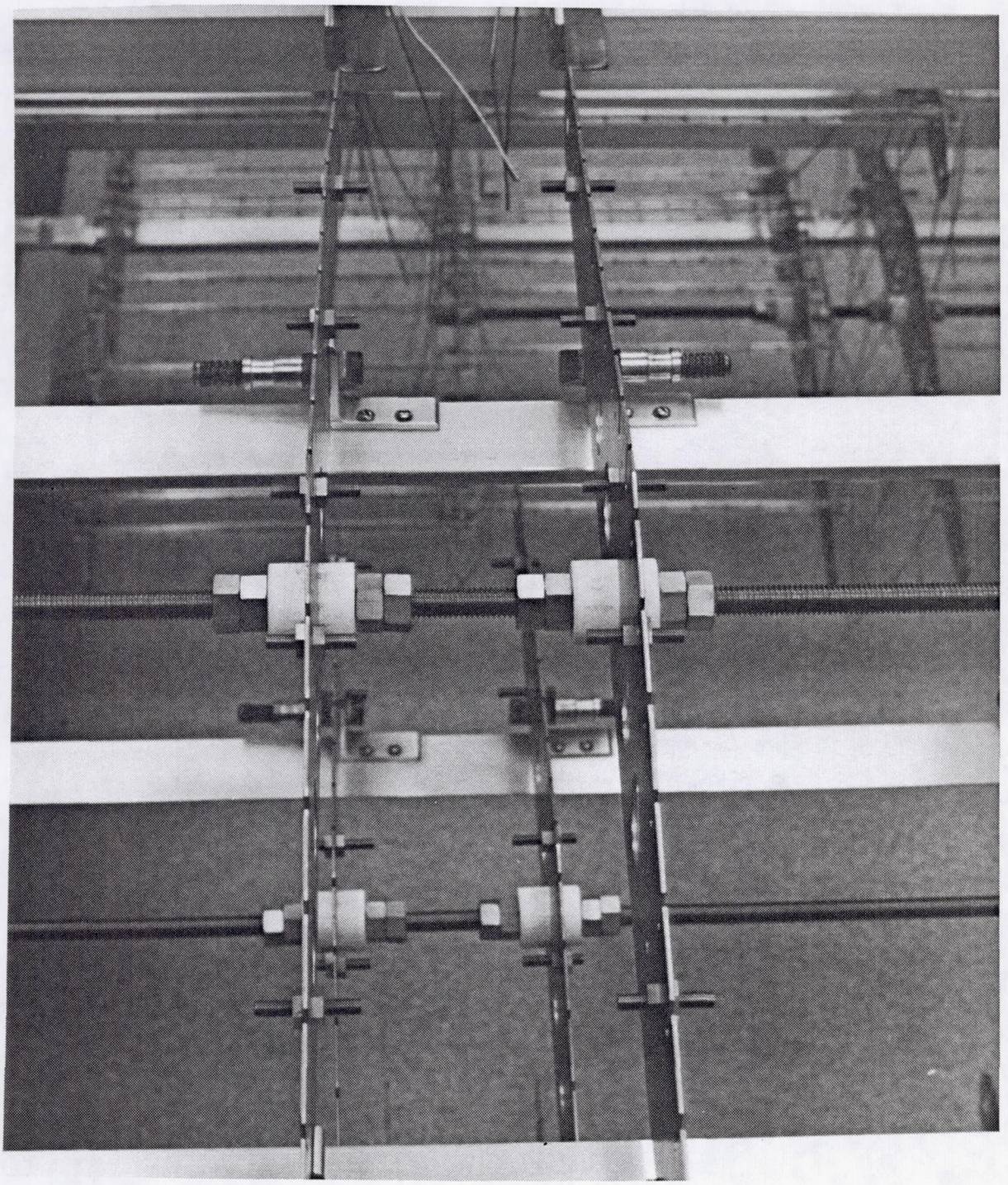

Figure 5-10: Negative Ground Bus Rod Isolation From Positive Lamp Bus Plates

alcohol. The ceramic spacers and pins were wiped with alcohol. The quartz lamps were wiped in acetone and wiped with alcohol per General Electric specification. All handling and assembly operations after cleaning were by "white-glove" only.

The 6 circumferential zones were attached to aluminum rails the required distance apart with "Cleco" clamps as shown in Figure 5-11. Metal lead protectors supplied with the lamps were removed and the lamps were installed in the notches in the plates. The leads were measured, excess length was clipped off, and the nickel ring terminals were crimped on.

Number 10 size molybdenum studs were attached to the plates for connecting the lamp leads to the plates and secured with molybdenum nuts. The lamp leads were then attached to the studs (2 to 4 leads per stud depending on location). After all the lamps were installed, they were secured to the plates with the 0.4 mm (0.015 in) diameter molybdenum wire as show in Figure 5-12. Next, the positive bus rods (6.4 mm diameter) were inserted into the plate and the location of spacers was marked. Each ceramic spacer was locked in position by installing a molybdenum washer on either end of the ceramic spacer and crimping the rod to locally increase its diameter. Figure 5-13 shows a completed position washer/ceramic on one of the bus rods. The washers are not able to pass the crimped region on the bus rod which positions the ceramic spacers where the are required.

The five positive bus rods were then attached to their respective plates using molybdenum nuts. The ceramic spacers used on the negative ground rod were position by locking two molybdenum nuts together on either side as shown previously in Figure 5-10. The ground rod was attached to appropriate plates with two molybdenum nuts on either side of the plate. A completed axial zone assembly is shown in Figure 5-14.

After the bus rod installation was completed, the assemblies were packed in styrofoam forms and placed in plywood crates for transportation to the Tulalip test site where they were assembled into the final lamp configuration as part of the ADRT test contract.

The aperture end of the receiver is closed off during the test of the receiver with an insulating plug with a 432 mm (17 in) aperture hole. The aperture plug is supported by stainless steel angles which attach to the front support ring of the receiver. Three cross pieces provide further support for the plug and also support the ends of the electrical bus rods from the quartz lamp heater as they exit out of the receiver cavity. The attachment point at the top support is also used to suspend the front end of the box beam.

A 152 mm (6 in) thick disc of Cerablanket ceramic fiber insulation (made up of 13 mm thick individual disks) is supported from the structure using 6, 13 mm (1/2 in) diameter molybdenum studs. Quartz cloth is sewn between the layers for stiffness and also covers the outer surface of the plug. Cutouts are included in the insulation for the penetrations by the box beam, bus rods, attachment studs, and the aperture hole in the center. The center aperture hole of 432 mm (17 in) diameter reflects the current space station design. The completed aperture plug is shown in Figures 5-5 and 5-6 (given previously) and in Figure 5-15 during the installation of the lamp array into the receiver cavity.

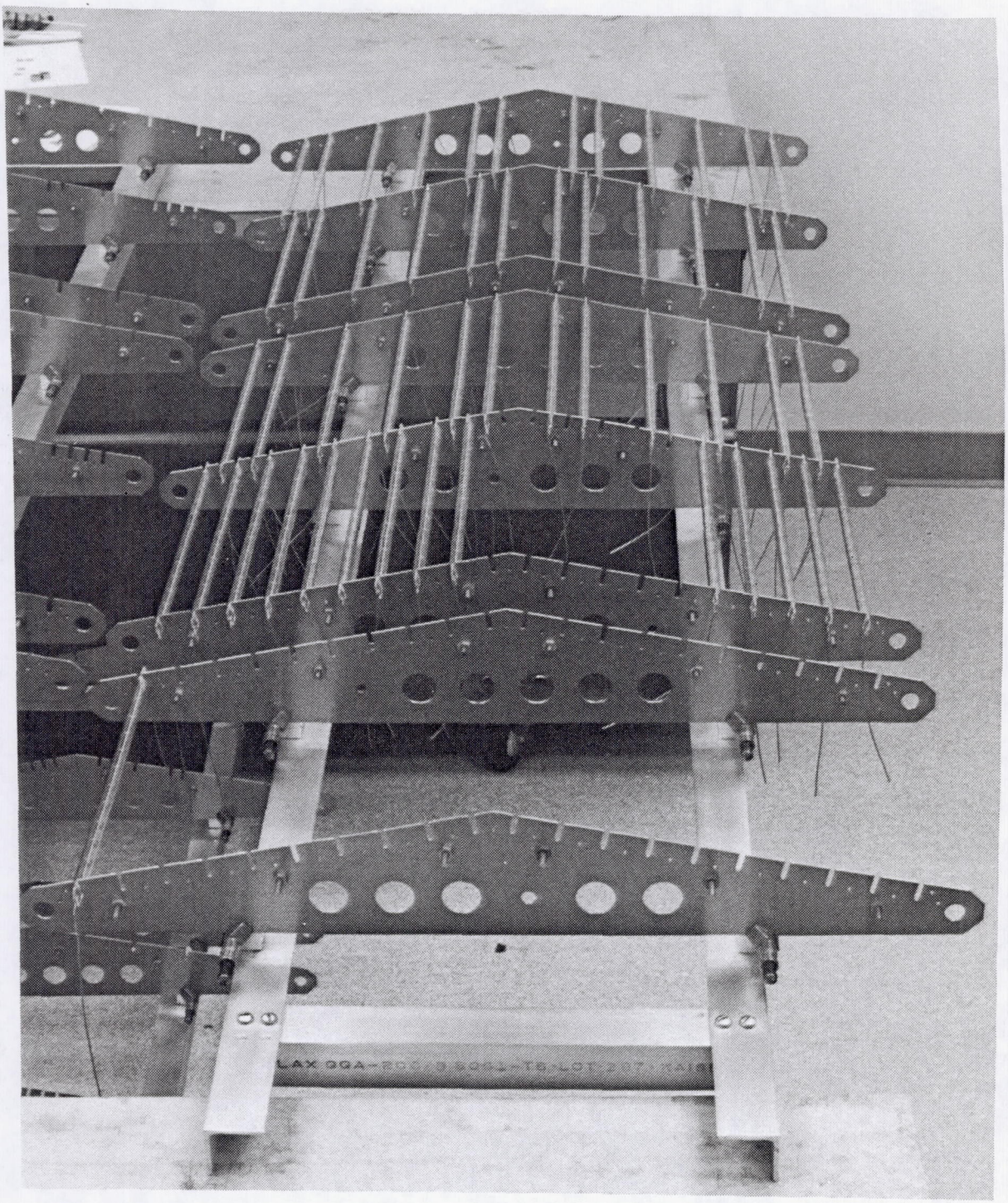

Figure 5-11: Positioning of Lamp Bus Plates On Rails For Assembly of Axial Zone

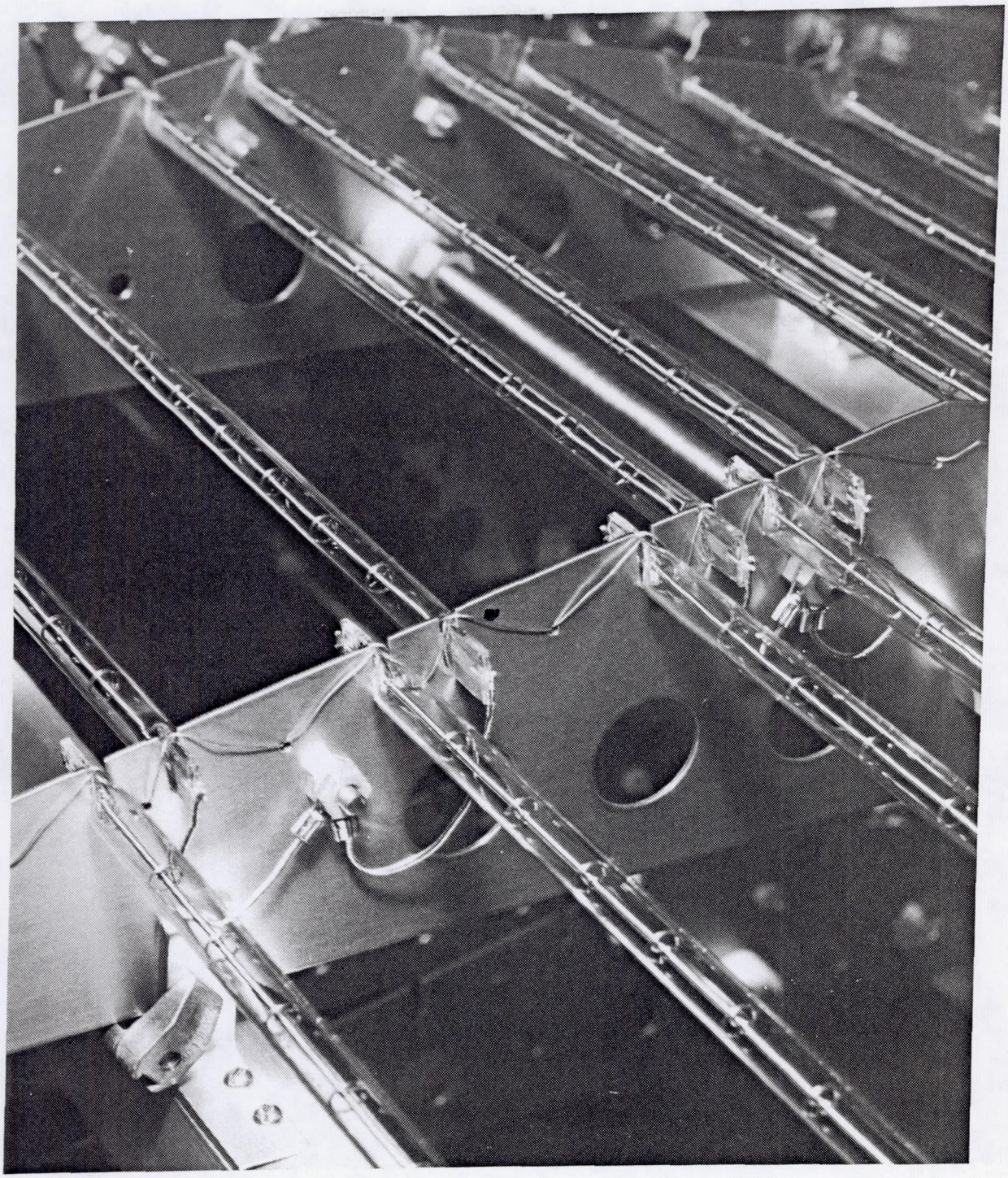

Figure 5-12: Securing Lamps Onto Bus Plates With Molybdenum Wire

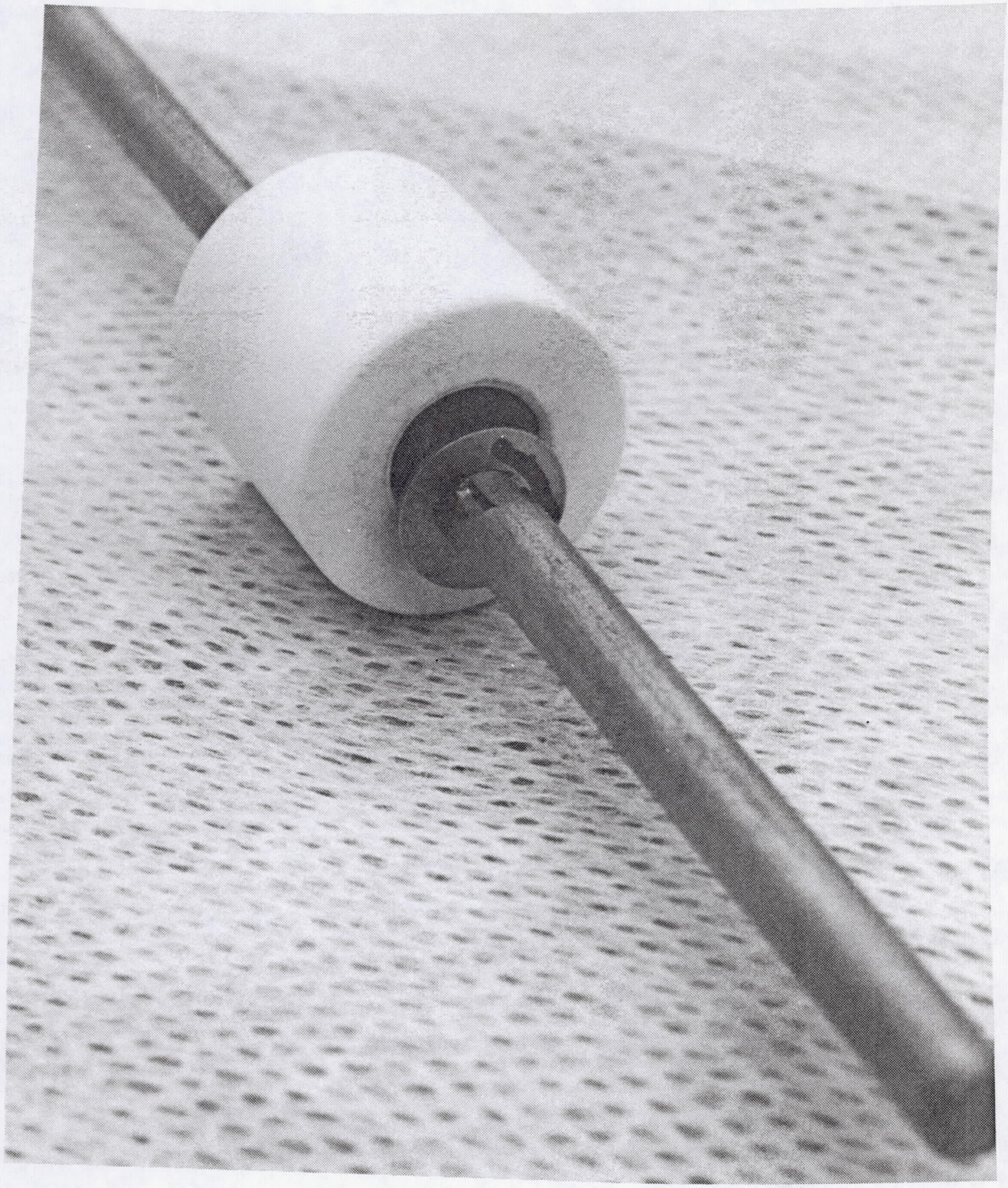

Figure 5-13: Crimped Washer To Position Ceramic Isolator On Positive Bus Rod

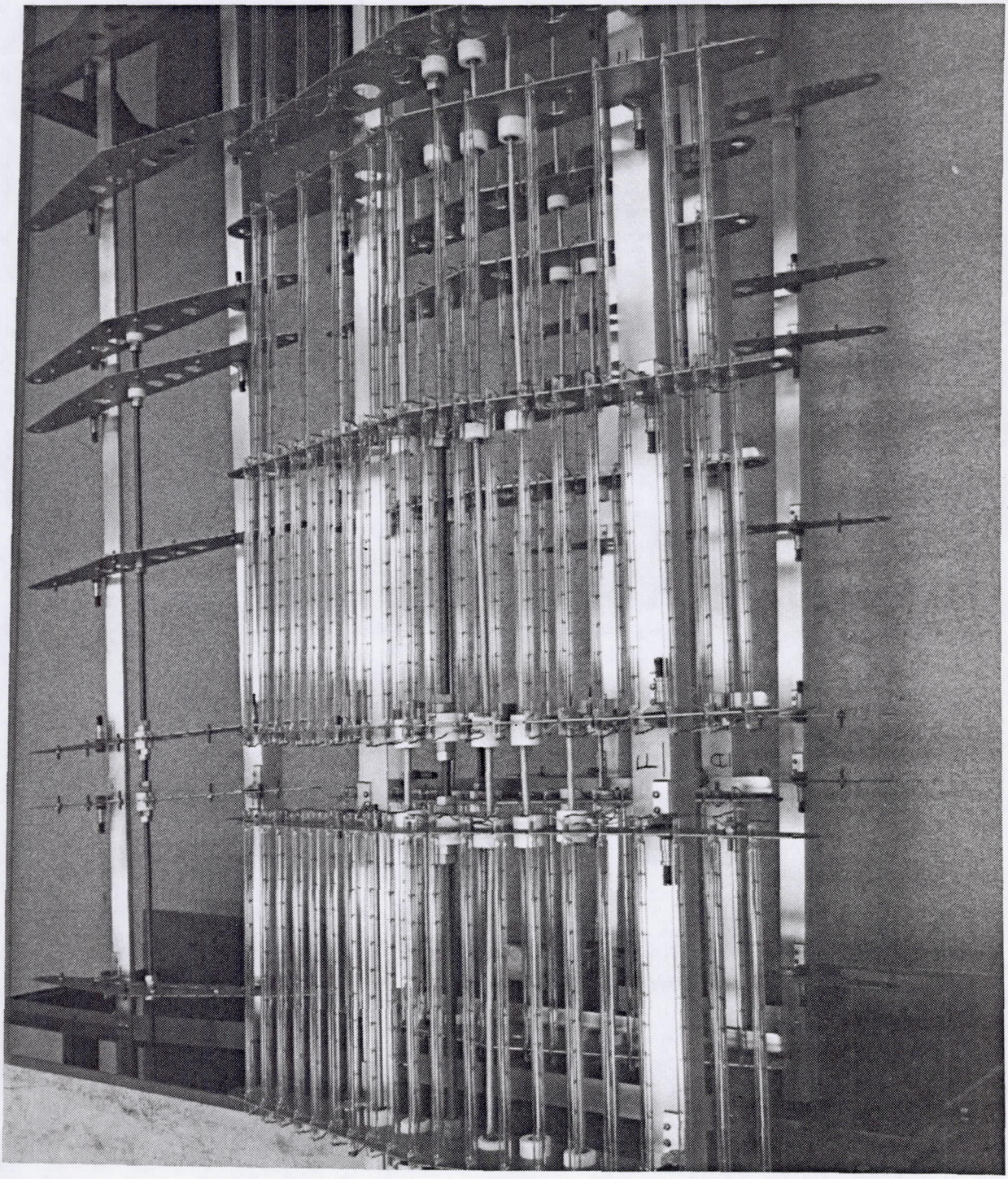

Figure 5-14: Completed Axial Zone Assembly

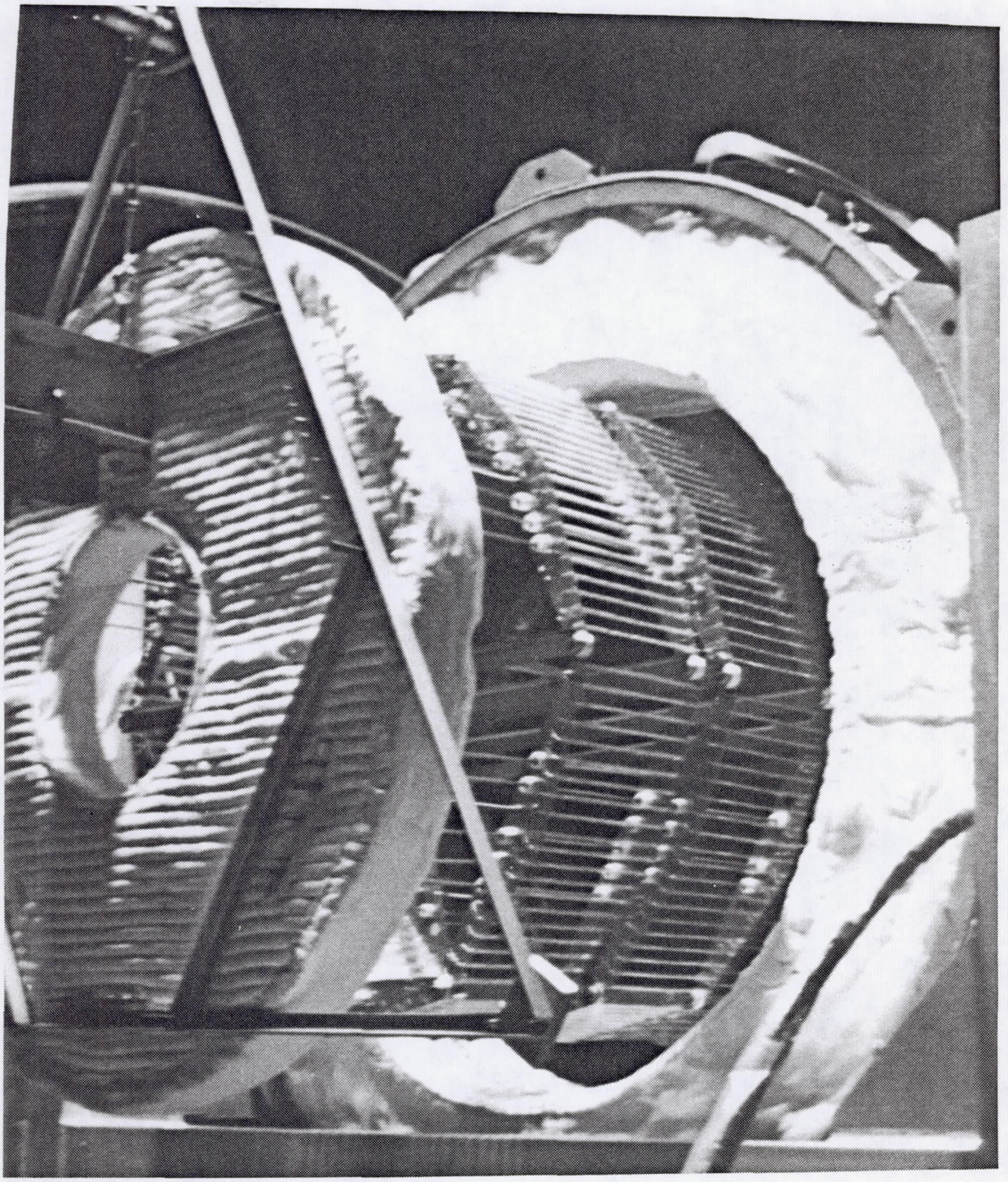

Figure 5-15: Quartz Lamp Array With Aperture Plug During Installation Into the Receiver Cavity

6.0 CONCLUSIONS AND RECOMMENDATIONS

The SDHRT program objectives, outlined previously in Section 2.1, have all been met except for quantifying the receiver performance in testing and the correlation of the test data with the thermal math model. These two objectives will be met upon completion of the ADRT program. Much has been learned about the real-life challenges associated with developing a full-size solar dynamic heat receiver for space flight, and in particular, Space Station application.

The SDHRT program began with a heat receiver conceptual design phase and, after choosing the most promising concept, continued with the detailed design and fabrication of the SDHRT heat receiver. A number of component level tests were also conducted to demonstrate fabrication methods and the performance of key elements of the design. In addition to the heat receiver, all of the test support hardware required to operate the receiver in a simulated LEO environment (except for gravity), was also designed and fabricated during the SDHRT program. To accomplish all of these tasks, program resources had to be carefully controlled and compromises in both scope and materials were made.

For example, a number of felt metal matrix materials are commercially available in a variety of densities, wire sizes, pore sizes, and material compositions. However, the costs of some of the better performing materials (reference 11) did not allow their use in the SDHRT receiver and there was no optimization of felt matrix parameters. Furthermore, the nickel felt used in the SDHRT receiver has shown that its material strength may not be adequate for this application as demonstrated by the compression of the felt disks during one of the molten salt fill operations (Section 4.2.4).

As part of the receiver optimization process, the entire heat storage tube design requires further analyses to quantify (1) the behavior of the salt in the matrix material and (2) ensure that the TES containment design has adequate margins for all operational modes. For example, no stress analyses was conducted of the cold start-up of the receiver, a condition which will dramatically increase the stresses induced in receiver components by thermal gradients. Also, the exact location of the salt inside the metal matrix and effects of salt inside the convolution volume need to be better understood for both normal and off-design operation. The optimization of the heat storage tube design will be required prior to any implementation of this configuration for space flight application.

In addition, the following significant areas were only briefly studied during the SDHRT program because they were not required for a ground test receiver:

1. The development of a low-cost and reliable aperture protection system.
2. The potential for contamination of the concentrator and/or the space craft from the off-gasing of receiver materials.
3. Damage potential from micrometeoroid and space debris.
4. The survivability and thermal performance of candidate cavity insulations in the solar wavelength.
5. Required make-up rates of helium because of diffusion and/or leaks from the pressure piping system and component seals.

The analyses that was performed in these areas (reference 11) shows that these topics are important to quantify before a operational SD module can become a reality. However, it must be emphasized that no SD module "show stoppers" were found during the conduct of the SDHRT program and all of these areas can be adequately addressed by proper design.

REFERENCES

1 JSC 30000, Space Station Program Definition and Requirements, Section 3 - Space Station System Requirements, Appendix 3.1, Natural Environment Definition for Design, NASA-JSC, 23 March 1986.

2 Boeing Document D180-29195-1, Solar Dynamic Heat Receiver Technology Work Plan, Boeing Aerospace, 15 November 1986.

3 Boeing Document D180-29709-1, Solar Dynamic Heat Receiver Interim Report and Conceptual Design Review, Boeing Aerospace, 16 July 1986.

4 Solar Dynamic Receiver Designs for Space Applications, L.M. Sedgwick, 1987 ASME Solar Energy Conference Paper, March 1987.

5 NASA-TM-82585/J8400040, Natural Environment Design Criteria for the Space Station Program Definition Phase.

6 LeRC-SS-0001, Rev. 6, Work Package 4 (WP04) Technical Requirements Document, NASA Lewis Research Center, 26 January 1989.

7 LeRC-SS-001, Electrical Power System (EPS) Requirements Document, NASA Lewis Research Center, 3 February 1987.

8 LeRC-SS-003, Solar Dynamic Power Module System Part 1 Control End Item Specification, NASA Lewis Research Center, 3 February 1987.

9 JSC 07700, Level 2 Program Definition and Requirements, National Space Transportation System.

10 JSC 20001, Orbital Debris Environment for the Space Station, D.J. Kessler.

11 Boeing Document D180-29711-1, Solar Dynamic Heat Receiver Technology, Design Analysis Report, Boeing Aerospace, September 1988.

12 Cotton, J.D., "Compatibility of Selected Superalloys With Molten LiF-CaF_2 Salt," Prepared for the 1989 IECEC Conference, August 1989.

13 Inconel 617 Product Catalog, Huntington Alloys.

14 Aerospace Structural Metals Handbook, Code 4215, Inconel 617.

15 NSRDS-NBS-61-PT-4, Physical Properties Data Compilations Relevant To Energy Storage, Part IV, Molten Salts, G.J. Janz, National Standards Reference System, July 1981.

16 Subcontract Report To Boeing Aerospace, Thermophysical Properties of Selected High-Temperature Salts and Metals, Institute of Gas Technology, 1986.

17 NASA Technical Memorandum 87320, Estimated Heats of Fusion of Fluoride Salt Mixtures Suitable for Thermal Energy Storage Application, A.K. Misra, NASA-LeRC, May 1986.

18 DOE/NASA/0806-79/1, NASA CR-159663, High-Temperature Molten Salt TES Systems, R.J. Petri, Institute of Gas Technology, February 1980.

19 Boeing Memorandum 2-3632-SDHR87-045, Measurement of Molten Lithium Fluoride-Calcium Difluoride Wettability and Wicking Heights of Several Different Thermal Conductivity Enhancement Materials, J.D. Cotton, Boeing Aerospace, September 1987.

20 Boeing Document D180-29233-1, Solar Dynamic Heat Receiver Technology Quality Assurance and Reliability Plan, Boeing Aerospace, November 1986.

21 ORNL-TM-2732, Filling Heat Storage Tubes for Solar Brayton Cycle Heat Receiver With Lithium Fluoride, R.A. Gnadt, July 1970.

22 Boeing Memorandum 2-3632-SDHR86-039, Pressure Assisted Molten Salt Filling, L.M. Sedgwick, Boeing Aerospace, October 1986.

23 Boeing Document D180-30536-1, Cleaning, Welding, and Inspection of TES Fill Tubes for the Solar Dynamic Heat Receiver, J.H. Lee, Boeing Aerospace, July 1990.

Appendix A

Summary of SDHRT Molten Salt Fill Operations

Summary of SDHRT Molten Salt Fill Operations

General Notes:

HLC = results of helium leak checking prior to laser welding
P = passed
F = failed

AFT = argon flow tests conducted at 10 psig inlet pressure
lpm = liters per minute argon flow
cfm = cubic feet per minute argon flow

U = unfilled
PC# = purge canister

SINGLE TUBE DEMO #1 (11 Nov 1988)

Tube Serial #	Dry Weight (lbs)	HLC	AFT #1 (lpm)	AFT #2 (lpm)	AFT #3 (lpm)	AFT #4 (lpm)	AFT #5 (cfm)	Manifold Order	Fill Order	Fill Time (min)	Filled Weight (lbs)
PC1	36.0	n/a	n/a	n/a	n/a	n/a	n/a	n/a	n/a	n/a	70.0
SS1	42.0	P	-	-	-	-	-	1	U	50	45.0

Notes:

No argon flow test was conducted on this TES tube or manifold; not yet part of the fill procedures.

Purge canister isolation freeze valve not capable of solidifying salt and purge canister was completely filled.

A small amount of salt was cast into the TES tube but salt could not continue to flow after filling purge canister because of improper transfer line insulation installation procedures caused salt to freeze.

Heat storage tube was section to examine salt content.

As a result of these problems, a high-temperature bellows valve was installed in the purge canister line. Procedures for installing insulation were changed to prevent view blockage of the transfer lines to heater surfaces.

SINGLE TUBE DEMO #2 (14 Feb 1989)

Tube Serial #	Dry Weight (lbs)	HLC	AFT #1 (lpm)	AFT #2 (lpm)	AFT #3 (lpm)	AFT #4 (lpm)	AFT #5 (cfm)	Manifold Order	Fill Order	Fill Time (min)	Filled Weight (lbs)
PC2	35.5	n/a	n/a	n/a	n/a	n/a	n/a	n/a	n/a	n/a	55.0
SS2	43.0	P	-	-	-	-	-	1	1	379	74.0

Notes:

No argon flow test was conducted on this TES tube; not yet part of the fill procedures.

Fill was successful but took much longer than expected and required higher static pressure than calculated for static head of the salt. Originally thought to be caused by improper gas flow meter calibration and back pressure in heat storage tube. Later discovered method of attaching manifolds to PCM tubes caused severe flow restriction and, therefore, salt flow was orificed into the TES tube.

TES tube was sectioned to confirm distribution of salt. Salt distribution was reasonably uniform from top to bottom of tube confirming the bayonet heat exchanger performed as desired.

No changes were made to the facility.

6-TUBE SDHRT FILL #1 (7 Apr 1989)

Tube Serial #	Dry Weight (lbs)	HLC	AFT #1 (lpm)	AFT #2 (lpm)	AFT #3 (lpm)	AFT #4 (lpm)	AFT #5 (cfm)	Manifold Order	Fill Order	Fill Time (min)	Filled Weight (lbs)
PC3	35.5	n/a	n/a	n/a	n/a	n/a	n/a	n/a	n/a	n/a	35.5
2	43.0	P	-	-	-	-	-	1	U	450	43.0
24	43.5	P	-	-	-	-	-	2	U	450	43.5
26	43.5	P	-	-	-	-	-	3	U	450	43.5
27	43.5	P	-	-	-	-	-	4	U	450	43.5
9	43.5	P	-	-	-	-	-	5	U	450	43.5
33	44.0	P	-	-	-	-	-	6	U	450	44.0

Notes:

No argon flow tests were conducted on these tubes; not yet part of the fill procedures.

Salt flow was never established. Salt only made it as far as the vertical transfer line above the tee. None of the six heat storage tubes (or inlet salt mainifold) was filled with any salt.

An anomaly investigation showed the cause was (1) severe restriction of the salt flow at of the weld connecting the manifolds with the PCM fill tubes and (2) improper heater and insulation installation at the tee section. The back side of the tee was unoxidized indicating a cold spot in the line.

The manifold to PCM tube weld connection was redesigned using a 5/16-inch diameter transition and a 1/4-inch diameter stub. The stub is first welded onto the 5/32-inch diameter PCM tube. This weld is visually inspected for blockage and is helium leak checked. A fillet weld is then made between the 5/16-inch transition and the 1/4-inch diameter stub. The procedures were changed to measure the argon flow rate through the heat storage tubes prior to welding, after attachment to the inlet manifold, and after connection to the exit manifold.

The heater and insulation installation procedures were changed to prevent cold spots in the salt transfer lines. More critical locations in the transfer line were instrumented with thermocouples.

Flow checking of the TES tubes showed no salt in the manifolds or in the heat storage tubes. Therefore, the inlet manifold and 6 heat storage tubes were installed back into the HTTES facilty for a 2nd attempt to cast salt into them.

6-TUBE SDHRT FILL #2 (19 May 1989)

Tube Serial #	Dry Weight (lbs)	HLC	AFT #1 (lpm)	AFT #2 (lpm)	AFT #3 (lpm)	AFT #4 (lpm)	AFT #5 (cfm)	Manifold Order	Fill Order	Fill Time (min)	Filled Weight (lbs)
PC3	35.5	n/a	n/a	n/a	n/a	n/a	n/a	n/a	n/a	n/a	36.0
2	43.0	P	10.3	10.5	-	10.0	2.2	1	U	141	43.0
24	43.5	P	9.6	9.5	-	9.5	2.2	2	U	141	43.5
26	43.5	P	10.3	10.0	-	9.9	2.2	3	U	141	43.5
27	43.5	P	10.3	10.0	-	9.8	2.2	4	U	141	43.5
9	43.5	P	10.3	10.3	-	10.4	2.2	5	U	141	43.5
33	44.0	P	11.0	11.0	-	10.5	2.2	6	U	141	44.0

Notes:

AFT = argon flow tests conducted at 10 psig inlet pressure
#1 = as received prior to modifications
#2 = transition weld fittings attached
#3 = not in the procedures at this time
#4 = inlet manifold attached
#5 = total cumulative flow after attachment to exit manifold

Salt flow again did not ever become established. Salt flow was observed all the way to the inlet of the TES tubes but ceased immediatly.

A new anomaly investigation team was formed to reevaluate the entire design and operational fill procedures of the HTTES facility.

The investigation focused on the salt. Salt samples were taken from various locations throughout the salt reservoir, salt transfer lines, manifolds, PCM tubes, TES tubes, and from the raw salt received from the supplier. The results showed (1) the composition of the as-received salt was only slighly off the eutectic compostion and was as-ordered; (2) the bulk of the salt inside the reservoir was at or very near the eutectic compostion; (3) the salt at the bottom of the reservoir was far off the eutectic composition and highly rich in CaF2; (4) the salt inside the transfer lines,

manifolds, PCM tubes, and TES tubes was far off the eutectic compositon and rich in CaF2; (5) the CaF2 was separating from the bulk salt inside the reservoir by gravity during melt and was being sucked up into the dip-leg during the fill; and (6) the CaF2-rich salt was blocking the salt transfer lines and preventing the fill.

Fixes included (1) adding active stirring to the salt reservoir; (2) adding a isolation valve to the salt transfer line; (3) boosting the compositon of the salt to the other side of the eutectic composition at 82LiF-18CaF2 by adding pure LiF to the salt reservoir prior to the additon of the existing eutectic; and (4) changing the facility fill temperatures to be coolest at the reservoir and to become progressively higher all the way to the heat storage tubes.

Examination of the heat storage tubes by CT showed the felt metal had compacted to the bottom end of the tube assembly because the tubes had been elevated to such high temperature for such a long period of time during the attempted fill operations.

A decision was made to scrap these 6 heat storage tubes and use them for a demonstration 6-tube fill operation. However, TES tube #9 was sectioned to examine the felt metal distribution and to confirm the presence of salt at the inlet of the heat storage tubes. Therefore, the last of 3 stainless steel tubes was used for the sixth tube in the demo fill.

6-TUBE DEMO FILL (29 Nov 1989)

Tube Serial #	Dry Weight (lbs)	HLC	AFT #1 (lpm)	AFT #2 (lpm)	AFT #3 (lpm)	AFT #4 (lpm)	AFT #5 (cfm)	Manifold Order	Fill Order	Fill Time (min)	Filled Weight (lbs)
PC3	36.0	n/a	n/a	n/a	n/a	n/a	n/a	n/a	n/a	n/a	41.0
2	43.0	P	10.3	n/a	22.0	22.0	1.4	1	1	9	74.5
24	43.5	P	9.6	n/a	22.0	20.0	1.4	2	5	43	74.5
26	43.5	P	10.3	n/a	24.0	24.0	1.4	3	3	36	74.5
27	43.5	P	10.3	n/a	24.0	24.0	1.4	4	4	38	75.0
33	44.0	P	11.0	n/a	23.0	22.0	1.4	5	2	12	74.5
SS3	43.0	P	11.0	n/a	26.0	26.0	1.4	6	6	43	74.5

Notes:

The inlet end PCM tubes were drilled past the end-caps to a depth of about 1 inch using a 3/32-inch diameter drill to ensure the compaction of felt at the bottom of the TES tubes would not prevent salt from entering the tube annulus. The new stainless steel tube was also drilled to match its argon flow rate with the other 5 heat storage tubes.

AFT = argon flow tests conducted at 10 psig inlet pressure
#1 = as received prior to SDHRT fill attempts #1 & #2
#2 = n/a
#3 = inlet drilled 3/32" dia to 1" depth and weld transitions attached
#4 = inlet manifold attached
#5 = total cumulative flow after attachment to exit manifold

The fill operation was a complete success and modifications to the facility and procedures became permanent.

A special trap was designed for the vacuum overflow line at the top of the chamber to collect and freeze out salt that exits the overflow salt manifold and prevents is from reaching the bottom of the chamber.

The disparity between the fill times for these 6 heat storage tubes was believed to be caused by flow pressure drop differences at the inlets because of felt metal compaction from the first 2 fill operations.

6-TUBE SDHRT FILL #3 (19 Dec 1989)

Tube Serial #	Dry Weight (lbs)	HLC	AFT #1 (lpm)	AFT #2 (lpm)	AFT #3 (lpm)	AFT #4 (lpm)	AFT #5 (cfm)	Manifold Order	Fill Order	Fill Time (min)	Filled Weight (lbs)
PC4	36.0	n/a	n/a	n/a	n/a	n/a	n/a	n/a	n/a	n/a	70.5
1	43.5	P	-	12.0	-	12.0	1.2	1	4	21	74.0
3	45.0	P	-	10.5	-	10.5	1.2	2	2	18	74.5
6	43.0	P	-	21.0	-	19.0	1.2	3	1	6	73.5
7	44.5	P	-	11.5	-	11.5	1.2	4	5	47	75.0
8	44.5	P	-	12.0	-	11.0	1.2	5	3	21	74.0
10	44.0	F	-	7.0	-	6.5	1.2	6	U	63	45.5

Notes:

Six new heat storage tubes were installed into the HTTES facility for fill. The inlets of these tubes were not drilled because (1) a need to drill the inlets had not been shown and (2) a potential exists for damaging the weld of the PCM fill tube to the end-cap. Damage to this weld would be extremely difficult to repair.

AFT = argon flow tests conducted at 10 psig inlet pressure
#1 = as received values measured but lost (close to #2 values)
#2 = weld transitions attached
#3 = not in the fill procedures at this time
#4 = inlet manifold attached
#5 = total cumulative flow after attachment to exit manifold

The fill operation was mostly successful. However, filling did not proceed as it did in the 6-tube demo. First, the salt did not freeze out at the top of the chamber in the exit manifold and some of the tubes were completely or partially filled from the top. Secondly, tube #10 was only filled to about 2-inches with 2.0 lbs of salt.

The data recorded during this fill operation was difficult to interpret. However, we believe that the reason the 6th did not fill was the failure to drill the inlets of the TES tubes. This tube had the lowest measured argon flow rate and was positioned last on the inlet manifold. The inlet end PCM tubes were drilled in all future fill operations.

The procedures were changed to operate the exit freeze valve during the active salt casting operation to prevent filling from the top overflow manifold.

Tube #10 will be filled in a future single-tube fill operation.

6-TUBE SDHRT FILL #4 (19 Jan 1990)

Tube Serial #	Dry Weight (lbs)	HLC	AFT #1 (lpm)	AFT #2 (lpm)	AFT #3 (lpm)	AFT #4 (lpm)	AFT #5 (cfm)	Manifold Order	Fill Order	Fill Time (min)	Filled Weight (lbs)
PC5	36.0	n/a	n/a	n/a	n/a	n/a	n/a	n/a	n/a	n/a	51.0
32	44.0	P	-	12.0	16.0	15.5	1.2	1	4	146	75.0
29	43.5	P	-	9.5	16.0	15.5	1.2	2	5	235	73.5
30	43.5	P	-	13.5	16.5	15.5	1.2	3	2	32	74.0
21	44.0	F	-	12.5	17.0	15.5	1.2	4	3	143	74.5
11	43.5	P	-	8.5	19.0	16.5	1.2	5	U	295	64.5
23	43.5	P	-	14.5	19.5	17.5	1.2	6	1	27	73.5

Notes:

Six new heat storage tubes were installed into the HTTES facility for fill. The inlets of these tubes were drilled with a 1/16-inch diameter drill to prevent damaging the weld of the PCM fill tube to the end-cap. Damage to this weld would be extremely difficult to repair.

AFT = argon flow tests conducted at 10 psig inlet pressure
#1 = as received values measured but lost (close to #2 values)
#2 = weld transitions attached
#3 = inlets drilled 1/16" dia to 1/2" depth
#4 = inlet manifold attatched
#5 = total cumulative flow after attachment to exit manifold

The fill operation was again mostly successful and the filling did not proceed as it did in the 6-tube demo. Five of the six tubes were completely filled.

We believe that the reason the 6th did not completely fill was due to blockage at the inlet by small metallic contaminents in the salt. Two changes were discussed to eliminate the problem. First, to control the rate of gas flow rate into the salt recervoir and flow salt through the transfer lines at verv low velocity. The low flow velocity would be too low to suspend particles up the 4-5 feet of vertical rise through the system. The second fix would be to design an in-line filter to remove the particles from the salt prior to the salt reaching the inlets of the PCM fill tubes. The decision was made to control the gas flow rate and slowly pressurize the salt reservoir.

If no more problems are encountered, tube #11 will be used as is with a 70% fill.

6-TUBE SDHRT FILL #5 (6 Feb 1990)

Tube Serial #	Dry Weight (lbs)	HLC	AFT #1 (lpm)	AFT #2 (lpm)	AFT #3 (lpm)	AFT #4 (lpm)	AFT #5 (cfm)	Manifold Order	Fill Order	Fill Time (min)	Filled Weight (lbs)
PC6	35.5	n/a	n/a	n/a	n/a	n/a	n/a	n/a	n/a	n/a	35.5
19	41.0	P	15.0	17.0	22.0	21.0	1.35	1	U	275	60.0
4	43.0	P	13.0	18.0	23.0	23.0	1.35	2	2	224	73.5
5	44.0	P	10.5	16.0	24.0	23.0	1.35	3	U	275	57.5
35	41.5	P	21.0	19.0	25.0	24.0	1.35	4	1	180	72.0
20	41.5	P	12.5	20.0	25.2	24.0	1.35	5	U	275	62.5
31	42.5	P	19.0	21.0	26.0	24.0	1.35	6	U	275	56.5

Notes:

Six new heat storage tubes were installed into the HTTES facility. The inlets of these tubes were drilled to 3/32" diameter to be the same as the tubes used in the 6-tube fill. Care was taken not to damage the weld of the PCM tube to the end-cap.

AFT = argon flow tests conducted at 10 psig inlet pressure
#1 = as received prior to modification
#2 = inlet and exit drilled 1/16" dia to 1" depth
#3 = inlet drilled 3/32" dia to 2" depth + exits 1/16" dia to 1"depth + transitions
#4 = inlet manifold attached
#5 = total cumulative flow after attachment to exit manifold

3050 g of the eutectic salt mixture from the first 6-tube fill attempt was loaded as part of the 174 lbs of salt eutectic for the fill because Cerac was unable to deliver all of the salt ordered on time. The salt was ground and examined under magnification and was found to contain less contaminants than the as-received salt from Cerac.

The gas flow into the salt reservoir was regulated to obtain 8-10 on the helium rotometer. This gas flow rate should result in a salt flow rate that will fill all of the heat storage tubes in a time period of not less than 1 hour. At this rate of flow, it took approximately 5 minutes for the molten salt to go from the reservoir to the vacuum feed through at the chamber. This translates into a salt velocity in the 3/8-in dia lines of about 2 ft/min.

It required 3 hours for the first tube to fill and almost 4 hours for the 2nd tube to fill. The remaining 4 tubes were only partially filled. The extremely low salt flow rate into the tubes eliminates viscous effects as a possible cause of flow stoppage. Therefore, the only possible reason flow could be stopped entering the heat storage tubes is because of particulate blockage at the felt metal interface. Analysis confirms that the only possible way for these tubes to fill in such a long time duration is due to severe restriction at the inlet.

The facility will be modified to include a in-line filter to remove metallic contaminats before they reach the inlets of the heat storage tubes. The filter design was checked by casting the 100 lbs of salt still left in the salt reservoir into a large, throw-away purge canister (not PC6; too much salt remained inside the reservoir to use the existing purge canister). This operation was successful and examination of the filter showed (1) adequate filter surface area to prevent clogging of the filter and (2) the presence of sufficient metallic contaminants to clog the inlets of the fill tubes.

An attempt will be made to complete the filling of the partially filled heat storage tubes in a separate 6-tube fill operation after the remaining 6 new tubes are filled.

6-TUBE SDHRT FILL #6 (20 Mar 1990)

Tube Serial #	Dry Weight (lbs)	HLC	AFT #1 (lpm)	AFT #2 (lpm)	AFT #3 (lpm)	AFT #4 (lpm)	AFT #5 (cfm)	Manifold Order	Fill Order	Fill Time (min)	Filled Weight (lbs)
PC6	35.5	n/a	n/a	n/a	n/a	n/a	n/a	n/a	n/a	n/a	42.0
17	44.0	P	27.0	27.0	27.0	n/a	1.48	1	n/a	9	75.5
12	43.5	P	29.0	28.5	27.5	n/a	1.48	2	n/a	9	74.5
16	44.5	P	28.5	29.0	27.0	n/a	1.48	3	n/a	9	75.5
18	45.0	P	28.5	29.0	26.0	n/a	1.48	4	n/a	9	75.5
34	44.5	P	28.0	29.0	27.0	n/a	1.48	5	n/a	9	75.5
22	44.0	P	30.0	30.0	26.0	n/a	1.48	6	n/a	9	75.0

Notes: All of the problems encountered during the previous fill operations have finally been corrected. The filter successfully prevented blockage at the tube inlets and all of the heat storage tubes were filled in the same length of time of 9 minutes.

AFT = argon flow tests conducted at 10 psig inlet pressure
#1 = inlets drilled 3/32" dia to 2" depth and exits drilled 3/32" dia to 1" depth
#2 = weld transitions attached
#3 = upper and lower manifolds attached
#4 = n/a
#5 = total cumulative flow after attachment to exit line

6-TUBE SDHRT FILL #7 (10 Apr 1990)

Tube Serial #	Dry Weight (lbs)	HLC	AFT #1 (lpm)	AFT #2 (lpm)	AFT #3 (lpm)	AFT #4 (lpm)	AFT #5 (cfm)	Manifold Order	Fill Order	Fill Time (min)	Filled Weight (lbs)
PC7	35.5	n/a	n/a	n/a	n/a	n/a	n/a	n/a	n/a	n/a	43.0
10	46.0	F	n/a	n/a	n/a	n/a	n/a	1	6	7	74.5
20	62.5	P	n/a	n/a	n/a	n/a	n/a	2	5	6	73.0
31	56.5	P	n/a	n/a	n/a	n/a	n/a	3	3	6	74.0
19	60.0	P	n/a	n/a	n/a	n/a	n/a	4	1	4	72.0
5	57.5	P	n/a	n/a	n/a	n/a	n/a	5	2	4	75.0
11	64.5	P	n/a	n/a	n/a	n/a	n/a	6	4	6	74.5

Notes: The fill of the partially filled tubes proceeded without incident. All of the tubes were completely filled in 7 minutes or less. Procedures were altered to carefully melt the salt inside the annulus and the lower freeze valve was operated until the salt flow was established in the transfer lines.

AFT No argon flow tests were conducted because the tubes were partially filled with salt.

The inlets were drilled to a 2-in depth using a 3/32-in dia drill to clear the flow passages of the tubes.

BOEING

ACTIVE SHEET RECORD

SHEET NO.	REV LTR	ADDED SHEETS				SHEET NO.	REV LTR	ADDED SHEETS			
		SHEET NO.	REV LTR	SHEET NO.	REV LTR			SHEET NO.	REV LTR	SHEET NO.	REV LTR
1						46					
2						47					
3						48					
4						49					
5						50					
6						51					
7						52					
8						53					
9						54					
10						55					
11						56					
12						57					
13						58					
14						59					
15						60					
16						61					
17						62					
18						63					
19						64					
20						65					
21						66					
22						67					
23						68					
24						69					
25						70					
26						71					
27						72					
28						73					
29						74					
30						75					
31						76					
32						77					
33						78					
34						79					
35						80					
36						81					
37						82					
38						83					
39						84					
40						85					
41						86					
42						87					
43						88					
44						89					
45						90					

ACTIVE SHEET RECORD

SHEET NO.	REV LTR	ADDED SHEETS				SHEET NO.	REV LTR	ADDED SHEETS			
		SHEET NO.	REV LTR	SHEET NO.	REV LTR			SHEET NO.	REV LTR	SHEET NO.	REV LTR
91											
92											
93											
94											
95											
96											
97											
98											
99											
100											
101											
102											
103											
104											
105											
106											
107											
108											
109											
110											
111											
112											
113											
114											
115											
116											
117											
118											
119											
120											
121											
122											
123											
124											
125											
126											
127											
128											
129											
130											
131											